Pavol Jozef Šafárik University in Košice

Faculty of Natural Science

BOOK OF ABSTRACTS

The 5th International Conference on Nanomaterials: Fundamentals and Applications

October 10-13, 2021

Organized by:

Department of Physical Chemistry
Faculty of Natural Science
Pavol Jozef Šafárik University in Košice
&
Slovak Chemical Society
Bratislava

Košice 2021

The 5th International Conference on Nanomaterials: Fundamentals and Applications

Book of Abstracts

Edited by: Veronika Niščáková, *veronika.niscakova@student.upjs.sk*

Ivana Šišoláková, *ivana.sisolakova@upjs.sk*

Institute of Chemistry, Pavol Jozef Šafárik University in Košice

Reviewed by: Renáta Oriňaková, *renata.orinakova@upjs.sk*

Andrea Straková Fedorková, *andrea.fedorkova@upjs.sk*

Institute of Chemistry, Pavol Jozef Šafárik University in Košice

Available at: www.unibook.upjs.sk
Publication date: 04.11.2021

ISBN 978-80-574-0039-4 (e-publication)

LIST OF CONTENTS

LIST OF AUTHORS

Preface

On behalf of the NFA 2021 Organizing Committees, we introduce with pleasure these proceedings devoted to contributions from the 5th NFA Nanomaterials: Fundamentals and Applications conference held in Štrbské pleso, High Tatras, Slovakia. The conference is organized by the Faculty of Science Pavol Jozef Šafárik Uninversity in Košice and Slovak Chemical Society. The conference program provides an opportunity for researchers interested in various applications of nanomaterials to discuss their latest results and exchange ideas on the new trends. The main objective of the conference umbrella is to encourage discussion on a broad range of related topics and to stimulate new collaborations among the participants.

The proceedings contains all papers of both: oral and poster presentations. We hope that these proceedings will give readers an excellent overview of important and diversity topics discussed at the conference. We thank all authors for submitting their latest work, thus contributing to the excellent technical contents of the Conference. Especially, we would like to thank the organizators that worked diligently to make this conference a success, and to the recenzents for the thorough and careful review of the papers.

We wish all attendees of NFA 2021 an enjoyable scientific gathering in High Tatras, Slovakia. I wish all participants enjoy this scientific meeting to collect new information form nanoscience.

Ivana Šišoláková

Invited Lecture 1

Ni-Rich Layered Oxide Cathode Materials for Automotive Li-Ion Batteries: Problems, Origins, and Solutions

Hieu Quang Pham[a]*, Jakub Reiter[a]

[a]R&D Department, Inobat Auto, Mostová 6, 811 02, Bratislava, Slovakia
*email: hieu.pham@inobat.eu

Lithium-ion batteries (LIBs) are widely used for portable devices, electrical vehicles, large-scale energy storage systems, and are subject to ongoing modifications to meet the growing demands for higher energy and power densities [1, 2]. In recent years, nickel-rich layered oxides ($LiNi_xM_yCo_zO_2$, $x \geq 0.6$, $x + y + z = 1$, Ni-rich NCMs), which are cheaper and contain significantly less of toxic cobalt, offer a higher specific capacity ($\geq$ 180 mAh g^{-1}) with an average voltage of ≈3.8 V vs Li^+/Li [3], as compared to traditional $LiCoO_2$ (145 mAh g^{-1}) and spinel-$LiMn_2O_4$ (120 mAh g^{-1}). So Ni-rich NCMs would be one of the most effective candidates for achieving high specific energy with over 300 Wh kg^{-1} at the cell level in the future.

However, large-scale application of Ni-rich NCM cathodes is hindered by severe capacity fading during long-term cycling, which is mainly caused by the instability of the Ni-rich NCM cathode–electrolyte interface at high-voltage (above 4.2 V vs Li^+ /Li), utilization of which would lead to higher energy densities. The highly oxidized state of Ni^{4+}, formed upon Li-deintercalation, is spontaneously reduced to Ni^{3+} and Ni^{2+} by accepting electrons from the electrolyte, causing severe oxidative decomposition of the electrolyte at the cathode−electrolyte interface [4]. This leads to the formation of nucleophilic fluoride (F^-) species, which in turn can corrode the transition metals from Ni-rich NCM, causing the structure deterioration of cathode. This leads to the formation of nucleophilic fluoride (F^-) species, which in turn can corrode the transition metals from Ni-rich NCM, causing the structure deterioration of cathode materials, when the standard $LiPF_6$ salt is used. In addition, the similar radius of Li^+ (0.76 Å) to Ni^{2+} (0.69 Å) leads to the intermixing of Ni and Li layers, which results in the well-known phase transition from layered hexagonal structure ($R\bar{3}m$) to spinel ($Fd\bar{3}m$) and to cubic rock-salt ($Fm\bar{3}m$), causing oxygen release and safety issues. This electrochemically inactive rock-salt phase hinders the Li^+ diffusion at the cathode–electrolyte interface, thus resulting in capacity fading. Additionally, crack formation, induced by internal stress in the secondary particles upon repeated Li^+-(de)intercalation, provides new sites for the cathode–electrolyte interface reactions, accelerating layered-to-rock-salt phase transition, causing voltage fade.

The details of problems and their origins of Ni-rich NCMs and the solutions attempted to mitigate these problems would be discussed in the meeting.

7

References

[1] X. Wang, Y.-L. Ding, Y.-P. Deng, Zh. Chen, Adv. Energy Mater. (2020) 1903864.
[2] H. Q. Pham, M. Mirolo, M. Tarik, M. E. Kazzi, S. Trabesinger, Energy Storage Mater. **33** (2020) 216-229.
[3] J. Li, L.E. Downie, L. Ma, W. Qiu, J.R. Dahn, J. Electrochem. Soc. 162 (2015) 162, A1401–A1408.
[4] H. Q. Pham, H. T. Tran; J. Han, S.-W. Song, J. Phys. Chem. C 1241(2020) 75-185.

 ISBN: 978-80-574-0039-4

Invited Lecture 2

Lightweight medium-entropy alloys for hydrogen storage

D. Varcholová[a,b], K. Kušnírová[a], L. Oroszová[a], N. Jasminská[c], M. Lazár[c], T. Brestovič[c], K. Saksl[a,b,d] *

[a] Institut of Materials Research, Slovak Academy of Sciences, Watsonova 47, 040 01 Košice, Slovak Republic
[b] Faculty of Materials Metallurgy and Recycling, Technical University of Košice, Letna 9, 042 00 Košice, Slovak Republic
[c] Faculty of Mechanical Engineering, Technical University of Košice, Letná 9, 042 00 Košice, Slovak Republic
[d] Faculty of Science, Institute of Physics, Pavol Jozef Šafárik University in Košice, Košice 041 80, Slovak Republic

Introduction

The decreasing cost of renewable energy is providing a path toward sustainable energy systems. Hydrogen is the ideal candidate as an energy carrier for both mobile and stationary applications while averting adverse effects on the environment, and reducing dependence on imported oil for countries without natural resources. It has a high energy density per unit mass (142 MJ kg^{-1}) but has a very low volumetric density of 11 m^3 kg^{-1} at ambient temperature and atmospheric pressure. Therefore, for efficient use of hydrogen, it is critical to increase its density by compression. Today, several types of hydrogen compression are industrially applied e.g. gas compression, liquefaction of hydrogen, storage of hydrogen molecules by adsorption and hydrogen storage in metals by absorption. Among them, the most effective way to compress hydrogen is to store it in a metal lattice where a stored amount of hydrogen can significantly exceed its liquid phase, e.g. Mg_2FeH_6 shows the highest known volumetric hydrogen density of 150 kg/m^3, which is more than double that of liquid hydrogen [1].

A "Superior" step forward in this respect represents publication of M. Sahlberg, et al. entitled "Superior hydrogen storage in high entropy alloys" [2] where the authors studied the hydrogenation of the high-entropy solid solution alloy TiVZrNbHf of bcc structure and observed that extremely large amounts of hydrogen (2.7 wt.% of H) can be absorbed in it. The amount of hydrogen corresponds to H/M ratio of 2.5 and becomes a world record in terms of volumetric energy density 219 kg H/m^3 exceeding by far the requested 40 kg H/m^3. The authors explain these phenomena by lattice strain favouring to absorb hydrogen in both tetrahedral and octahedral interstitial sites.

In our work, we focus on study of hydrogen absorption in Al-Ti-Nb-Zr medium-entropy lightweight alloys designed for transport applications.

8

Prediction

In the first step, we verify whether the assumed Al-Ti-Nb-Zr alloys fall into the area of solid solutions stability (Medium-Entropy Alloys, MEA). Conventionally, MEAs solid solution is defined as alloys comprised of 3 or 4 elements with non-equiatomic concentrations for which the configurational entropies at a random state are between 1 R and 1.5 R. [3].

Zhang et al. [4] proposed the use of two parameters for the design of multicomponent solid solutions, namely, the atomic size difference δ and the mixing enthalpy ΔH_{mix} [5]:

$$\delta = \sqrt{\sum_{i=1}^{n} c_i \left(1 - \frac{r_i}{\sum_{j=1}^{n} c_j r_j}\right)^2} \quad (1)$$

where c_i and r_i denote the atomic fraction and atomic radius of the i^{th} element, respectively,

$$\Delta H_{mix} = \sum_{i=1, i\neq j}^{n} \Omega_{ij} c_i c_j = \sum_{i=1, i\neq j}^{n} 4\Delta H_{ij}^{mix} c_i c_j \quad (2)$$

where ΔH_{ij}^{mix} is the enthalpy of mixing of the binary liquid between the i^{th} and j^{th} elements at an equiatomic composition.

MEAs generally tend to form single-phase solid solutions in the case of low mixing enthalpy and atomic size difference. In general, the formation of a single-phase solid solution corresponds to the region $\Delta H_{mix} > -12$ kJ/mol and $\delta \leq 6.6\%$.

 ISBN: 978-80-574-0039-4

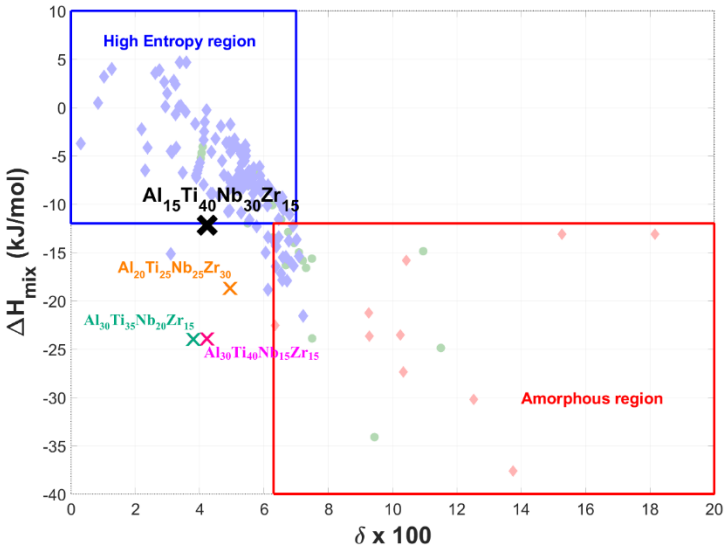

Fig. 1 The plot delineating the phase selection in MEAs. The regions highlight the individual region to form simple solid solutions, and amorphous phases [12]. Position of the studied Al-Ti-Nb-Zr is highlighted in colour

Figure 1 shows in the upper left corner a stability region of multicomponent MEA solid solutions. The Al-Ti-Nb-Zr alloys are shown in the plot in colour. From this graphical comparison, it is clear that none of the alloys falls within the stability range of MEA solid solutions. On the other hand, all the alloys were prepared as single solid solutions of body-cantered-cubic lattices and thus the basic requirements on MEA were met.

Results

Tab. 1 The prepared Al-Ti-Nb-Zr alloys listed with experimentally obtained data: density, amount of hydrogen absorbed at 200°C and 2MPa H_2 within 1 hour expressed by weight increase percentage and hydrogen to metal atoms ratio, residual amount of hydrogen after desorbtion realized at 380°C in vacuum for 2 hours, mixing enthalpy - ΔH_{mix}, atomic size mismatch δ, corresponding mixing entropy - ΔS_{mix} , and concentration of valence electrons - VEC.

Sample	Density [g/cm^3]	Absorbed H [wt. %] ; H/M	Desorbed H [wt. %] ; H/M	ΔH_{mix} [kJ/mol]	δ × 100	ΔS_{mix}	VEC
$Al_{15}Ti_{40}Nb_{30}Zr_{15}$	6.11	1.34 ; 0.89	0.21 ; 0.14	-12.2	1.85	10.9	4.2
$Al_{20}Ti_{25}Nb_{25}Zr_{30}$	6.15	1.29 ; 0.88	0.25 ; 0.17	-18.75	1.22	11.5	4.9
$Al_{30}Ti_{35}Nb_{20}Zr_{15}$	5.66	1.07 ; 0.60	0.18 ; 0.10	-24.0	0.83	11.0	3.8
$Al_{30}Ti_{40}Nb_{15}Zr_{15}$	5.48	0.97 ; 0.56	0.00 ; 0.00	-23.9	0.84	11.0	4.2

As can be seen from the table, the highest storage capacity of hydrogen has the $Al_{15}Ti_{40}Nb_{30}Zr_{15}$ alloy with an H/M value of 0.89. This alloy did not completely desorb hydrogen even after annealing in vacuum at 380°C for 2 hour indicating a strong hydrogen bonding to metal atoms in this alloy. The value of residual hydrogen expressed by the

ISBN: 978-80-574-0039-4

H/M ratio is 0.14. On the other hand, alloys with lower proportion of Nb (less than 25 at.%) show a significantly lower value of hydrogen storage (reduction by more than 33%) and residual hydrogen. This indicates a significant effect of Nb, which affects strongly also the mixing enthalpy of the alloys.

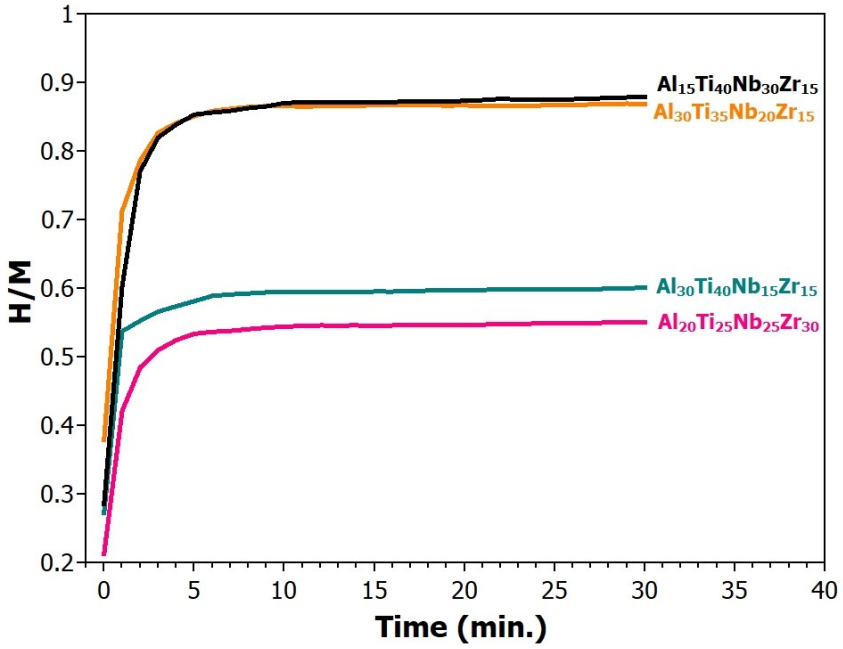

Fig. 2 Hydrogen absorbtion curves of the Al-Ti-Nb-Zr alloys at 200°C and 2MPa of H_2

All these studied alloys show extremely fast hydrogen absorption kinetics, see figure 2. Full saturation of all alloys was achieved within a first three minutes.

Acknowledgements

This work was supported by the Slovak Research and Development Agency under contract No. APVV-20-0205, APVV-20-0068, APVV-20-0138 and APVV-15-0202. Authors are grateful to the Scientific Grant Agency of the Ministry of Education, Science, Research and Sport of the Slovak Republic and the Slovak Academy of Sciences (VEGA project No. 2/0013/19, No. 1/0108/19, No. 1/0626/20 and KEGA No. 005TUKE-4/2019) and DAAD project No. 57560249.
All measurement of hydrogen absorbtion ware realized at the Institut für Nichtklassische Chemie e.V. Lipzig Germany.

References

[1] A. Züttel, Materialstoday, **6** (2003) 24-33.
[2] M. Sahlberg, et al., Sci. Rep. **6** (2016) 36770.
[3] Y. Zhou et al., Sci Rep, **8** (2018) 1236.
[4] Y. Zhang et al., Adv. Eng. Mater.**10** (6) (2008), 534-538.
[5] S. Guo , et al., Intermetallics. **41** (2013) 96–103.

 ISBN: 978-80-574-0039-4

Invited Lecture 3

Nanotechnology in biosensing and bioanalysis

J. Tkáč[a]*, T. Bertok [a], L. Lorencova [a], M. Hires [a], E. Jane [a], V. Gajdosova [a], A. Blsakova [a]

Institute of Chemistry, Slovak Academy of Sciences, 821 04, Bratislava, Slovakia,
jan.tkac@savba.sk

In this contribution we will describe application of various forms of nanomaterials applicable in biosensing and bioanalysis. In particular 2D nanomaterials such as graphene oxide or MXene will be presented, but also other types of nanomaterials including hybrid magnetic nanoparticles and magnetic nano/microparticles will be discussed, as well. Another aspect which will be described is to control immobilisation process at the nanoscale by carefully tuned modification of interfaces.
Such devices were extensively optimized to resist non-specific interactions allowing to work with complex samples such as human serum from patients having various diseases including cancer *i.e.* prostate cancer, breast cancer, *etc.* The clinical potential of magnetic enzyme-linked lectin assays for diagnostics of prostate cancer will be discussed in detail.

Acknowledgement:
The financial support from APVV (17-0300), VEGA (2/0137/18); from the Ministry of Health of the Slovak Republic under the project registration number 2018/23-SAV-1 and 2019/68-CHÚSAV-1 is acknowledged.

 ISBN: 978-80-574-0039-4

Electrochemical Determination of EGFR

R. Gorejová [a]*, I. Šišoláková, J. Shepa, M. Panigaj, R. Oriňaková

[1] Department of Physical Chemistry, Pavol Jozef Šafárik University in Košice, Moyzesova 11, 040 01 Košice, Slovak Republic

[2] Institute of Biology and Ecology, Pavol Jozef Šafárik University in Košice, Moyzesova 11, 040 01 Košice, Slovak Republic

E-mail: radka.gorejova@student.upjs.sk

Epidermal growth factor receptor (EGFR) is a predictor of the various types of cancer. In case of lung cancer, patients undergo EGFR testing before targeted therapy. Different methods, such as enzyme assay, denaturing high-performance liquid chromatography, and direct automatic sequencing, were used as a detection techniques. Nevertheless, these methods display several limitations like cumbersome procedures, long duration, and high cost [1]. In general, electrochemical biosensors attracted recently considerable attention. Electrochemical methods offer many advantages as high sensitivity, good selectivity, low cost, and fast detection [2]. Various electrochemical methods lie cyclic voltammetry, chronoamperometry, electrochemical impedance spectroscopy, linear sweep voltammetry etc. can be considered as the suitable way to EGFR determination. Moreover, the favorable properties of protein detection by bond creation with the specific aptamer are well known. Various aptasensors were studied for detection of leukemia biomarkers, various viruses and so on.

Herein, we studied aptasensor for EGFR detection as an another approach to cancer diagnostics. Screen-printed carbon electrodes (SPCE) modified by streptavidin were studied due to this simplicity and good electrochemical properties. Both methods, cyclic voltammetry and electrochemical impedance spectroscopy were used to evaluate electroanalytical properties of these electrodes in more details.

Modification of SPCE by streptavidin and specific aptamer led to good electroanalytical characteristics which were studied via cyclic voltammetry (Figure 1). The modified electrodes display wide linear concentration rage from 10 ng/ml to 250 ng/ml. Limit of detection was calculated as 48 ng/ml. Sensitivity of modified electrodes was 19.7 nAml/ng. Therefore, we can confirm that studied electrodes are suitable platform for EGFR detection and are suitable for application in amperometric and impedimetric sensors.

12

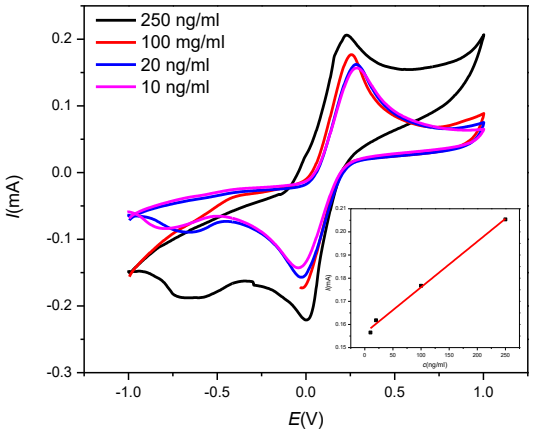

Fig. 1 Cyclic voltammograms for different concentration of EGFR protein. Inset: Calibration curve

ISBN: 978-80-574-0039-4

Acknowledgements

This work has been supported by the project of the Slovak Research and Development Agency APVV-PP-COVID-20-0036 and Visegradfund project number 22020140.

References

[1] J. Hu, Y. Yu, M. Guo, M, Yuan, W. Liu, Biosens. Bioelectron. **77** (2016) 215-219.
[2] M. M. Qaid, M.M. Adbelrahman, Cogent Food Agric. **2** (2016) 1-18.

 ISBN: 978-80-574-0039-4

Preparation of The Screen Printed Carbon Electrodes Modified by Polypyrrole and Nickel Nanoparticles for Electrochemical Insulin Determinantion

F. Chovancová[a]*, I. Šišoláková[a], J. Shepa[a], R. Oriňaková[a]

[a] Deparrtment of Physical Chemistry, Faculty of Science, Pavol Jozef Šafárik University, Moyzesova 11, 04011 Košice, Slovak Republic
* frederika.chovancova1@gmail.com

Insulin is known as an anabolic hormone created by two different chains – A and B connected by disulfide bridges [1][2]. Thus, the glucose level is controlled by a careful amount of insulin [3]. However, a mistake in insulin production or insulin activity is caused by abnormal glucose levels and subsequently leads to a condition known as diabetes mellitus [4]. Diabetes mellitus is a group of metabolic diseases represented by chronic hyperglycemia [5] caused by insulin resistance or absolute insulin deficiency [6][7].

Diabetes has gotten a worldwide pandemic with significantly expanding occurrences [8]. The numbers of diabetics in the following 20 years relied upon to ascend to 642 million. Thus, on the off chance that no further move is to be made, the mortality identified with diabetes will keep on expanding in the next many years [5]. Furthermore, inadequately controlled diabetes is related to extreme hazardous complications [8][9] , such as renal diseases [10] , various cardiovascular problems [11] or limb amputation [9].

Direct detection focused on glucose concentration in the blood is essential to prevent or diabetes treatment [12]. These days, the third generation of enzymatic glucose electrochemical sensors is commonly used for glucose testing and diagnosis of diabetes [13][14]. However, enzymatic sensors suffer poor pH stability and unstable temperatures over 40°C [15][16]. Two primary methods for insulin determination are immune and non-immune [1]. However, these methods are unsuitable for commercial applications [17]. Electrochemical techniques could beat the inadequacies of different strategies portrayed previously [13].

Researchers have been working intensively to developed insulin sensors as a relevant alternative to enzymatic glucose sensors [14]. Electrochemical insulin sensors have stood out due to their direct electrocatalytic detection and suitable analytical properties [2].

This work deals with the preparation of screen printed carbon electrodes modified by combination of the polypyrole and nickel nanoparticles. Firstly, screen printed carbon electrodes were electropolymerized by 0,1M pyrrole monomer and 0.5M KCl at constant current 0.2 mA for 50 s. The modified surface of electrodes NiNPs were electrodeposited at potential E = - 0,5 V for 45s in the solution of 0.06 M $NiCl_2$. The surface of electrodes were activated in 0.1 M NaOH. Secondly, activated electrodes surface were applied potential of 1.6 V for 60 s in acid medium consisted of 0.5 M H_2SO_4 and 0.1 M KCl. The last step was electrodeposition of NiNPs at constant potential 0.5 V during 45s.

Acknowledgements

This work has been supported by the project of the Slovak Research and Development Agency APVV-PP-COVID-20-0036 and Visegradfund project number 22020140.

References

[1] J. Hovancova, A. Orin, D. R. Garcia, O. Shylenko, and J. Radon, Electroanalysis. (2018) 1–11.
[2] J. Hu, M. Yuan, W. Liu, M. Guo, and Y. Yu, Biosens. Bioelectron. **77** (2015) 215–219.
[3] Y. Yu, M. Guo, M. Yuan, W. Liu, and J. Hu, Biosens. Bioelectron. **77** (2016) 215–219.
[4] A. K. Srivastava, P. Bajpai, and A. Jain, Elsevier Ltd. **1** (2018).
[5] S. S. K. Reddy and M. Tan. Elsevier Inc. (2020).
[6] F. Gómez-Peralta, C. Abreu, X. Cos, and R. Gómez-Huelgas. *Rev. Clínica Española (English Ed.)* **220** (2020) 305–314.

 ISBN: 978-80-574-0039-4

[7] I. Ahmed and B. Goldstein. Elsevier Inc. **24** (2006).
[8] G. Päth, N. Perakakis, C. S. Mantzoros, and J. Seufert. Metabolism. **90** (2019) 1–15.
[9] S. M. Blackman and D. W. Cooke. *Encycl. Biol. Chem. Second Ed.* **1** (2013) 649–658.
[10] I. Šišoláková, J. Hovancová, F. Chovancová, R. Oriňaková, I. Maskaľová, A. Oriňak, J. Radoňák, Electroanalysis. (2020).
[11] S. Y. Tan, J.L.M. Wong, Y. J Sim, S. S. Wong, S. A. M.Elhassan, S. H. Tan, G. P. L. Lim, M. W. R. Tay, N. W. R.Tay, N. C. Annan, S. K. Bhattamisra, M. Candasamy *Diabetes Metab. Syndr. Clin. Res. Rev.* **13** (2019) 364–372.
[12] H. Chen, G. Fan, J. Zhao, M. Qiu, P. Sun, Y. Fu, D. Han, G. Cui. New J. Chem. **43** (2019) 7806–7813
[13] J. Hovancová, I. Šišoláková, R. Oriňaková, A. Oriňak. (2017) 2147–2166.
[14] I. Šišoláková, J. Hovancová, R. Oriňaková, A. Oriňak, L. Trnková, I. Tříšková, Z. Farka, M. Pastucha, J. Radoňák, J. Electroanal. Chem. **860** (2020).
[15] J. Hovancová, I. Šišoláková, P. Vanýsek, R. Oriňaková, I. Shepa, M. Kaňuchová, N. Király, M. Vojtko, P.Čudek, A. Oriňak, J. Electroanal. Chem. **878** (2020).
[16] I. Šišoláková, J. Hovancová, R. Oriňaková, A. Oriňak, L. Trnková, D. R. Garcia, J. Radoňák, Bioelectrochemistry. **130** (2019).
[17] N. Amini, M. B. Gholivand, and M. Shamsipur, J. Electroanal. Chem. **714–715** (2014) 70–75.

 ISBN: 978-80-574-0039-4

Optimization of Thin Electrodeposited Layers for Lithium – ion Batteries

J. Maca[a]*, J. Libich[a], P. Cudek[a], T. Kazda[a]

[a] Brno University of Technology, Department of Electrical and Electronic Technology, Technická 10, 616 00 Brno, Czech Republic
*macaj@vut.cz

Introduction

Lithium ion batteries are one of the most used batteries in the industry. The development of green and renewable energy opens new areas for application of lithium ion batteries in large storage batteries. Current lithium ion batteries are made from positive electrode based on LiFePO4, LiNiMnCoO2, LiNiCoAlO2 and the most modern nickel rich materials NCM 111 or NCM 811. For negative electrode two main materials are used some form of carbon or lithium titanite ceramic material (Li4Ti5O12).

Current boom in electromobility was also a big push for research in batteries. The state of research is focused on development electrode materials with higher capacity, lower weight, almost zero self-discharging, maximum safety and low cost. Most of these parameters cannot be obtained at the same time so a compromise must be done. One of the research branches is focused to move from intercalation mechanism to a conversion reaction. The substituting of present used intercalation mechanism to conversion is due a much higher capacity of metallic oxides used in conversion-based batteries.

This paper is focused on optimization of thin layers based on cobalt and lead for applications in batteries. The capacity of Co3O4 material is almost 2.3 times higher than common used carbon-based negative electrode. The lead layers can be interesting in sodium ion batteries applications. The area of sodium-based batteries in growing a lot in recent years. The electrodeposited layer should serve as a base for growing a 3D nanostructure on it. The main disadvantage of conversion principle is significant volume change during charging and discharging. The nanostructure in form of nanowires should compensate the volume change in x and y axis[1-8].

Experimental

Thin layer based on cobalt and lead were prepared by electrodeposition. On a foil made from cupper was through a suitable mask deposited a thin layer of cobalt oxide or lead oxid from solution. Deposition solution for cobalt was used 0.01 M CoSO4 · 7 H2O and 0.1 M ammonium acetate (CH3COONH4) dissolved in deionized water. The pH of the solution was set by 25% solution of ammonia (NH4OH). The pH was set to 7. The time of electrodeposition was change from 15 to 45 minutes depends on the sample. The electrodeposition voltage was 1.2 V against standard calomel electrode (SCE). The surface of cobalt deposition for 45 minutes is shown in figure 1A. From the picture is visible that he sizes of the “trees” is approximately 9 μm.

The layer based on lead was prepared in solution of 0.2 M lead(II) nitrate (Pb(NO3)2) and 0.3 M nitric acid (HNO3). The current density was calculated to 10 mA·cm-1. The signal alternation was changed from 1:5 to 5:1. A current a rectangular signal was used. The electrodeposition was always running till charge of 20 C flowed through. There was no magnetic stirring used for both materials depositions. The deposited lead layer is shown in figure 1B, the alternation 1:5 was used (1 time unit current flow versus 5 time units current is cut off). The size of the “leaves” is approximately 22 μm.

 ISBN: 978-80-574-0039-4

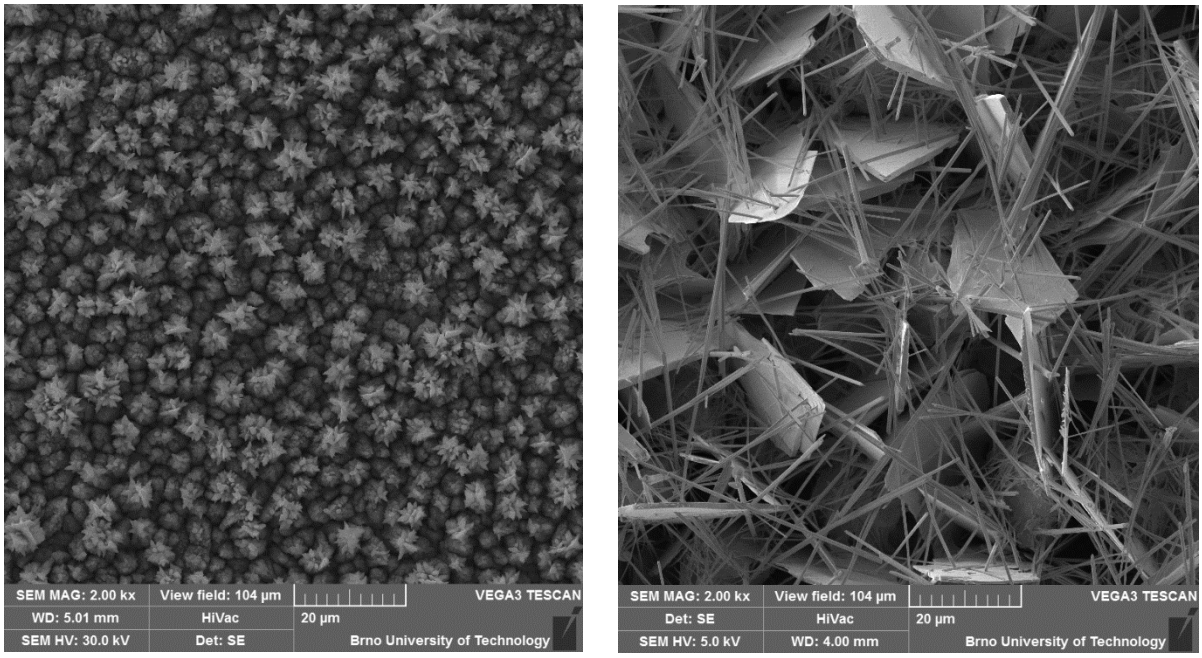

A) B)

Fig. 1 A) Cobalt electrodeposited layer, B) Lead electrodeposited layer

Conclusion

From presented figure 1A and 1B it is obvious that much smaller structures are crated by deposition of cobalt layer. The cobalt layer is without long spikes and more uniform truth the whole surface. The deposited surface of lead is more random with larger depth differences. The main influence of signal alternation is in suppressing of the needle shape structures growth. From the EDS spectrum 43 wt.% is cobalt present sample shown on 1A. The lead sample contain 88 wt.% of lead. The cobalt layer seems to be more suitable for use as base for the following nanowires growth due the uniformity of the layer.

The conversion reaction is promising for use in batteries but many obstacles have to be overcome to by usable in commercial industry. The nanostructure management can be the solution of the main problem, the volume change during cycling. The material and structure research need to be done.

Acknowledgements

Authors gratefully acknowledge the financial support from the Ministry of Education, Youth and Sports of the Czech Republic under project No. LTT19001 and BUT specific research programme (project No. FEKT-S-20-6206).

References

[1] A. N. Dey, J. Electrochem. Soc. 1971, 118, (2012).
[2] T. Simons, A. K. Pearson, S. J. Pas, D. R. Macfarlane, J. electacta, 174, (2015).
[3] A. M. P. Sakita, R. Della Noce, E. Vallés, A. V. Benedetti, J. apsusc, 434, (2018).
[4] C. Cui, R. Zhang, CH. Fu, B. Sun, Y. Wang, H. Hou, Y. Ma, Y. Gao, P. Zuo, J. apmt, 24, (2021).
[5] J-L. Wang, E. Alasonati, P. Fisicaro, M.F. Benedetti, J.jhazmat, 422, (2022).
[6] N.I. Liu, X. Zhang, E. He, W. Zhou, L. Yu, X. Yan, J. apsusc, 568, (2021).
[7] A. Gupta, CH. Srivastava, J. surfcoat, 425, (2021).
[8] L. Anicai, I. Sin, O. Brincoveanu, S. Costovici, A. Cotarta, A. Cojocaru, M. Enachescu, T. Visan, J. apsusc, 475, (2019).

 ISBN: 978-80-574-0039-4

Epoxy/Carbon Fiber Composites with Designed Interface Interaction

Matej Mičušík[a]*, Mária Omastová[a], Michal Procházka[a], Zbynek Vorac[b], Marie Bohacova[c], Vladimír Spacek[c]

[a] Polymer institute, Slovak Academy of Sciences, Dubravska cesta 9, Bratislava 84541, Slovakia
[b] Departments of Physics at the Faculty of Science, Masaryk University in Brno, Kotlářská 267/2, 611 37 Brno, Czech Republic
[c] Synpo a.s., S. K. Neumanna 1316, Pardubice 532 07, Czech Republic
*matej.micusik@savba.sk

In polymer composites interfaces are very important and the manufactured components not always have the expected properties derived from the reinforcement (fillers as fibres or various nanoparticles) and polymer matrix separately [1, 2]. Our objective was the development and manufacturing of new hybrid composite materials based on epoxy/carbon fibre composites combined with certain types of special structured molecules and/or with the use of carbon or inorganic nanostructures.
Better compatibility and interconnection of polymeric system with carrying carbon-based fillers will be achieved by suitable chemical modification of primary materials. New types of organically modified nanostructured composites will significantly decrease delamination and crack propagation in epoxy carbon composites. If necessary, functionalization of carbon fibres by -NH2 groups will be carried out enabling chemical bond with carrying polymeric system.
Expected result is a composite design, which can be applied in more challenging applications in terms of mechanical properties and durability.
Systems intended for the transport industry (aviation, automotive, etc.) and for the construction industry (concrete structures reinforcement) will be aimed for industrial implementation.

Star-like and star polymers were synthetized. The aim of the initial experimental phase was to start from syntheses of hydroxy-functional star polymers with different number of arms and different arm lengths, which are prepared by ionic polymerization of a suitable polyol and caprolactone and / or lactide. After proper carboxy or amine functionalization, the polymer thus formed is being tested for compatibility in admixture with a suitable epoxide.
We have modified carbon nanostructures, especially carbon nanotubes (CNT) with polyhedral oligomeric silsesquioxane (POSS) (Scheme 1). POSS is a hybrid molecule with an inorganic silsesquioxane part at the core and organic (isobutyl, isooctyl, methacrylate, etc.) groups attached at the corners of the cage. Therefore, we chose aminopropyl isobutyl POSS (POSS-NH2), which has a reactive amino group suitable for creating bonds to nanotubes. CNT were purified and then oxidized by hydro-chloric acid. XPS analysis showed the presence of hydroxyls (C1s signal at ca 286 eV) and carboxyls (C1s signal at ca 289 eV). The carboxyl groups were converted to acylhalogenide by chlorinating agent to increase their reactivity with POSS-NH2. Modified POSS was characterized by SEM, EDX, Raman and XPS. Unfortunately, we are not able to confirm, that POSS is chemically bonded to CNT from the available data. It is possible that POSS is mixed with the fibres of CNT only physically, without any covalent bond between POSS and CNT. In the next phase of the study, we will investigate other possibilities of incorporation of POSS into CNT.
We also successfully introduced amino groups on the surface of CNT by radiofrequency plasma modification. For this experiment, outlet of plasma afterglow was placed directly into the liquid medium (allylamine as a source of nitrogen) containing CNT. EDX showed the increase of nitrogen content from 0 % for original CNT to about 30 % for modified CNT.
Mechanical properties of final composites were studied and will be presented.

 ISBN: 978-80-574-0039-4

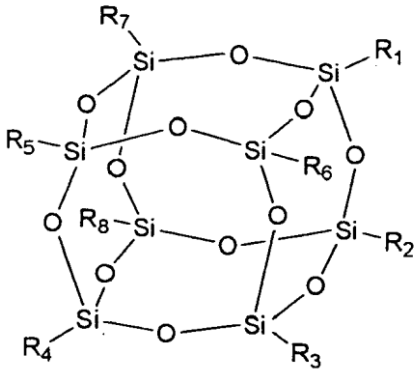

Scheme 1 The POSS structure (https://www.reade.com/products/poss-polyhedral-oligomeric-silsesquioxane-molecules)

Acknowledgements
This work was developed under the M-Era.Net 2 research project entitled EPIC - European Partnership for Improved Composites. This work was supported by the Slovak Research and Development Agency under the project APVV-SK-BY-RD-19-0011 and project VEGA 02/0010/18.

References
[1] Hughes J.D.H.: Comp. Sci. Tech. 41, 13 (1991).
[2] Karger-Kocsis J., Mahmood H., Pegoretti A.: Prog. Mater. Sci. 73, 1 (2015).

 ISBN: 978-80-574-0039-4

Application of Electrochemical Biosensors in Clinical Diagnostics

R. Oriňaková[a]*, I. Šišoláková[a], J. Shepa[a]

[a]Department of Physical Chemistry, Institute of Chemistry, Faculty of Science of Pavol Jozef Šafárik University in Košice, Moyzesova 11, 040 01 Košice
*renata.orinakova@upjs.sk

In recent years, much attention has been paid to personalized medicine to enable an accurate diagnosis to be made before any symptoms of the disease appear which is essential for patients' survival. The main challenge in medical diagnostics is early diagnosis and personalization of patient care using non-invasive methods. To achieve this goal, reliable methods of detecting and monitoring specific biomarkers that indicate a pathological phenomenon are needed. In this light, electrochemical biosensors are a very attractive alternative to other analytical devices and provide multiplexed analysis, fast response, sensitivity, specificity and lower costs compared to proven analytical methods. Electrochemical biosensors are among the oldest and most widespread catalytic sensor devices and are based on conversion of biochemical processes, such as the reaction between the enzyme and the substrate, or the antigen-antibody interaction, on electrical signals. The most common electrochemical sensors are enzymatic sensors, nanomaterial-based sensors, immunosensors, DNA sensors, and apatasensors. The main advantages of electrochemical sensors are simple construction of the measuring system, low costs, excellent sensitivity and specificity. In addition, these systems can be integrated into miniaturized analytical devices (lab on chip), which represent excellent analytical platforms for the point of care or on site analysis, which fully replace commercial laboratory instruments for in vitro diagnostics [1, 2]. Biosensor (Fig. 1) applications are expanding rapidly due to the growing demand for fast and accurate quality or quantity control and detection of very low concentrations of substances.

20

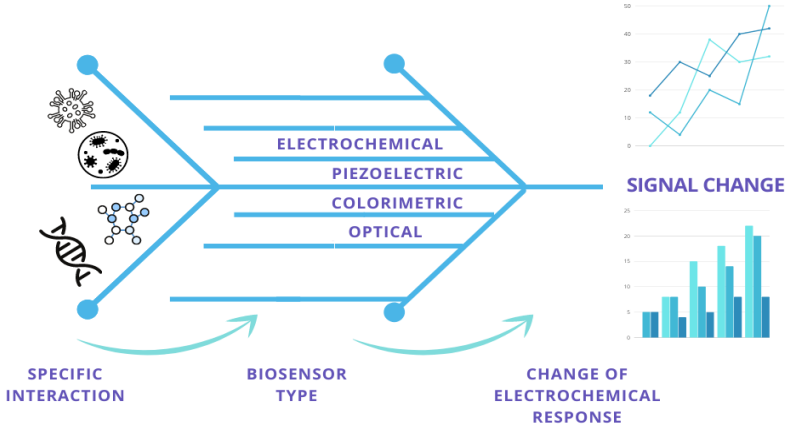

Fig. 1 Schematic representation of biosensor principle

Acknowledgements
The work has been supported by the Slovak Research and Development Agency (project APVV-PP-COVID-20-0036) and Visegrad fund (project No. 22020140).

References
[1] I.H. Cho, D.H. Kim, S. Park, *Electrochemical biosensors: Perspective on functional nanomaterials for on-site analysis*, Biomat. Res. **24** (2020) 6.
[2] N.K. Bakirhan, B.D. Topal, G. Ozcelikay, L. Karadurmus, S.A. Ozkan, *Current Advances in Electrochemical Biosensors and Nanobiosensors*, Crit. Rev. Anal. Chem. **50** (2020) 1-16

 ISBN: 978-80-574-0039-4

NiAg nanocavities film for SERS detection of organic molecules

O.Petruš[a]*, M.Strečková[a], J. Macko[b], R.Oriňaková[b], V.Socha[c]

[a] Institute of Materials Research, SAS, Watsonova 47, 040 01 Košice, Slovakia
[b] Department of Physical Chemistry, UPJŠ, Moyzesova 11, 040 01 Košice, Slovakia
[c] Department of Air Transport, ČVUT, Horská 3, 128 03, Prague, Czech Republic
*opetrus@saske.sk

The first assumptions of signal enhancement were due to the enlargement of the surface area of the substrates [1]. Later, in 1978 Moskovits published the theory proposing that Raman signal enhancement occurs when the preresonant or resonant excitations of conduction electron resonate in metal structures on the surface with adsorbed analyte [2]. The enhancement of the local electric field in close proximity to the surface depends on the shape and geometry of nanostructured objects. For these reasons, it is necessary to prepare nanostructured films or nanoparticles with the desired shape and geometry [3,4], which are capable of producing localized surface plasmons after illumination by the excitation laser source.
Surface Enhanced Raman Spectroscopy (SERS) is a suitable technique to detect a very low concentration of organic molecules using nanostructured films or nanoparticles to enhancement analytical signal. In present work we prepared nickel nanocavity array by colloidal litography combined with electrochemical deposition. After removal of colloidal mask, the Ag nanoparticles was electrochemically deposited on the as-prepared Ni nanocavites. Advantage of the NiAg nanocavity film is hydrophobicity with contact angle 140.2° ± 6.1°, which leads to preconcentration of the analytes during drying of the solution droplet of analyte as shown in Figure 1.

21

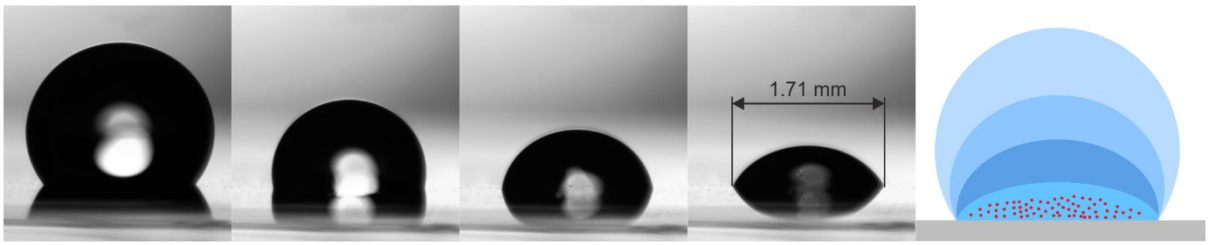

Fig. 1 The lateral image of 1×10-6 mol.dm-3 R6G water solution droplet on NiAg nanocavity film at different times of drying. The scheme on the right shows the drying and preconcentration process of analytes on the substrate

As a analyte organic molecules we selected Rhodamie 6G (R6G), Crystal violet (CV), Methylene blue (MB) and Malachite green oxalate (MGO). SERS spectrum of individual organic molecules are shown in Figure 2. The RSD for R6G, CV, MB, and MGO was 20.1%, 13.8%, 16.7%, and 19.3%. The concentration dependence was measurement from from 1.10^{-5} to 1.10^{-12} mol.dm^{-3} for R6G and from 1.10^{-5} to 1.10^{-10} mol.dm^{-3} for CV, MB and MGO and the detection limit limit was 1.3×10^{-12}, 1.5×10^{-10}, 1.4×10^{-10}, 7.5×10^{-11} mol.dm^{-3}, respectively. Finally, we performed the principal component analysis to extract the differences in complex spectra of the dyes where the first and second PCs carry 42.43 % and 31.39 % of the sample variation, respectively. The achieved results demonstrated the suitability of AgNi nanocavity films for the SERS-based detection of organic dyes, with a potential in other sensing applications.

 ISBN: 978-80-574-0039-4

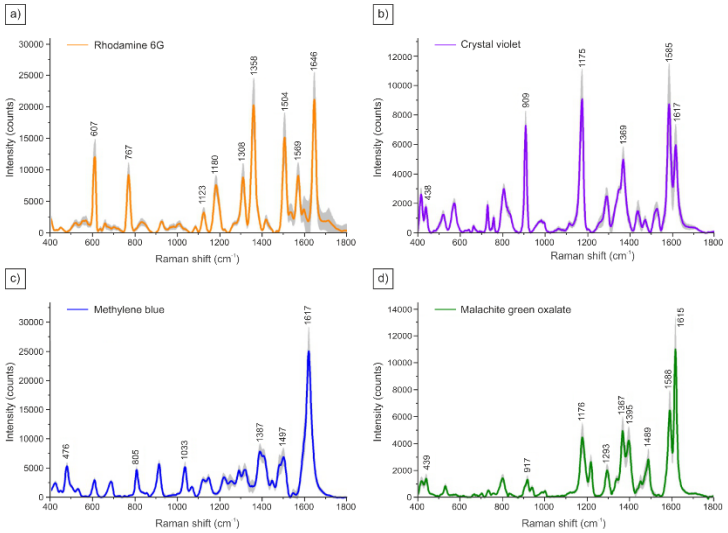

Fig. 2 Comparison of mean SERS spectra of selected organic dyes. The shaded areas represent the standard deviations of the means (n = 6)

Acknowledgements
This research was financially supported by projects VEGA 1/0074/17 of the Slovak Scientific Grant Agency, APVV-16-0029 and APVV-COVID-20-0036 of the Slovak Research and Development Agency.

References

[1] M. Fleischmann, P. J. Hendra, and A. J. McQuillan, Chem. Phys. Lett. **26**, 163 (1974).
[2] M. Moskovits, J. Chem. Phys. **69**, 1 (1978).
[3] Z. Luo, L. Chen, C. Liang, Q. Wei, Y. Chen, and J. Wang, Microchim. Acta **184**, 3505 (2017).
[4] P. A. Atanasov, N. N. Nedyalkov, N. Fukata, W. Jevasuwan, T. Subramani, D. Hirsch, and B. Rauschenbach, AIP Conf. Proc. **030001**, (2019).

ISBN: 978-80-574-0039-4

Electrochemical Determination of Insulin on Cobalt Naoparticles Modified Carbon Electrodes

K. Sisáková a*, I. Šišoláková[a], J. Shepa[a], R. Oriňaková[a]

[a] Department of Physical Chemistry, Pavol Jozef Šafárik University in Košice, Moyzesova 11, 040 01 Košice, Slovak Republic
*katarina.sisakova@student.upjs.sk

Various transition metal nanoparticles represent promising low-cost materials for catalysis of insulin oxidation. Combination of transition metal nanoparticles with multi walled carbon nanotubes (MWCNTs), ensure the enlargement of the active surface area of the electrode, can improve the analytical characteristics of electrodes in many ways [1]. Usage of polymer membrane on the electrode surface prevents the occupation of active sites with Cl^- ions present in body fluids and improves the stability of the electrode by fixing the nanoparticles on the electrodes surface during the electrochemical measurements [2]. In this work screen-printed carbon electrodes (SPCEs) modified by the combination of cobalt (CoNPs) polymer membrane (chitosan) and MWCNTs was prepared. The surface of prepared electrode was studied via atomic force microscopy (AFM) and scanning electron microscopy (SEM) (Figure 1). In the effort to find the most suitable modification for electrochemical insulin determination, stability, analytical characteristics, and selectivity of the electrode was determined. The results proved low limit of detection (25 nM), high sensitivity (0.031 mA μM^{-1}) and wide linear range (0.05 µM to 5 µM) of CoNPs/chitosan-MWCNTs/SPCE. The stability of the CoNPs/chitosan -MWCNTs/SPCE was very high, with only 1.7% decrease of maximal current value after 50 measurements. Therefore, CoNPs/chitosan-MWCNTs/SPCE can be considered as the suitable modification for new electrochemical sensor for insulin determination, with suitable analytical characteristics.

Acknowledgements
This work has been supported by the project of the Slovak Research and Development Agency APVV-PP-COVID-20-0036 and Visegradfund project number 22020140.

References
[1] Šišoláková I., Hovancová J., et al.: Bioelectrochemistry, 130 (2019), 107326.
[2] Shepa J., Šišoláková I., et al.: Sensors, 21 (2021), 5063.

 ISBN: 978-80-574-0039-4

Carbon Electrodes as a Novel Platform for EGFR Detection

I. Šišoláková[a*], J. Shepa[a], M. Panigaj[b], R. Oriňaková[a]

[1] Department of Physical Chemistry, Pavol Jozef Šafárik University in Košice, Moyzesova 11, 040 01 Košice, Slovak Republic
[2] Institute of Biology and Ecology, Pavol Jozef Šafárik University in Košice, Moyzesova 11, 040 01 Košice, Slovak Republic
E-mail: radka.gorejova@student.upjs.sk

Epidermal growth factor receptor (EGFR) is a cellular trans-membrane protein activated through binding to its specific ligands. Over expression of EGFR can leads to deregulation of cell processes and initiation of cancer in the lung, breast, rectal, and oral tissues [1]. Currently used techniques for EGFR detection require sophisticated instrumentation and specially trained person. So, development of a sensitive, fast, low-cost , and simple method is crucial for the point-of-care cancer biomarker detection. Several methods have been developed for the detection of the EGFR, such as microfluidic nano-biochip, cell-based sensor (lab-on-chip, LOC), quartz crystal microbalance immunosensors. Electrochemical methods display ability to evaluate the interfacial properties of biological processes [2]. Other benefits of these methods are fast response, simplicity, and effectivity. In this paper we report a preparation of electrochemical sensor for EGFR detection. The screen-printed carbon electrodes (SPCE) were modified by gold nanoparticles, which were modified by oligonucleotide chain with the biotin. In the second step the streptavidin molecules were bonded to oligonucleotide chain. The modification of electrode was studied via scanning electron microscopy (SEM) and fluorescence microscopy (Figure 1).

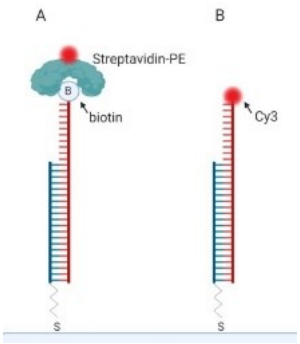

Fig. 1 Schematic illustration of SPCE modification by biomolecules

Acknowledgements
This work has been supported by the project of the Slovak Research and Development Agency APVV-PP-COVID-20-0036 and Visegradfund project number 22020140.

References
[1] J. Hu, Y. Yu, M. Guo, M, Yuan, W. Liu, Biosens. Bioelectron. **77** (2016) 215-219.
[2] M. M. Qaid, M.M. Adbelrahman, Cogent Food Agric. **2** (2016) 1-18.

 ISBN: 978-80-574-0039-4

Investigation of TiSiN/AlTiSiN/TiSiN nanocomposite coatings

P. Šulhánek [a]*, I. Černičková [a], L. Ďuriška [a], P. Babincová [a], Ľ. Čaplovič [a]

[a] Slovak University of Technology in Bratislava, Faculty of Materials Science and Technology in Trnava
J. Bottu 25, 917 24 Trnava, Slovak Republic
*patrik.sulhanek@stuba.sk

TiN and AlTiN hard coatings have been widely used for improving properties and prolonging lifetime of machining tools. By adding silicon to TiN and AlTiN systems a nanocomposite structure is created, which results in improved hardness, thermal stability, as well as oxidation and corrosion resistance of the coating. These properties are important requirements for the coatings to serve their purpose well [1-2]. In this work, samples of nanocomposite coatings in as-deposited and annealed state were investigated. The coatings were deposited by LARC® technology on a high speed steel substrate. Structure and morphology of the coatings were observed using SEM, chemical composition was measured by EDX. Finally, the results obtained from each sample were compared with one another.

Acknowledgements
The authors would like to thank the project of VEGA Grant Agency of the Ministry of Education, Science, Research and Sport of the Slovak Republic and Slovak Academy of Sciences, No. 1/0540/19 and the Slovak Research and Development Agency project number APVV-20-0124 for providing financial support.

References

[1] A. M. Palacios, J. J. Olaya, J. E. Alfonso. Influence of Si on the Structural, Electrical, and Optical Properties of (Al, Ti, Si)N Films Deposited Via Reactive DC Sputtering. *Materials Research.* **23** (2020) doi: 10.1590/1980-5373-mr-2019-0687.
[2] H. Çaliskan, P. Panjan, C. Kurbanoglu. *Hard Coatings on Cutting Tools and Surface Finish.* In: *Comprehensive Materials Finishing.* (Yilbas, B. S., ed.) Vol. 3 - Surface Coating Processes, (2017), Chap. 3.16, (pp. 230–242). ISBN: 9780128035818

 ISBN: 978-80-574-0039-4

Biocompaibility Evaluation of Polymer Coated Zinc-based Degradable Material

R. Gorejová[a]*, J. Macko[a], V. Čákyová[a], R. Oriňaková[a]

[a]Department of Physical Chemistry, Institute of Chemistry, Faculty of Science of Pavol Jozef Šafárik University in Košice, Moyzesova 11, 040 01 Košice
*radka.gorejova@student.upjs.sk

Biodegradable zinc implants gained a higher attention recently due to their ideal behaviour in physiological environment [1]. Their degradation properties in the simulated human body fluids predetermine them for application in the field of degradable biomaterials. In addition to suitable degradation and mechanical properties, biological compatibility is a key parameter for a choice of ideal implant material. The safety of released products and nanoparticles *in vivo* influence biomaterial biocompatibility and need to be carefully monitored [1]. In our study, zinc-based biodegradable materials were prepared and modified. Powder metallurgy route was chosen as a suitable method for metallic material preparation. Zinc pellets with diameter of 12 mm were prepared from raw powder after uniaxial compression at 600 MPa. Green compacts were subsequently sintered in the inert atmosphere (Argon, 4l/min) at 350 °C. Sintered pellets were ultrasonically cleaned in acetone and ethanol for 10 minutes in each and then immersed into 10 wt% solution of polyethyleneglycol (PEG) to bio-activate the sample surface. Indirect cytotoxic effect of extracts (prepared by immersion of Zn and Zn-PEG samples in simulated body fluids for 4 hours and further diluted to 50% and 10% concentration) on adult human dermal fibroblast (HDFa) cells was tested by the MTS assay. Cells without extracts were used as a negative control (NC). The relative viability of HDFa cells after 4 hours of incubation with Zn sample extracts decreased vs. the NC, however, the viability remained relatively high (above 80%) for all dilutions. PEG layer further positively influenced resulting viability of zinc material (above 90% for all dilutions). Differences between the diluted and un-diluted samples were not significant predicting their acceptable biocompatibility even after longer time of immersion.

Acknowledgements
This work was supported by the Slovak research and development agency (projects APVV-16-0029 and APVV-20-0278).

References
[1] P. K. Bowen, J. Drelich, J. Goldman, Adv. Mater. **25**(18) (2013) 2577-2582.
[2]Y. Yoshioka, K. Higashisaka, Y. Tsutsumi, *Biocompatibility of nanomaterials;* in: *Nanomaterials in Pharmacology.* Humana Press, New York, 2016, pages 185-199.

 ISBN: 978-80-574-0039-4

Glycerol citrate modified biodegradable metal cellular material

J. Macko[a], T. Sopčák[b], R. Gorejová[a], R. Oriňaková[a], A. Oriňak[a]

[a] Department of Physical Chemistry, Institute of Chemistry, Pavol Jozef Šafárik University in Košice, Moyzesova 11, 041 54 Košice
[b] Institute of Materials Research of SAS, Slovak Academy of Sciences, Watsonova 47, 040 01 Košice
*jan.macko@upjs.sk

Biodegradable materials are of the group of materials belonging to the bioactive biomaterials. Their task is to temporarily prolong gradually regenerating tissue *in vivo*. Iron powder has been used to prepare degradable metallic cellular materials precisely because of its advantageous properties. Cellular materials were prepared by a combination of the replication method and the powder metallurgy method. The prepared cellular material was modified by applying a thin layer of glycerol citrate (GCA) prepolymer by deep coating methods from ethanol solutions containing GCA prepolymer content of 10% and 20%, which was polymerized in an oven at 100 °C, 135 °C and 165 °C for 90 minutes. In the case of a solution containing 10% GCA, the applied layer was incomplete. In the case of 20% GCA content, the applied layer was significantly thicker. Corrosion properties were determined in Hanks' solution in the form of static and dynamic corrosion. The highest rate of degradation results in a 10% GCA solution. All prepared samples corroded faster than the original pure iron material.

Acknowledgements
This work was supported by grants APVV-16-0029 and APVV-20-0278 of the Slovak Research and Development Agency and within the framework of scientific cooperation between SAS and MAV (Low-temperature electrohydrodynamic techniques used for preparation of bioceramic coatings).

 ISBN: 978-80-574-0039-4

Nanoporous Modified Fe-based Degradable Materials

A. Morovská Turoňová[a*], M. Kupková[b], M. Hrubovčáková[b]

[a]Institute of Chemistry, Faculty of Science, P. J. Šafárik University, 040 01 Košice, Slovakia
*andrea.morovska.turonova@upjs.sk
[b]Institute of Materials Research, Slovak Academy of Sciences, 040 01 Košice, Slovakia

Biodegradable materials are needed for maintenance sufficient mechanical properties during regeneration and growth of new tissue in the implanted area. At the same time, controlled degradation is required and dissolved particles they are expected to be eliminated by excretion from the body without causing any side effects or toxicity [1].

Iron is one of the best candidates for biodegradable metallic materials due to its properties, excellent elastic modulus and high strength. Therefore, biodegradable iron-based alloys have a wide range of applications in various fields of medicine. It is important to examine the basic data on iron metabolism and its biocompatibility, the mechanism of the corrosion process, as well as the rate of iron degradation. Compared to zinc and magnesium, for example, iron has a very low corrosion rate, so pure iron can hardly be called "biodegradable". But due to its biocompatibility and excellent mechanical properties, it is important to work on modifications that could accelerate corrosion. It is clear that the evolution of H_2 gas, the formation of anodic and cathodic sites on implants and the formation of pits are the main reasons for the slow degradation of Fe-based materials in aggressive environments. Due to the low rate of corrosion, it is necessary to modify this material with various additives, nanoparticles, composites, or to treat the surface of the material with various nanoporous coatings.

In a previous study, ZnO and MgO nanoparticles were chosen as an additive to the iron matrix. ZnO nanoparticles are known as active antibacterial additives in antibacterial polymeric matrix composite biomaterials. In addition to antibacterial activity in a pH-neutral environment, it is a source of zinc, which is an essential element for the human body. Another reason for such a choice was that ZnO already showed catalytic activity in various situations [2]. Similarly, MgO with ultrafine particles in nanoscale with a high specific surface area has shown great promise as a destructive adsorbent for toxic chemicals [3]. All materials were prepared by powder metallurgy and treated by spark plasma sintering. The electrochemical measurements confirmed that the corrosion properties and the rate of degradation depend on the amount of nanoparticles present. In all these cases, the material appeared more compact, the surface was more homogeneous.

In the next research, the Fe-based samples were treated in various ways. The aim was investigate the effect of surface treatments on corrosion rate, corrosion potential, corrosion current density and polarization resistance.

The materials were modified in the first step by phosphating and in the next step by calcination, sintering and by hydroxyapatite coating (HAp). The surface treatment of Fe-based samples leads to the formation of nanoscale and micro-dimensional defects and the porous surface is more active for degradation processes, fig. 1. From the corrosion measurements we determined, that the result of degradation processes which take place on the nanoporous surface is a shift in the corrosion potential, a change of current density, and thus an increase in the degradation rate of materials. For pure iron, the corrosion rate was 0.117 mm/y, for phosphated modified materials the degradation rate increased up to 0.390 mm/year. Further treatment by sintering and by HAp coating again slightly reduced the corrosion rate to 0.305 mm/year and to 0.358 mm/year, respectively.

Calcination of the samples did not contribute to accelerated degradation. By changing the current density, the kinetic resistance of the material to the corrosion process decreases and the distribution of surface particles changes. The distribution of surface heterogeneities in the nanoscale can lead to more uniform corrosion.

 ISBN: 978-80-574-0039-4

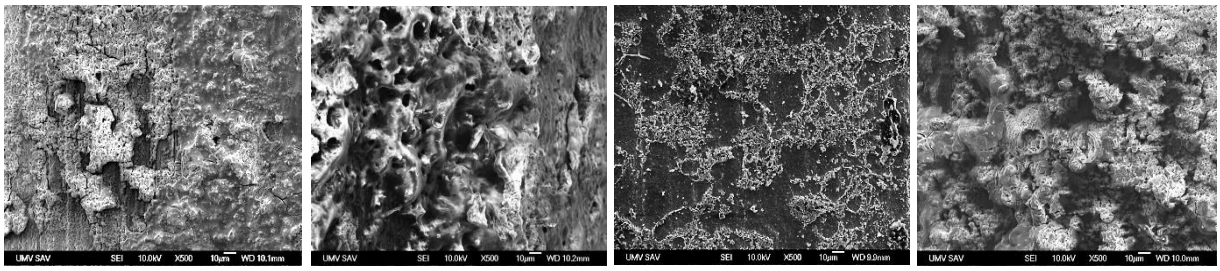

Fig. 1 SEM images of modified Fe-based materials, a) FeP, b) FeP calcined, c) FeP sintered, d) Fe HAp

Acknowledgements
This research was supported by the Slovak Research and Development Agency, project number APVV-20-0278.

References
[1] Manivasagam G. and Suwas S., *Biodegradable Mg and Mg based alloys forbiomedical implants*, J. Mater. Sci. Technol. **30**, 5 (2014) 515-520.
[2] Kupková M., Kupka M., Hrubovčáková M., Oriňaková R., Morovská Turoňová A., Puchý V*., Study on Corrosion of Iron-Zinc Oxide Particulate Composites Produced by a Spark Plasma Sintering in Hanks' Solution* Int. J. Electrochem. Sci. **13** (2018) 11839 – 11852.
[3] Ramanujam K., Sundrarajan M., *Antibacterial Effects* of *Biosynthesized MgO Nanoparticles Using Ethanolic Fruit Extract* of *Emblica officinalis. J. Photochem. Photobiol. B: Biol. **141** (2014) 296–300.*

 ISBN: 978-80-574-0039-4

Bioactive coating influence on the biocompatibility of iron-based biomaterials

M. Petráková[a]*, R. Oriňaková[a], R. Gorejová[a], J.Macko [a], A. Oriňak[a]

[a]Department of Physical Chemistry, Institute of Chemistry, Faculty of Science, P. J. Šafarik University in Košice, Moyzesova 11, 040 01 Košice
*martina.petrakova@student.upjs.sk

Microorganisms that grow in biofilms and adhere to the implant surface in a highly hydrated extracellular matrix often cause implant infections. The solution to this problem can be the application of bioactive nano-coatings to the surface of biomaterials [1]. Bioactive and nano-coatings have proven to be advantageous because they could improve the process of permanent implantation as well as reduce the need for repeated surgeries. For this purpose, drug molecules can be integrated into the coating, allowing therapeutic doses to be delivered to target sites [2].
In this work, the influence of the bioactive polymer coating on the biocompatibility of Fe biomaterials was studied. Samples were prepared from carbonyl iron powder (CIP) by cold pressing into 12 mm diameter pills at 600 MPa. Then the pressed samples were sintered at 1120 °C in a reducing atmosphere for 1 hour. The surface of the iron samples (Fe) was modified with a polymer coating layer of polyethylene glycol (PEG). Part of the samples was coated with a PEG polymer layer containing gentamicin. The biocompatibility of the materials was tested using the MTS cytotoxicity assay of the samples. Fibroblast viability in cell sample extracts did not fall below the critical value of 70% in any sample type. After 24 hours of culture, however, we observed a slight decrease in viability below 90% in all tested samples, which means that no extract from the substrates of the tested samples was cytotoxic.

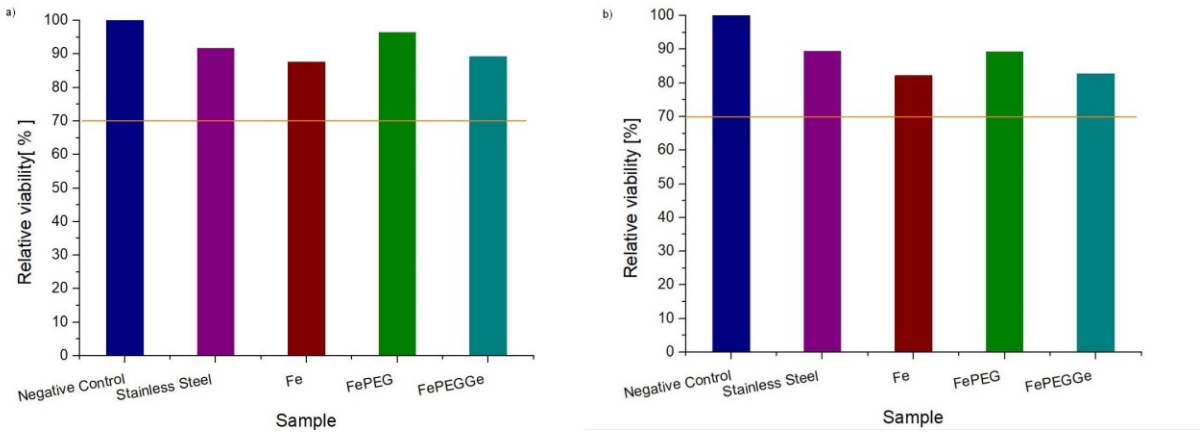

Fig. 3 Relative viability of fibroblasts after a) 4 hours b) 24 hours

Acknowledgements
This work was supported by the project APVV-20-0278 of the Slovak Research and Development Agency.

References
[1] B. G. X, Zhang, *et al*. International Journal of Molecular Sciences **15** (7) (2014) 11878-11921.
[2] M. Gimeno, *et al.* European Journal of Pharmaceutics and Biopharmaceutics. **96** (2015).

 ISBN: 978-80-574-0039-4

Sulphur PAN/PVP Fibres based Composite Material as Cathode for Li-S Batteries

K. Benková[a]*, D. Capková[a], A. Straková Fedorková[a], I. Šišoláková[a], R. Oriňaková[a], M. Strečková[b],
M. Hečková[b]

[a] Department of Physical Chemistry, Faculty of Science, Pavol Jozef Safarik University in Košice, Moyzesova 11, 040 01 Košice, Slovakia

b Institute of Material Research, Slovak Academy of Sciences, Watsonova 47, 040 01 Košice, Slovakia

*katarina.gavalierova@gmail.com

Introduction

These days, lithium-sulphur batteries (Li-S) belong to very attractive field of study because of their high theoretical energy density, cost effectiveness and non-toxicity of sulphur. Li-S batteries are rechargeable devices and consist of a sulphur-based cathode, binder, separator, organic liquid electrolyte, lithium anode and current collector. A schematic diagram of a Li–S battery is shown in Fig. 1. During the discharging process, sulfur in the solid phase ($S_{8(s)}$) is firstly dissolved in the electrolyte and then transforms to $S_{8(l)}$. Then $S_{8(l)}$ is gradually reduced to high-order lithium polysulfides (Li_2S_n , $4 \leq n \leq 8$), which are easily soluble in the electrolyte and diffuse from the cathode to the electrolyte. As discharge continues, the high order lithium polysulfides are further reduced to low order lithium polysulfides (Li_2S_2 and Li_2S) which are less soluble in the electrolyte. During the charging process, the discharge products (Li_2S_2 and Li_2S) are gradually oxidized to high order lithium polysulfides and eventually oxidized to elemental sulfur [1].

There are more different techniques to prepare materials for composites. One of them is electrospinning. Electrospinning is a widely used technique for electrostatic fibre formation. The technique utilizes electrical forces to prepare polymer fibres with diameters in a range between 2 nm to several micrometres [2].

31

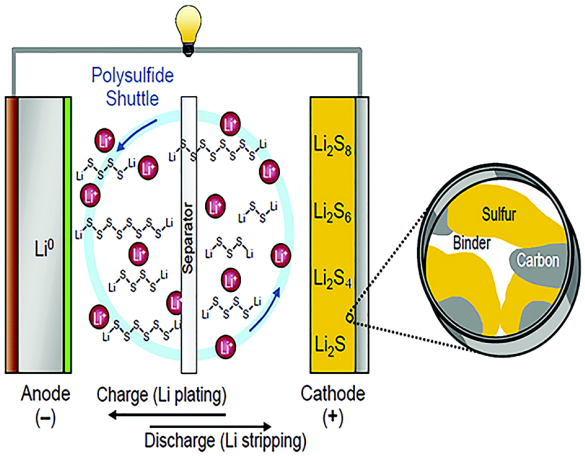

Fig. 1 Schematic diagram of Li-S battery [3]

Lithium-sulphur battery belongs to a conversion type of battery. It means, new electrochemical compounds during charge-discharge process are formed what can cause some scientific problems [4, 5]. Various forms of sulphur, called polysulfides (PS), are produced during discharging and show poor ionic and electronic conductivity. The next problem is related to the volume variation of the sulphur cathode. Sulphur can change its volume of about 79%, what can cause the losing the electrical contacts with the conductive substrate or the current collector. The drastic volume variation of the electrodes can lead to serious safety problems [6, 7].

 ISBN: 978-80-574-0039-4

In our work, we are focusing on composite material based on sulphur and electrospun carbon microfibers to eliminate above-mentioned scientific problems of Li-S batteries.

Experiment

In this work, the carbon fibres were prepared by electrospinning using polyacrylonitrile (PAN) and polyvinylpyrrolidone (PVP) polymers. The S/C composite was prepared by mixing S/CS_2 solution and PAN PVP carbon fibres in ratio 40:60. The electrode slurry was prepared by mixing S/CS_2–PAN PVP carbon fibres composite as the active material with PVDF in N-methyl-2-pyrrolidone. Finally, CS_2 solution was added to the commercial electrolyte. Circular electrodes with 12 mm diameter were cut out of the coated foil. Test cells were assembled using these cathodes in a Swagelok two electrode cell with lithium metal foil anodes and a fiber glass separator.
The electrochemical measurements such as galvanostatic cycling with potential limitation and electrochemical impedance spectroscopy were performed with AUTOLAB potentiostat.

Results

Figure 2 shows the Nyquist plot of electrochemical impedance spectroscopy (EIS) of the above-mentioned sample. The full line indicates the measured data, and the red dots represent data obtained from fitting in a software, whereas the equivalent circuits are also depicted. We can observe two semicircles. The first small semicircle (corresponds to R1 element) describes the charge transfer resistance, and the second significant semicircle (corresponds to R2 element) is associated to the polysulfide coating resistance.
The charge-discharge cycling of the sample S-CS_2/PAN PVP is seen in Fig. 3. We observe the initial charge and discharge curves. All the processes took place in the range between 1,0 and 3,0 V. The measurements were performed at the C/10 rate. From the figure can be seen that the initial discharge specific capacity is 1890 mAh/g.

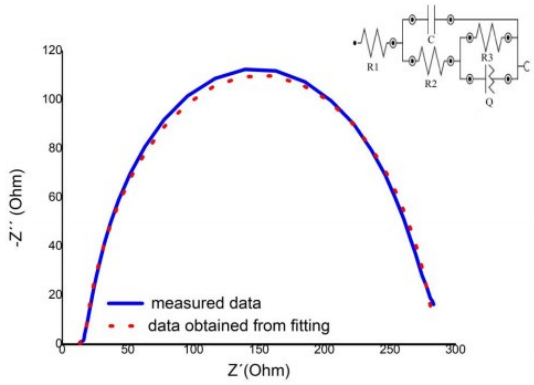

Fig. 2 EIS spectra of the sample S-CS_2/ PAN PVP

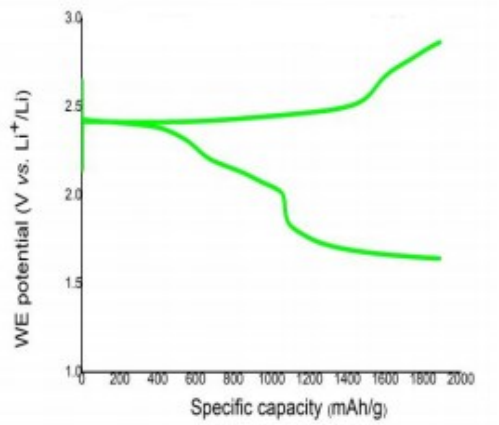

Fig. 3 Charge-discharge profile of the sample S-CS_2/ PAN PVP

EDX map analysis of the sample S-CS_2/PAN PVP is shown in Fig. 4. Fig. 4b depicts the distribution of carbon mostly related to carbon fibres. From Fig. 4c we can see a homogenously distribution of sulphur.

ISBN: 978-80-574-0039-4

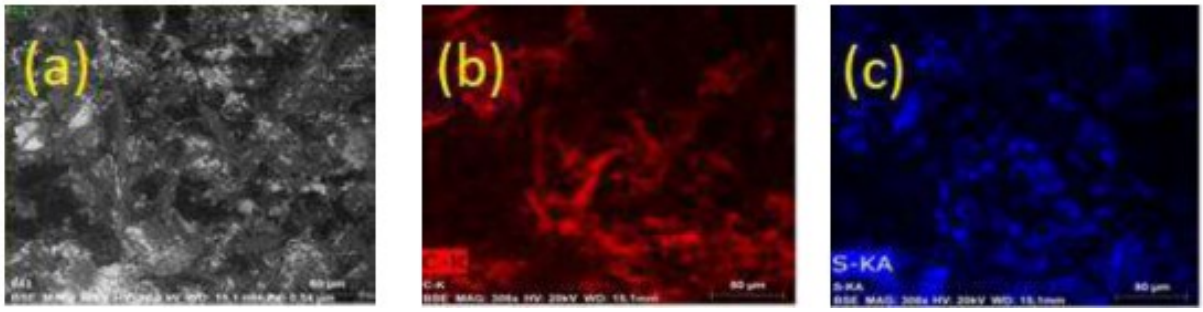

Fig. 4 EDX map analysis of the sample S-CS2/PAN PVP (a), analysis for carbon (b), analysis for sulfur (c)

Conclusion

- PAN PVP microfibres were prepared by electrospinning and S-CS_2/PAN PVP composite was prepared by mixing as cathode material for Li-S battery.
- Electrochemical impedance spectroscopy, galvanostatic charge/discharge and scanning electron microscopy were used.
- A higher initial discharge capacity of 1890 mAh/g was achieved.

Acknowledgements

This work was supported by the Operational program Integrated Infrastructure within the project: Innovative Solutions for Propulsion, Power and Safety Components of Transport Vehicles, 313011V334, co-financed by the European Regional Development Fund and by projects VVGS-PF-2021-1756, APVV-20-0138 and APVV-20-0111.

References

[1] Y. Liu, Ch. Cui, Y. Liu et al., RSC Advances **13**, (2020) 7384.
[2] Y. Diao, K. Xie, X. Hong et al., Acta Chim. Sin. **71**, (2013) 508.
[3] A. Mathiram, Y. Fu, S. Chung et al., Chem. Rev. **114**, (2014) 11751.
[4] A. Strakova Fedorkova, T. Kazda, K. Gavalierova et al., Int. J. Electrochem. Sci. **13**, (2018) 551.
[5] X. Zhang, B. Jin, L. Lin et al., J. Electrochem. Chem. **26**, (2016) 780.
[6] D. Capková, T. Kazda, A. Straková Fedorková et al., ECS Transactions **95**, (2019) 19.
[7] H.D. Yoo, E. Markevich, G. Salitra et al., Materials Today **17**, (2014) 110.

ISBN: 978-80-574-0039-4

Development of new catalytic materials for aqueous electrolysers

R. Bodnárová[a]*, M. Kožejová[a], V. Latyshev[a], S. Vorobiov [a] and V. Komanický[a]

[a] Department of Condensed Matters Physics, Faculty of Science, P. J. Safarik University, Park Angelinum 9, 041 54, Kosice, Slovak Republic

*renata.bodnarova@student.upjs.sk

In the present article, we focused on the preparation of the catalyst and testing the catalytic activity and stability of catalytic materials for the hydrogen economy. The electrocatalysts for hydrogen evolution reaction (HER) were fabricated by magnetron sputtering deposition of metallic Mo-Ni thin film at different temperatures. The catalytic activity of HER and the stability of MoNi compositions in the alkaline electrolyte NaOH were tested by cycling. The formed MoNi thin films were studied by voltammetry techniques and characterized by scenning electron microscopy.. The MoNi alloy prepared at elevated temperatures showed the best catalytic activity of HER and a good structure in an alkaline solution compared to Mo or Ni alone. The optimal composition of as-deposited Mo-Ni catalyst was defined as $Mo_{63}Ni_{37}$. The MoNi catalyst demonstrates low HER overpotential of 195 mV at 10 mA·cm^{-2} current density.

Introduction

One of the most urgent challenges is to find sustainable solutions to the impending energy crisis on a small and large scale to reduce our dependence on conventional fossil fuel-based energy sources. The industry has introduced several new technologies that provide electricity from renewable sources. Electrochemistry plays an important role, because it allows the conversion between electrical and chemical energy. It allows the storage of energy in the form of chemical bonds. [1]

Hydrogen storage is a suitable and sustainable energy source compared to commonly used fossil fuels. Regarding the environment, it is necessary to develop alternative energy approaches to natural fossil energy, such as the production of hydrogen by electrolysis of water. HER is a reaction of the transfer of two electrons. Sufficiently active catalysts are needed to reduce energy barriers. In recent years, research has focused on the development of new catalysts to increase the rate of the kinetic reaction, reduce the voltage of hydrogen evolution, high electrical conductivity and be stable in the environment. [2]

Catalysts for HER depended on chemical properties can be divided into three groups based on precious metals (Pt, Pd), based on base metals (Ni, Mo, Co, Fe, W), based on non-metallic materials (C, P, N, Se, B). Non-precious metal catalysts promise good catalytic properties. By increasing the electrode area, we can increase the overall activity of the electrode. [3]

We focused on the preparation of a thin layer of MoNi. The activity of pure nickel alone in an alkaline environment is worse than that of other metals. The reason is the absorption of atomic hydrogen by nickel, which causes the disruption of the strength of the H-H surface bond. In this process, the metal dissolves into the electrolyte. This shortcoming can be eliminated by alloying another more stable metal (Mo) on the substrate together with nickel. This improvement is due to the strong synergistic effect between the given transition metals. Nickel alloys are characterized by high corrosion resistance and good catalytic properties. [4]

Experimental

From our previous measurements, we have found out that the Mo / Ni alloy provides the best values for HER activity. Therefore, the next step of our work was to optimize the sputtering parameters, and thus to change the Mo: Ni concentration ratio, to achieve the ratio with the best possible catalytic HER activity. In our work, we prepare samples on a standard glassy carbon substrate, and thus the final comparative patterns are correct. It was gradually changed the powers of the DC magnetron gun as follows: 1. Ni-15W, Mo-200W; 2. Ni-30W, Mo-200W; 3. Ni-50W, Mo-200W; 4. Ni-100W, Mo-200W and 5. Ni-200W, Mo-80W.

By EDS analysis, it was found concentration of prepared samples: Mo: Ni. 1. (92:8) %; 2. (86:14) %; 3. (79:21) %; 4. (63:37) %; 5. (28:72) %. All samples were prepared with ~ 30 nm thickness. The results of HER activity

 ISBN: 978-80-574-0039-4

measurements of the samples are shown in Figure 1. An MoNi alloy with ratio 63:37 appears to be best catalyst for HER in alkaline solution. Catalysts with a higher molybdenum content also show better HER activity as catalyst with more as 50 % of Ni.

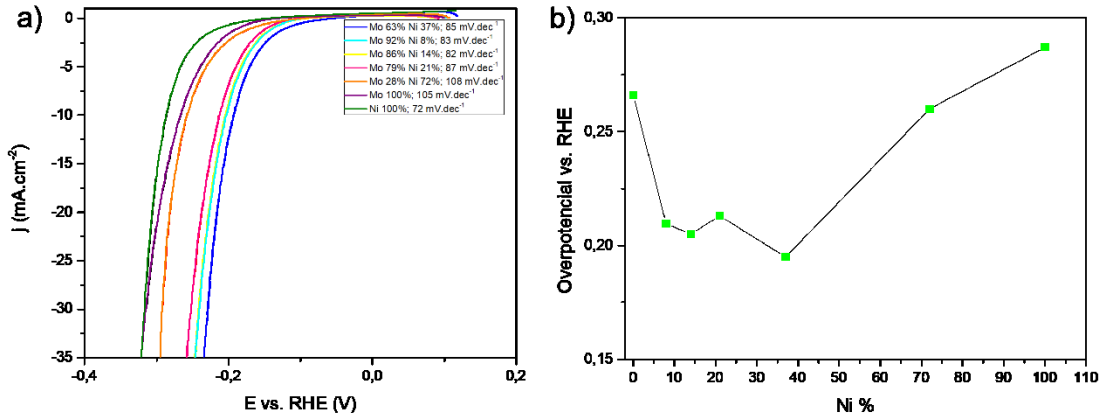

Fig. 1 a) Voltamogrammes of the prepared MoNi thin alloys films (b) Dependence overpotential at 10mV.dec-1 versus amount of Ni in MoNi alloy

The combination of nickel with molybdenum or molybdenum compounds is one of the most effective approaches. It is well-known that molybdenum atoms can incorporate into the nickel lattices to form nickel - molybdenum alloys. Nickel is active in water dissociation while molybdenum has good adsorption properties for hydrogen thanks to its unique electronic structure. Therefore, nickel-molybdenum alloys are attractive electrocatalysts due to the synergistic effect of these two components. [5]

The sample of Mo 63% and Ni 37% has the highest exchange current density (0.0589 $mA.cm^{-2}$) and the Tafel slope has a lower value (85 $mV.dec^{-1}$), which predetermines it as a suitable catalyst.

Conclusion

Considerable progress has been made in the development of HER catalysts in alkaline media. We prepared thin layers of MoNi at different temperatures by magnetron sputtering. We investigated their activity and structure in an alkaline environment using voltametric methods. We found that a series of MoNi samples at high temperature showed better activity and stability values. To determine the amount of Mo and Ni in the sample, we analysed the thin films in detail by EDS. The measured HER activity of the samples shows a shift to lower values of overpotential (195mV) in the sample MoNi with a concentration of Mo 63% and Ni 37%.

Acknowledgements

This work has been supported by grant 313011V334, Innovative Solutions for Propulsion, Power and Safety Components of Transport Vehicles.

References

[1] X. Zou, et al., "Noble metal-free hydrogen evolution catalysts for water splitting." In *Chemical Society Reviews* 44.15 (2015): 5148-5180.

[2] M. Kozejova, M., et al. "Evaluation of hydrogen evolution reaction activity osf molybdenum nitride thin films on their nitrogen content." In *Electrochimica Acta*. 2019, vol. 315, p. 9-16.

 ISBN: 978-80-574-0039-4

[3] H. Knozinger, et al.: "Heterogeneous Catalysis and Solid Catalysts" In *Ullmann's Encyclopedia of Industrial Chemistry.* 2002.
[4] Y. Wang, et al.: "Structural stability of Ni-Mo compounds from first-principles calculations." In *Scripta Mater*. 2005, vol. 2005, p. 17-20.
[5] Y. Zhou, et al. "Mechanistic study on nickel-molybdenum based electrocatalysts for the hydrogen evolution reaction." In *Journal of Catalysis* 388 (2020): 122-129.

 ISBN: 978-80-574-0039-4

Synthesis of Sulphur-Carbon Nanotubes Composite via Carbon Disulphide Solution for Li-S Batteries

D. Capková[a]*, T. Kazda[b], M. Almáši[c] and A. Straková Fedorková[a]

[a] Department of Physical Chemistry, Faculty of Sciences, Pavol Jozef Šafárik University in Košice, Moyzesova 11, 041 54, Košice, Slovak Republic
[b] Department of Electrical and Electronic Technology, Faculty of Electrical Engineering and Communication, Brno University of Technology, Technická 10, 616 00, Brno, Czech Republic
[c] Department of Inorganic Chemistry, Faculty of Sciences, Pavol Jozef Šafárik University in Košice, Moyzesova 11, 041 54, Košice, Slovak Republic
*dominika.capkova@upjs.sk

Demant for high energy density batteries are increasing and current used lithium-ion batteries do not meet the requirements for high energy density and specific capacity. Lithium-sulphur batteries may replace lithium-ion batteries in their applications, such as personal portable devices, electromobility or stationary energy storage systems due to high theoretical capacity. Though, lithium-sulphur batteries have some major drawbacks, that block commercialization. Porous, conductive materials and optimization of electrode material preparation can suppress shortcoming of lithium-sulphur batteries. Metal-organic framework in combination with carbon Super P and multiwall carbon nanotubes can effectively confine and capture sulphur. The initial discharge capacity of the S/MOF-76(Gd)/C-CS_2 electrode is 735 mAh g^{-1} with capacity retention of 107 % after 50 cycles.

Introduction

Particular attention is currently paid to batteries that have expected energy density values in the range of several watt-hours per kilogram. The theoretical specific energy density of 2600 Wh kg^{-1} is provided by lithium-sulphur (Li-S) batteries which are one of the alternatives to such battery cells. Moreover, sulphur is abundant element, environmentally benign and the theoretical capacity of Li-S battery is 1675 mAh g^{-1} [1].

Despite several advantages of Li-S batteries, there are several shortcomings that prevent them from reaching the market. The major issues are volumetric expansion of sulphur during cycling at approximately 80 %, insulating character of sulphur and the polysulphide shuttle. Process of discharging starts with reaction of sulphur cyklo-S_8 with lithium ions. The intermediates products are divided to higher (Li_2S_8, Li_2S_6, Li_2S_4) and lower polysulphides (Li_2S_2, Li_2S). Higher polysulphides participate in shuttle effect, they are soluble in the electrolyte which leads to loss of active material from cathode [2, 3].

To solve these issues, various conducting and porous matrix, such as carbon nanotubes (CNTs) [4], amorphous carbon [5] or metal-organic framework (MOF) [6]. Porous carbon materials can effectively trap and confine polysulphides to prevent shuttle effect or decrease the influence of volumetric expansion. Furthermore, ultrasonication in solvents can improve homogenization and aggregate-free dispersions [7].

Herein, we propose the application of combination of MOF-76(Gd), carbon Super P and multiwall carbon nanotubes (MWCNTs) saturated by sulphur from solution of carbon disulphide (CS_2) and homogenized by ultrasonication as a cathode material in Li-S batteries.

Experimental

Sulphur was dissolved in a 10 wt.% solution of carbon disulphide (CS_2) and MWCNTs were added during mixing. Prepared solution was placed into ultrasonic bath for 15 min. While stirring at 60 °C, CS_2 was evaporated. Mixture of sulphur and MWCNTs, MOF-76(Gd) and carbon Super P were milled together in mortar (final electrode was denoted as S/MOF-76(Gd)/C-CS_2). Comparative sample was prepared by milling of sulphur, MOF-76(Gd), Super P and MWCNTs (electrode was marked as S/MOF-76(Gd)/C). The mass ratio of prepared electrode samples was 60:15:15:10:10 for sulphur, MOF-76(Gd), Super P, MWCNTs and binder polyvinylidene fluoride (PVDF). Firstly, PVDF was dissolved in N-metyl-2-pyrolidone (NMP) and then the electrode material was added to prepare slurry. The electrode slurry after homogenization for 24 h was coated on aluminium current collector with surface carbon modification and dried in the oven at 60 °C for 24 h. Cut-out electrodes with diameter of 18 mm were pressed using a pressure of 315 kg cm^{-2}. Resulting mass of sulphur in the electrodes was controlled around 2 mg cm^{-2}.

 ISBN: 978-80-574-0039-4

Electrochemical testing of prepared electrode materials was performed in test cells (El-Cell®). The assmebly of cell was done in argone-filled glove box (Jacomex). The electrolyte composition was as follows: 0.25 M of lithium nitrate ($LiNO_3$) + 0.7 M of lithium bis(trifluoromethanesulfonyl) imide (LiTFSI) solution in 1,2-dimethoxyethane (DME) and 1,3-dioxolane (DOL) with the volume ratio 2:1. Metal lithium was used as a counter electrode, and the glass fibre separator was placed between the electrodes a saturated by the electrolyte.
Comparision of cyclic voltammograms of the S/MOF-76(Gd)/C and S/MOF-76(Gd)/C-CS_2 electrodes is shown in Figure 1. Oxidation and reduction peaks are clearly visible for both electrodes. First cathodic peaks are at 2.35 V and second cathodic peaks can be observed around 2.0 V. Positions of this peaks related to the reduction of the elemental sulfur to higher polysulfides and then their reduction to lower polysulfides in both electrodes. The S/MOF-76(Gd)/C-CS_2 electrode reach higher current densities than S/MOF-76(Gd)/C electrode.

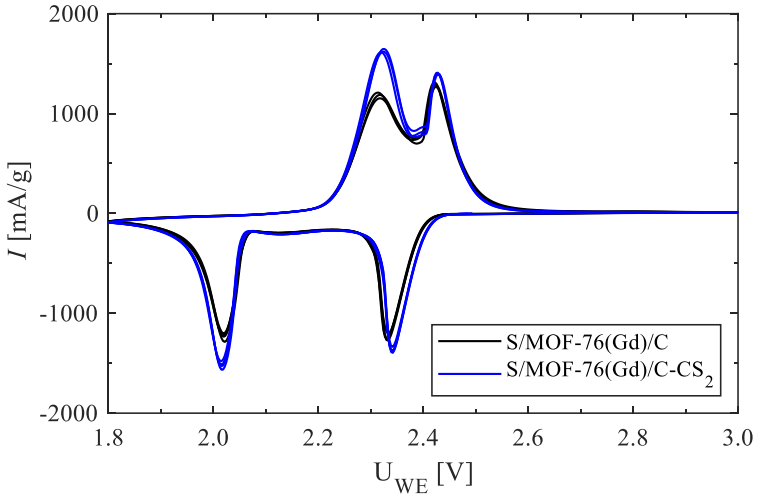

Fig. 1 Comparison of cyclic voltammograms of the electrodes S/MOF-76(Gd)/C and S/MOF-76(Gd)/C-CS_2

Galvanostatic cycling of the S/MOF-76(Gd)/C and S/MOF-76(Gd)/C-CS_2 electrodes id depicted in Figure 2. The initial discharge capacity of the S/MOF-76(Gd)/C-CS_2 electrode is 735 mAh g^{-1} and after 50 cycles the capacity retention is 107 %. In comparison, the initial discharge capacity of the S/MOF-76(Gd)/C electrode is 646 mAh g^{-1} with capacity retention of 106 % in fiftieth cycle.

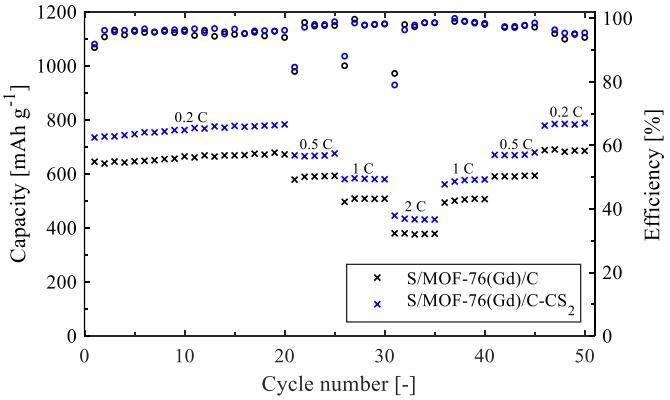

Fig. 2 Galvanostatic cycling of the S/MOF-76(Gd)/C and S/MOF-76(Gd)/C-CS_2 electrodes despite various current densities

ISBN: 978-80-574-0039-4

Conclusions

Fabrication of electrode material with MOF-76(Gd), carbon Super P and MWCNTs was demonstrated. Prepared electrode materials were tested as cathodes in Li-S batteries. The S/MOF-76(Gd)/C-CS_2 electrode obtained higher discharge capacities at all current densities compared to S/MOF-76(Gd)/C electrode. The initial discharge capacity of the S/MOF-76(Gd)/C-CS_2 electrode was 735 mAh g^{-1} compared to 646 mAh g^{-1} for the S/MOF-76(Gd)/C electrode. It can be concluded, that both materials with MOF-76(Gd) can be used in Li-S batteries, but the S/MOF-76(Gd)/C-CS_2 electrode reaches higher capacities with stable cycle performance.

Acknowledgements

This research was sponsored by the following projects: APVV-20-0138, Development of Novel 3D Materials for Post Lithium Ion Batteries with High Energy Density; APVV-20-0111, Towards Lithium Based Batteries with Improved Lifetime; iCoTS No. 313011V334, Innovative Solutions for Propulsion, Power and Safety Components of Transport Vehicles; vvgs-pf-2021-1756, Development of Electrode Materials for Lithium-sulfur Batteries; VEGA 1/0074/17, Nanomaterials and Nanostructured Layers with Specific Functionality, VEGA 1/0294/22, Porous Coordination Polymers for Environmental Applications, and specific graduate research of the Brno University of Technology No. FEKT-S-20-6206.

References

[1] J. B. Robinson, et al., "2021 Roadmap on Lithium Sulfur Batteries", *Journal of Physics: Energy,* 3 (2021) 031501.

[2] T. Kazda, et al., "Carrageenan as an Ecological Alternative of Polyvinylidene Difluoride Binder for Li-S Batteries", *Materials*, 14 (2021) 5578.

[3] S. Li, et al., "Inhibition of polysulfide shuttle in Li–S batteries: Modified separators and solid-state electrolytes", *Adv. Energy Mater.*, 11 (2021) 2000779.

[4] J. Xu, et al., "Progress in Mechanistic Understanding and Characterization Techniques of Li-S batteries", *Adv. Energy Mater*., 5 (2015) 1500408.

[5] D. Capková, et al., "Carbon Materials as the Matrices for Sulfur in Li-S Batteries", *ECS Trans,* 95 (2019) 19-26.

[6] D. Capková, et al., "Metal-Organic Framework MIL-101(Fe)-NH_2 as an Efficient Host for Sulphur Storage in Long-Cycle Li-S Batteries, *Electrochim. Acta*, 354 (2020) 136640.

[7] L. Qiang, et al., "A Simple Synthesis of Hollow Carbon Nanofiber-Sulfur Composite via Mixed-Solvent Process for Lithium–Sulfur Batteries", *J. Power Sources*, 256 (2014) 137-144.

 ISBN: 978-80-574-0039-4

Carbon fibres doped with transition metal phosphide nanoparticles as efficient hydrogen evolution reaction catalysts

A. Gubóová [a]*, R. Oriňaková[a], M. Strečková[b], O.Petruš[b]

[a] Department of Physical Chemistry, Faculty of Science, P.J. Šafarik University in Košice, Moyzesova 11, 041 54, Košice
[b] Institute of Materials Research, Slovak Academy of Sciences, Watsonova 47, 040 01 Košice
* alexandra.guboova@student.upjs.sk

To accelerate the kinetics of water splitting, efficient catalysts for hydrogen evolution reaction are continuously pursued. Great efforts have been made to enhance the catalytic activity of hydrogen evolution reaction (HER) catalysts to minimize energy consumption in electrochemical water splitting [1]. Traditional ways to improve the electrochemical kinetics for the HER catalysts focus on surface modification, which has meet the demanding requirements for practical water electrolysis.
Due to their low production cost, metalloid property, and good electrical conductivity as well as high activity and good stability in all environments, transition metal phosphides (TMP) incorporated in carbon porous fibers are considered to be promising catalysts for the hydrogen evolution. [2].

Carbon fibers doped with nanoparticles of transition metal phosphides were prepared by well-known needle-less electrospinning. However, innovative method of sintering these samples between two plates into a layer as thin as a few hundred micrometers was employed. This approach allows direct incorporation of catalyst fibers into electrolyzers.
The samples were electrochemically characterized in an acidic and an alkaline environment in a three-electrode system connected to a potentiostat. The fibers in the form of a layer were connected as a working electrode.
The significant potential shift to more positive values was observed for fibers doped with transition metals in comparison with bare carbon fibers. Moreover, samples doped with nickel/cobalt phosphide nanoparticles in acidic media demonstrated higher activity than iron/cobalt phosphide nanoparticle samples which may be caused by poor behavior of iron in acids. However, in an alkaline media their roles were reversed, indicating better catalytic performance of FeNiP in non-acidic environment.

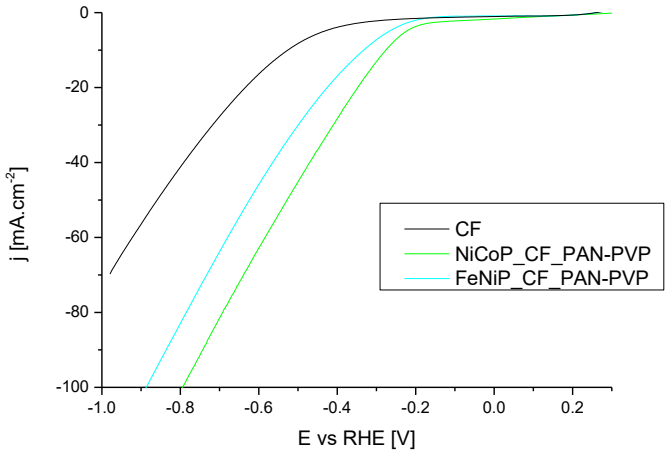

Fig. 4 Polarization curves measured in 0.5 M H_2SO_4 for samples NiCoP_CF_PAN-PVP, FeCoP_CF_PAN-PVP and bare carbon fibers CF for comparison

 ISBN: 978-80-574-0039-4

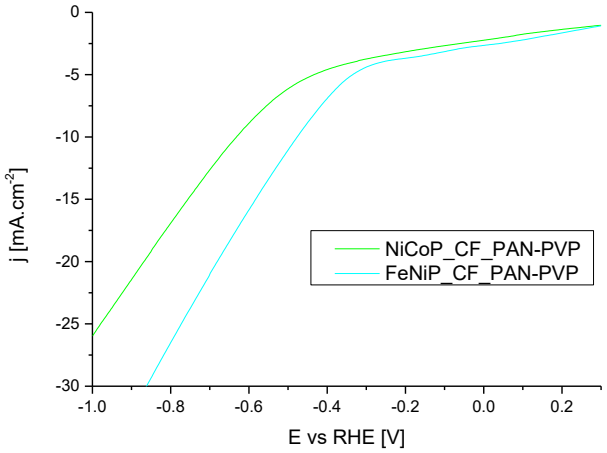

Fig. 5 Polarization curves measured in 0.1 M KOH for samples NiCoP_CF_PAN-PVP, FeCoP_CF_PAN-PVP

Acknowledgements
This work was supported by Grant Agency of Slovak Academy of Sciences, project no. VEGA 1/0095/21 and Slovak Research and Development Agency under the contract no. APVV-20-0299.

References
[1] Liu, G., Bai, H., Ji, Y., Wang, L., Wen, Y., Lin, H., … Peng, H. (2019). *Highly efficient alkaline HER Co-Mo bimetallic carbide catalyst with optimized Mo d-orbital electronic state. Journal of Materials Chemistry A.* doi:10.1039/c9ta02886b
[2] Li, Z., Niu, W., Yang, Z., Kara, A., Wang, Q., Wang, M., … Yang, Y. (2020). *Boosting Alkaline Hydrogen Evolution: Dominating Role of Interior Modification in Surface Electrocatalysis. Energy & Environmental Science.* doi:10.1039/d0ee01750g

 ISBN: 978-80-574-0039-4

Extraction efficiency of different solvents for $LiFePO_4$ type of cathode material

P. Guricová[a], T. Kazda[a]

[a] Department of Electrical and Electronic Technology, Faculty of Electrical Engineering and Communication, BUT, Technická 10, 616 00 Brno, Czech Republic

Abstract

This article focuses on separation of the commercial battery UR18650 with $LiFePO_4$ cathode chemistry. Recycling techniques are described with the emphasis on direct recycling. Disassembly of the $LiFePO_4$ cell is performed with the aim of extracting the cathode material. Two groups of solvents, conventional and ecological variants are compared. Separation efficiency of each of six different types of solvents is discussed.

Introduction

Lithium-ion batteries (LIBs) are increasingly used in all sorts of application nowadays (electronics, electric vehicles, power backups, energy storage systems, ect.). Lithium iron phosphate ($LiFePO_4$) was firstly synthesized in 1996 [1] and has a structure of olivine. Main advantage of this cathode material is high theoretical capacity (170 mAh/g). Thanks to the olivine structure, Li^+ ions can easy intercalate and deintercalate through the structure, and the cell have better stability at higher loads. Disadvantage of this type of cathode material is low potential against Li and from it resulting lower gravimetric energy density [2].

Recently, there has been accumulation of end-of-life LIBs due to their high rise in production. If the batteries are not going to be used in some secondary application, they can be recycled. The need for strategic recycling approach of these types of cells is desired from environmental and economic point of view. There are three main technologies used nowadays: pyrometallurgy, hydrometallurgy and direct recycling. First two methods are not originally designed to recycle LIBs and they are causing concerns because of their damage to the environment (high emissions of CO_2, production of toxic gases, etc.). Another disadvantage is that most of the valuable materials are lost during the process of recycling. To overcome this problem direct recycling has been developed to directly regenerate the battery material. Although it is possible to recycle almost all parts of the battery, cathode is the one on which the most attention is paid to [3, 4].

For the direct recycling technique of LIBs, it crucial to extract the cathode mass from the battery the most efficient and fastest way possible. One of the approaches on how to separate cathode material is to use some sort of solvent, which causes dissolving of the binder, mostly polyvinylidenfluorid (PVDF). Main advantage of direct recycling is lesser steps and high theoretical recycling efficiency (more than 80%) [5]. Cathode substance after separation needs only little adjustments, for example relithiation, and after this treatment is ready to be used in another application. This means simplification of overall process and lower impact on environment in comparison to conventional pyrometallurgical and hydrometallurgical processes.

Experimental

Battery UR18650 (1 400 mAh) with $LiFePO_4$ cathode chemistry was used in this work. As it was new commercial cell, it needed to be aged by cycling so that we can get cathode material with similar damage in the structure, as it is in the cells that are ready to be recycled (less than 50% of the original capacity). Firstly, the battery was characterised by rate capability test, using range from 0.1-1C rates. Followed by galvanostatic cycling, which was set to 500 cycles with 1C rate, to simulate the process of how the battery works in normal use. After cycling, another rate capability test was made.

Afterwards, battery was discharged and disassembled. Because the electrolyte largely evaporates after disassembly of the battery, it was necessary to do all the work in a fume hood. Electrolyte was present at quite large amount and was leaking from the electrodes, even causing several flares of fire. After removing the metal cover, it was possible to unroll the individual layers of the cathode, anode and separator. On both cathode and anode were visible damage in some areas, the material has fallen of some regions. The cathode was taken for the further experiment.

 ISBN: 978-80-574-0039-4

Efficiency of the solvents

As the first solvents for these experiments, group of three commercially used organic solvents were picked: N-methylpyrrolidon (NMP), dimethylformamid (DMF), Dimethylacetamide (DMAC). These are reliably good solvents, but they are toxic, carcinogenic and mutagenic so it is demanding to find alteration. Dimethylsulfoxide (DMSO) is the first from the second category, which serves as another option for the solvents mentioned above. It is relatively non toxic and the price is lower than for NMP. Last one picked was ethyl acetate and Cyrene. Most interesting and most ecologic in this case is dihydrolevoglucosenone, mostly known as Cyrene, which is cellulose-derived solvent, and can be recycled itself after use.

Samples 4x3 cm were immersed in the 60 ml of solvents. The experiment was perfomed at room temperature and possible changes were checked after every couple of hours. Photos of the samples after the extraction are shown in Fig. 6.

1. hour

Most of the solvents, NMP, DMF, DMAC and DMSO, showed similar behaviour and effective and fast results. At room temperature after approximately 30 minutes, it was possible to see waviness on the surface of the samples. After removal of the sample from the solution, mass was easily detached from metal collector. In most cases, 1 hour was sufficient enough to separate all of cathode material. For DMSO and DMF, it was needed to left the samples in the solution for longer time.

Ethyl acetate was quickly evaporating from the sample surface, but the layer was breaking and little pieces were peeling off, mostly from the edges. With Cyrene it was possible to see reddish colour of the solvent after couple of minutes, which indicated that the matter was dissolving. Afterwards however, it was not possible to scrape it off even with scalpel.

2. hour

By the DMF, DMSO and ethyl acetate it was possible to remove left bits and get separated aluminium collector and cathode material. At Cyrene, the cathode slowly started to set off.

10. hour

Only Cyrene left in the experiment, after 5 hours in the solution most of the material went off, to completely isolate the substance it took 10 hour in total. After the experiment at room temperature was successful for most of the solvents, only Cyrene was taken for the attempt with higher temperature. At 50°C of the solvent however, there were not significant changes, and the process was predominantly similar to that at room temperature.

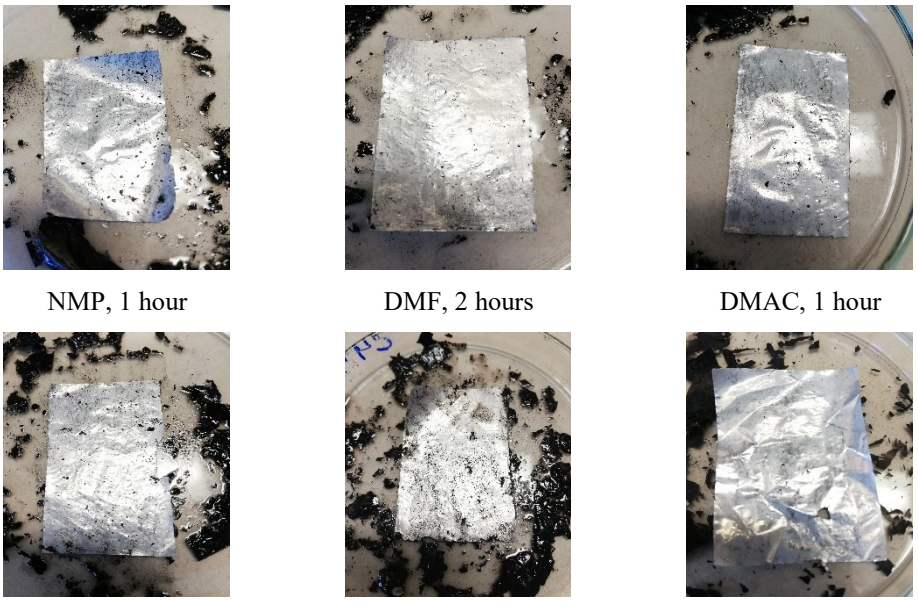

NMP, 1 hour | DMF, 2 hours | DMAC, 1 hour

DMSO, 2 hours | Cyrene, 10 hours | Ethyl acetate, 2 hours

Fig. 6 Samples shown after extraction, best result for each solvent is shown (room temperature)

ISBN: 978-80-574-0039-4

Conclusion

Extraction of material from positive electrode from UR18650 $LiFePO_4$ cell was performed. Cathode material was fully extracted using six different solvents. From the energetic point of view, it was possible to gain good results for of all the solvent with just room temperature. This would reduce overall energetic and economic cost of the recycling process, as the need for energy consumption for heating is eliminated. As expected, strong organic solvents, e.g. NMP, are effective and fast at dissolving the PVDF binder. It was shown that toxic organic solvents can be in the case of $LiFePO_4$ replaced by other alternatives. Significant results were achieved even at room temperature using ecologic Cyrene and ethyl acetate. Separation of the material can depend on used binder but also at pressure that is used when manufacturing the electrodes.

Acknowledgements

This work was supported by the specific graduate research of the Brno University of Technology No. FEKT-S-20-6206 and by grant CEITEC VUT-K-21-6938.

References

1 Forte, F., et al. "Lithium Iron Phosphate Batteries Recycling: An Assessment of Current Status." *Critical Reviews in Environmental Science and Technology* 51.19 (2021): 2232-59. Print.
2 Kazda, Tomáš. "Modifikace Materiálů Pro Kladné Elektrody Lithno-Iontových Akumulátorů." Brno University of Technology, 2015. Print.
3 Li, X. L., et al. "Direct Regeneration of Recycled Cathode Material Mixture from Scrapped Lifepo4 Batteries." *Journal of Power Sources* 345 (2017): 78-84. Print.
4 Padhi, A. K., K. S. Nanjundaswamy, and J. B. Goodenough. "Phospho-Olivines as Positive-Electrode Materials for Rechargeable Lithium Batteries." *Journal of the Electrochemical Society* 144.4 (1997): 1188-94. Print.
5 Song, X., et al. "Direct Regeneration of Cathode Materials from Spent Lithium Iron Phosphate Batteries Using a Solid Phase Sintering Method." *Rsc Advances* 7.8 (2017): 4783-90. Print.

 ISBN: 978-80-574-0039-4

Organic Cellulose-Based Binder for Lithium-Sulfur Batteries

K. Jasso[a]*, T. Kazda[a], P. Cudek[a]

[a] Department of Electrical and Electronic Technology, Brno University of Technology, Technicka 10, 616 00 Brno, Czech Republic
*kamil.jasso@vut.cz

Abstract
With the advancement of mobile technology, there has been an increase in the demand for batteries capable of meeting the requirements for high-energy power sources and low-cost. Although, lithium-ion batteries are constantly improving, they are struggling to meet these requirements as they are approaching to their technological and electrochemical limits. Due to their high theoretical energy density and potentially low cost, lithium-sulfur batteries are a promising successor to current lithium-ion batteries in many areas. Unfortunately, some shortcomings in lithium-sulfur battery technology must be addressed before it can be deployed in the commercial sector. Some of the shortcomings could be solved or at least supressed by binder. Due to environmental concerns, research is mostly focused on non-toxic binders, especially water-soluble binders used in food and cosmetics industry are of particular interest. The aim of this paper is to investigate the possibility of using the organic binder carboxymethyl cellulose in lithium-sulfur batteries.

Introduction
Lithium-sulfur batteries (Li-S batteries or LSBs) have a potential to overcome the limits of current Lithium-ion (Li-ion) technology and meet the demand for high energy density and low-cost energy sources. Li-S batteries are promising successor mainly due to the high theoretical energy density (2600 Wh kg^{-1}), high availability and low-cost, resulting from the use of sulfur as the cathode material. However, before they can be deployed in commercial production, several problems associated with the use of a combination of sulfur and lithium metal still need to be resolved. The most significant negative effects include low conductivity of sulfur and reaction products, lithium dendrite growth, sulfur volume changes, and the shuttle effect. The vast volume change during reversible conversion of sulfur species causes sulfur cathode cracking, pulverization, and structure collapse, which results in rapid capacity fading and short cycle life 0. Furthermore, the combination of weak electronic and ionic conductivity of the charge and discharge products with poor electrochemical reversibility of sulfur cause a relatively low rate capability of Li-S cell 0. To improve the weak electrical conductivity, conductive additives, most often carbon, are added to the positive electrode material, thus reducing the sulphur content in the positive electrode volume at the expense of the conductive element.

One possible way to prevent or at least suppress some of these drawbacks is to use special functional binders. Binders are an integral part of almost every battery electrode and greatly influence the resulting electrochemical parameters of the cell. Polymer binders play a critical role in maintaining the structural integrity and stability of the electrodes of lithium batteries. Binders serve two main purposes: (1) they establish a suitably close contact between active materials and conducting agent, (2) they ensure the electrode's mechanical integrity and strong adhesion to the current collector, and (3) they can possibly aid the chemical interactions 0. Their role is even more important in the case of lithium-sulfur batteries, which undergo large volume changes during cycling that cause mechanical stress in electrode material that can result in loss of contact between individual elements but also between the electrode material and current collector. Carefully chosen binder could potentially reduce or completely prevent these types of shortcomings. The structural integrity and mechanical qualities of the electrode are determined by the physical properties of the binder 0. Polymers with strong stickiness and elasticity are appropriate candidates for achieving these aims.
Carboxymethylcellulose (CMC) is cheap, nontoxic and biodegradable polymer. It is a anionic derivative of cellulose with carboxymethyl groups (-CH_2-COOH) commonly available with a degree of substitution (DS) in the range of 0.38-1.4. It is often used in the food, pharmaceutical and cosmetics industries as a viscosity modifier, stabilizer or thickener.

 ISBN: 978-80-574-0039-4

Experimental

Materials

The following materials were used to produce the positive electrode: Sulfur powder (Sigma-Aldrich, St. Louis, USA), Super P Carbon black (Timcal, Bodio, Switzerland) and CMC binder (CP Kelco, Atlanta, USA) in form of highly purified sodium carboxymethylcellulose. The electrolyte was prepared from 0,25M $LiNO_3$ and 0,7M LiTFSI lithium salts dissolved in a mix of DME and DOL (2:1) solvents (all Sigma-Aldrich, St. Louis, USA).

Electrode preparation

First, an electrode slurry was prepared from the materials using a classical method: dissolving the binder (10%wt.) in water with the help of a magnetic stirrer, followed by the addition of a conductive agent and an active material. Positive electrodes for LiS cells were prepared by applying the slurry to the aluminium current collector and allowing it to dry. One electrode sample before pressing was used for analysis under a scanning electron microscope (see Figure 1A), and the other was used in the assembly of the LiS cell, which was subjected to electrochemical analysis. Inspection of the electrode structure and electrochemical studies revealed that this method of manufacture was not suitable since the electrode components were not uniformly mixed. Therefore, a more precise preparation method was chosen and the amount of binder in electrode material was reduced to 7%wt. The electrode prepared in this way was again subjected to analyses, which showed a visible improvement in the structure (see Figure 1B) but also in the electrochemical properties of the electrode. Last, the electrodes were prepared by a fine-tuned method, with an even greater reduction in the amount of binder to 4% wt. (see Figure 1C).

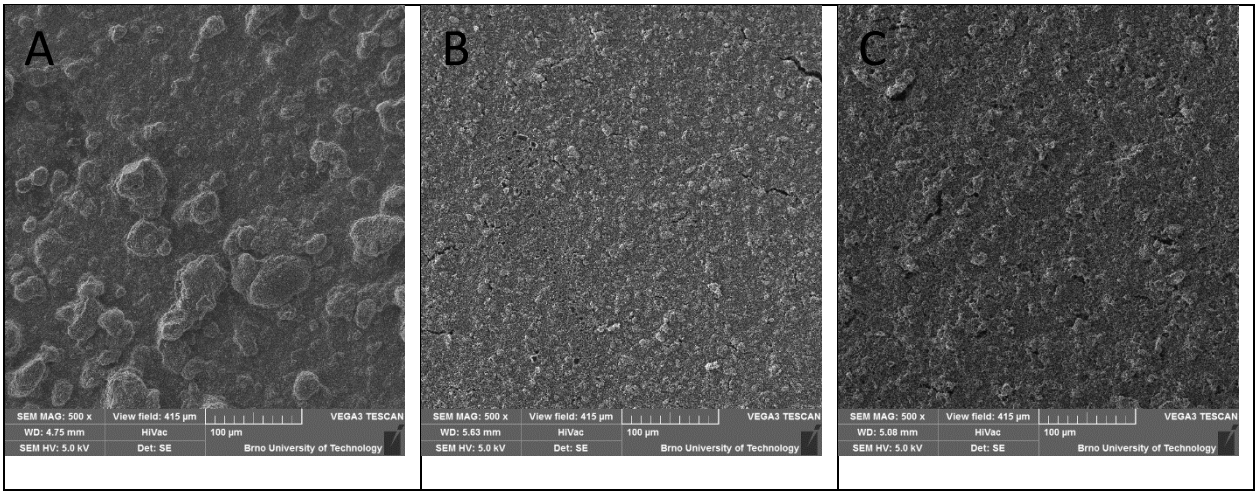

Fig. 7 Analysis of prepared electrodes under SEM: A) Classical preparation B) Modified preparation with less binder content C) Improved preparation with even less binder content

From the comparison of the structure of the prepared electrodes (Figure 1), it can be seen that a more porous electrode with a more uniform distribution of materials can be prepared with the aid of a modified more precise preparation method and a reduction in the binder content.

Electrochemical analysis

The remaining electrode samples were used in the assembly of LiS cells, which were subsequently subjected to electrochemical analyses. After initialization analyses, 50 cycles of galvanostatic cycling at variable loads (0.2C, 0.5C, 1C, 2C, 1C, 0.5C and again 0.2C) were performed (see Figure 2).

 ISBN: 978-80-574-0039-4

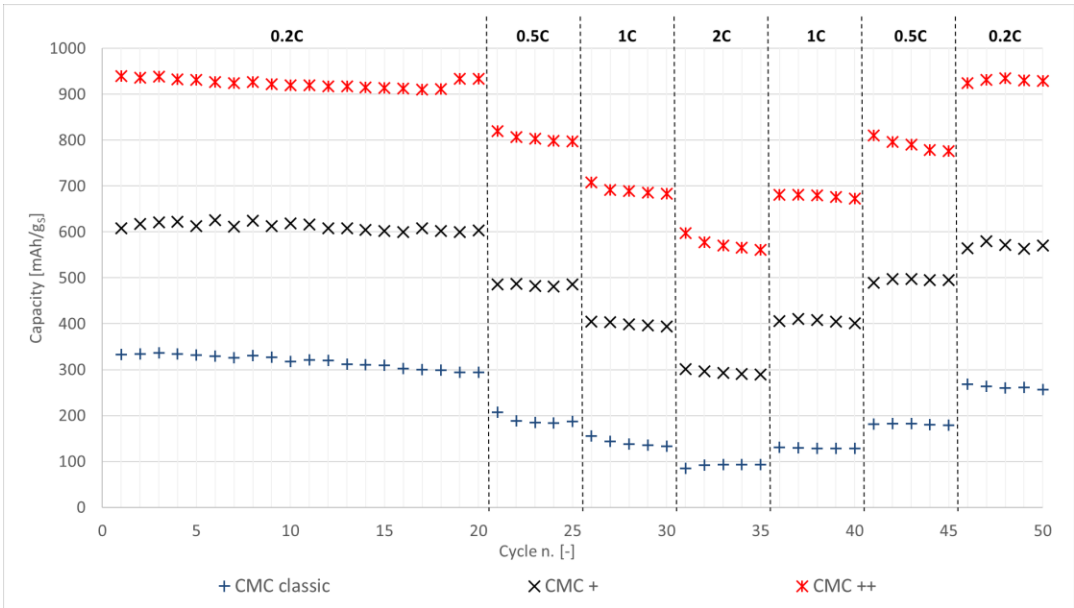

Fig. 8 Comparison of cell discharge capacities with respect to a positive electrode prepared by different preparation methods

From the galvanostatic cycling results, it is clear that the cell with the electrode prepared by the classical method of slurry preparation on a magnetic stirrer (CMC classic) is the worst off in terms of capacity values and stability, reaching the highest capacity equal to 336 mAh g^{-1} at 0.2C rate. The use of a more precise preparation method and a slight reduction in binder content resulted in better electrochemical properties of the LiS cell (CMC+). The LiS cell with the electrode prepared in this manner reached almost double the capacity at 0.2C rate at 626 mAh g^{-1}. After fine-tuning the electrode preparation method and reducing the binder content even further, a significant improvement in the electrochemical properties of the resulting LiS cell (CMC++) can be seen. The cell with such electrode showed the highest capacity values, at around 940 mAh g^{-1} at 0.2C rate, which is almost three times the capacity of the CMC classic. Furthermore, the capacity of this cell also shows the best recoverability to the original values at the end of cycling.

Conclusion

Since the classical slurry preparation method proved to be unsuitable for the CMC binder, the preparation method was modified during the experiment and the binder content was reduced. The measured results showed that the use of carboxymethyl cellulose as a binder for lithium-sulphur batteries is suitable, whereby it is possible to reduce the binder content and thus increase the energy density of the cell.

Acknowledgements

Authors gratefully acknowledge the financial support from the Ministry of Education, Youth and Sports of the Czech Republic under project No. LTT19001, BUT specific research programme (project No. FEKT-S-20-6206).

References

[1] H. Yuan et al., *Advanced Energy Materials*, 8 (2018).
[2] M. J. Lacey et al., *Journal of Power Sources*, 264, 8-14 (2014)
[3] Y. Li, Q. (R.) Zeng, I. R. Gentle, and D. -W. Wang, *Journal of Materials Chemistry* A, 5, 5460-5465 (2017)

 ISBN: 978-80-574-0039-4

Novel electrode materials for Li-S Batteries

J. Macko[a]*, D. Capková[a], A. Straková Fedorková[a], R. Oriňaková[a], A. Oriňák[a].

[a] Department of Physical Chemistry, Institute of Chemistry, Pavol Jozef Šafárik University in Košice, Moyzesova 11, 041 54 Košice
*jan.macko@upjs.sk

Lithium-sulfur (Li-S) batteries attract increasing attention because of their high energy density up to ~2600 Wh kg^{-1} [1]. They are inexpensive, environmentally friendly, and sulfur is naturally abundant in the environment [2]. There is an increasing demand for energy storage in modern applications, such as electromobility, or stationary energy storage systems for renewable energy sources [3]. However, sulfur cathodes suffer from several scientific and technical issues which are related to polysulfide ion migration. The polysulfide shuttle effect occurs during the charging and discharging of the Li-S battery. In the initial state, cyclo-S_8 is reduced during discharging to higher lithium polysulfides (Li_2S_8, Li_2S_6, Li_2S_4) between 2.4 and 2.1 V vs. Li and then, between 2.1 and 1.7 V vs. Li, lower lithium polysulfides (Li_2S_2, Li_2S) are formed (Fig. 1.). Currently, several methods were developed to prevent the shuttle effect and decrease the influence of sulfur volumetric expansion. A widely used technique is polysulfide trapping by porous carbon materials, which can bind lithium polysulfides in its porous structure and subsequently increase the conductivity of the electrode structure [3]. Despite enormous developments accomplished in the Li-S battery, the commercialization of this battery still has a long way to go, relying on technological breakthroughs in solving the key issues such as low sulfur conductivity, volume changes, and shuttle effect. Recently, nanostructured carbons, such as meso/micro-porous carbons, hollow carbon spheres, graphene, carbon nanotubes, and nanofibers, have been proposed to host sulfur materials [2].

48

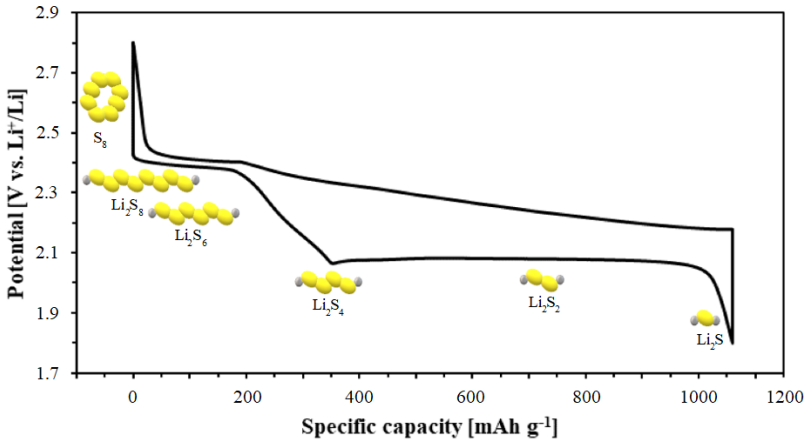

Fig. 1 Li-S Battery charge-discharge profile

Acknowledgements
This work has been supported by grants APVV-20-0138 by Slovak Research and Development Agency

References
[1] J.-Z. Wang, L. Lu, M. Choucair, J. A. Stride, X. Xu, H.-K. Liu, Journal of Power Sources. 196 (2011) 7030-7034.
[2] J. Pu, Z. Shen, J. Zheng, C. Zhu, Q. Zhou, H. Zhang, F. Pan, Nano Energy. 37 (2017) 7-14.
[3] T. Kazda, D. Capková, K. Jaššo, A. Straková Fedorková, E. Shembel, A. Markrvich, M. Sedlaříková, Materials. 14 (2021) 5578.

 ISBN: 978-80-574-0039-4

Use of recycled materials in Li-ion batteries

V. Niščáková[a]*, D. Capková[a], A. Straková Fedorková[a], S. Hatokova[b], M. Čigaš[b], Š. Hanigovský[b]

[a] Pavol Jozef Safarik University of Kosice, Department of Physical chemistry, Srobarova 2, 040 01, Kosice
[b] Fecupral, Jilemnickeho 3578/2, 080 01, Presov
*veronika.niscakova@student.upjs.sk

In this work, a positive electrode was prepared for a Li-ion battery having the following composition of 80% NMC (from recycled material); 10% amorphous carbon, and 10% PVDF (polyvinylidene fluoride as a binder). The prepared electrode was tested by various electrochemical procedures such as cyclic voltammetry, galvanostatic cycling. The cycling took place in the range of potentials from 3 V - 4, 2 V. The initial discharge capacity of the prepared electrode at 0.1 C was 134 mAh/g. Material from recycled batteries will be used as active material. Despite not the best results, such recycled materials will be usable in the future, as recycling processes are only being set up at this time and greater purity of materials is expected.

Introduction

Lithium-ion batteries are a power source for numerous common electronic devices such as mobile phones, laptops, cameras, and are also widely used nowadays as a power source in electric vehicles such as automobiles, buses, or scooters [1,2]. Such batteries are constantly evolving, studying their properties from a chemical, physical, structural, also the electrochemical point of view. The properties of cathode and anode materials are especially important, as they affect the overall performance of the battery [1,3]. Research within nanomaterials is on the rise, mainly since they improve cyclability compared to electrodes made from conventional larger particle sizes. The nanoparticles can quickly absorb and store vast amounts of lithium ions, without causing any deterioration in the electrode [3].

Experimental

Electrode material slurry was prepared by mixing 80 % NMC; 10 % amorphous carbon and 10 % PVDF in 2 ml NMP (N-methyl-2-pyrrolidone). After 24 h of stirring the slurry was coated on aluminum foil with a coating bar and dried in an air oven at 60 °C for 24 hours. The test cell was compiled in the glove box with an argon atmosphere. As counter electrode was used metal lithium and as the working electrode was used prepared cathode. The electrolyte was $LiPF_6$.

Results and discussion

Morphological characterization of the prepared electrode was investigated by scanning electron microscopy (SEM). The SEM image is shown in figure 1 with a view field of 415 μm. The electrode surface is full of grains that are homogenously dispersed through the electrode.

 ISBN: 978-80-574-0039-4

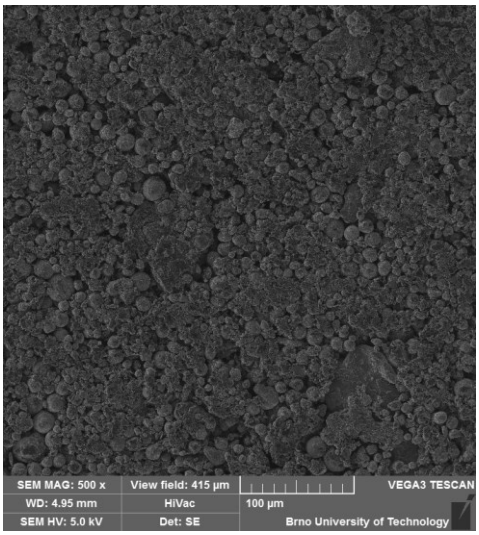

Fig. 1 SEM images of the prepared electrode, view field: 415 µm

The prepared electrode was investigated by cyclic voltammetry and galvanostatic cycling. CV curves were measured in the potential window from 1,5 V to 4,5 V at 0,1 mV/s and 5 mV/s at room temperature. The Li^+ insertion (cathodic peak) and extraction (anodic peak) occur at the potential of 3,8 V and 3,6 V. In voltammogram we can see a decrease of current with a gradual increase of cycles which causes a decrease in the activities of the cathode material. Galvanostatic charge and discharge curves in the potential window from 3 V to 4,2 V are in figure 2. The initial discharge capacity of the prepared electrode at 0.1 C was 134 mAh/g.

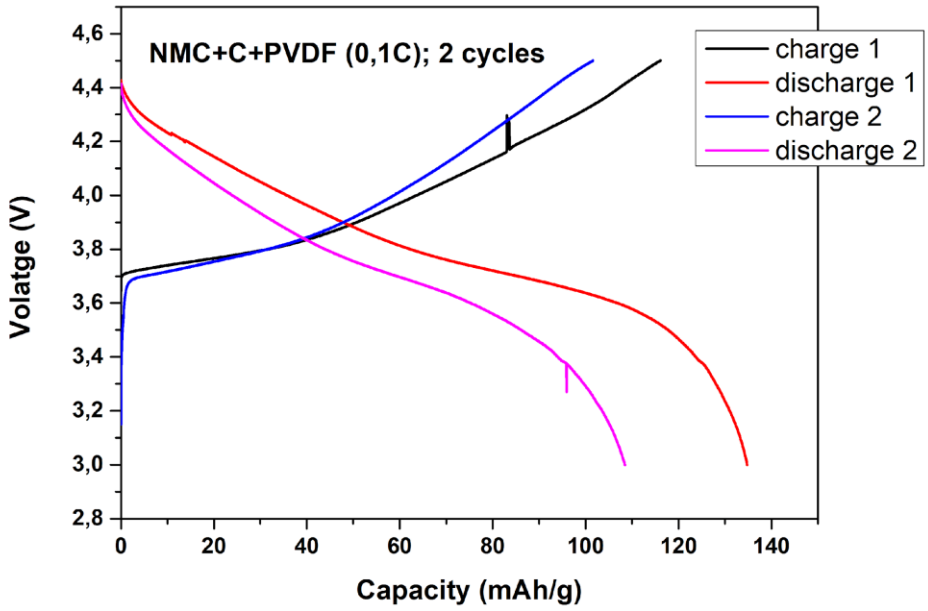

Fig. 2 Iniatial charge and discharge curves at 0.1C

ISBN: 978-80-574-0039-4

Conclusion

It was proven that recycling material (NMC) demonstrates some electrochemical activity. Due to the origin and nature of the material used, the results such as chemical composition, electrochemical characteristics and values of measured capacities are very good. Such recycled materials will be usable in the future, as recycling processes are only being set up at this time and greater purity of materials is expected.

Acknowledgments

This publication was supported by the Operational program Integrated Infrastructure within the project: Innovative Solutions for Propulsion, Power and Safety Components of Transport Vehicles, 313011V334, cofinanced by the European Regional Development Fund and of the Slovak Research and Development Agency APVV-20-0138 and APVV-20-0111.

References

[1] N. Li, C.R. Martin, B. Scrosati, Nanomaterial-based Li-ion battery electrodes, c (2001) 240–243.
[2] M. Jiang, Q. Zhang, X. Wu, Z. Chen, D.L. Danilov, R.A. Eichel, P.H.L. Notten, Synthesis of Ni-Rich Layered-Oxide Nanomaterials with Enhanced Li-Ion Diffusion Pathways as High-Rate Cathodes for Li-Ion Batteries, ACS Appl. Energy Mater. 3 (2020) 6583–6590. https://doi.org/10.1021/acsaem.0c00765.
[3] H.K. Liu, G.X. Wang, Z. Guo, J. Wang, K. Konstantinov, Nanomaterials for lithium-ion rechargeable batteries, J. Nanosci. Nanotechnol. 6 (2006) 1–15. https://doi.org/10.1166/jnn.2006.103.

 ISBN: 978-80-574-0039-4

Preparation and properties of epoxy composites with MXene and carbon nanotubes

Y. Soyka[a]*, M. Prochazka[a], M. Micusik[a], M. Omastova[a]

[a] Polymer Institute, Dubravska cesta 9, 845 41 Bratislava, Slovakia
*yaryna.soyka@savba.sk, maria.omastova@savba.sk

Introduction

MXenes are a large family of two dimensional (2D) materials with unique optoelectronic properties and tuneable surface termination. The physical and chemical properties of 2D nanoparticles can be efficiently tuned using various methods. These include control of their dimensions, crystallographic structure, reduction of structural defects, doping with heteroatoms, or chemical modification of their surface. Different MXenes are prepared from different MAX phases of the formula $M_{n+1}AX_n$ (n = 1–3), where M is the most common transition metal, A is an element of the 13 or 14 group of the periodic table of elements, X is usually C and/or N [1]. By etching of the A layers from MAX phase, MXene are formed. The surface of etched MXenes contains functional group e.g., -O, -F, -OH, leads negatively charged surface.

Carbon nanotubes (CNTs) were discovered in the 1990s. It is easy to describe carbon nanotubes as rolling one of the molecular layers of graphene — into a tube. Usually the ratio of length to diameter of CNT is about 1000 and more, so they can be considered as an almost one-dimensional structure [2].

Carbon nanotubes in polymer matrices have a great influence and electrical conductivity, shear strength and other transport properties, being hybrids of nanoscale fillers and additives and enabling obtaining "smart" materials, such as sensitive to pressure switch. Due to its excellent mechanical and physical properties, CNTs [2] have become one of the promising subordinates for the adaptation of the power structures of polymer-based nanocomposites. Low weight percentages of CNTs can significantly improve the conductive and mechanical properties of CNT-based composites. Allaui et al. [3] achieved significant improvement of mechanical power systems of epoxy composition reinforced with CNT. In his study, the Young's modulus and yield strength were doubled for a nanocomposite of 1 and 4 wt.% of multiwall CNTs, respectively, compared with pure epoxy matrix. Meguid and Sun [4] showed that a homogeneous dispersion of CNTs in an epoxy matrix can improve the tensile and shear strength of the obtained synthesized nanocomposite. However, at higher concentrations of CNTs, the mechanical properties of the nanocomposite deteriorate due to the formation of CNT agglomerates, which act as stress concentrators.

52

Previously the sandwich-like composites with CNT/MXenes have been investigated. It is noteworthy that a well-thought-out structure is of paramount importance in this process. For example, sandwich-like hybrids of graphene/carbon nanotube made by in situ growth methods show much better performance than those produced by direct mixing [5]. Influence of preparation methods on the electrical and nanomechanical properties of composites with CNT were studied [6]. Up to now, there is no literature data on epoxy-based composites with CNT and MXenes used as fillers. This topic is attractive for our research. Combination of 2D and 1D nanoparticles can increase conductivity of composites because of more conductive pathways are developed by combination of 1D particles and 2D nanostructures.

Experimental part

For preparation of composites, Ti_3C_2 type of MXenes was used. MXene layers were prepared by delamination of MXene paste prepared at Drexel University, USA. The composites with different concentration of nanofillers were prepared by solvent casting method. CHS-EPOXY 582, and Telalid 0402 hardener (Spolchemie, Czech Republic), and Nanocyl 7000 (NANOCYL, Belgium**)** have been used for experiment.

Firstly, epoxy/MXene and epoxy/CNT composites were prepared. MXenes were mixed with epoxy resin using mechanical stirrer. In the next step, epoxy/CNT/MXene composites were prepared. CNT were mixed with ethanol in ultrasonic bath. Then CNT were added to epoxy/MXenes dispersion and all compound were mixed together by magnetic stirrer. After that, the hardener was added and mixed for 15 min by hand and composites were poured into round shapes form. Composites were dried in the air overnight and then 4-6 h in vacuum oven at 60 °C. The conductivity of samples was measured by 4-point method.

 ISBN: 978-80-574-0039-4

Results and discussion

Conductivity of all samples was measured with 4-point-probe methods. Epoxy/MXene composites were not conductive, when MXene content was up to 2 wt.%. Conductivity of epoxy/1 wt.% CNT was 0.10 S/m and after month about 0.079 S/m. Epoxy/2%CNT on the second day after preparation showed conductivity 2.05 S/m and after 3 months –conductivity dropped to 0.36 S/m.

First results showed, that epoxy/CNT/MXene composites reached good conductivity, when using at least 1 wt.% of 1D and 2D filler. Changes of composites conductivity were monitored within 3 months. The conductivity of epoxy/1%CNT/2%MXene increased with time, from 1.69 S/m to 2.74 S/m and epoxy/2%CNT/2%MX – from 12.00 S/m to 13.18 S/m of staying at ambient condition. It means that samples were not oxidized in the air.

The combined composites epoxy/2%CNT/2%MXene were more conductive then the other samples, where only 1D or 2D nanofillers were used. All composites provide good flexible properties. This work will continue with increasing concentration of nanofillers in composites and study of their properties.

Composites based on MXenes can be used in energy storage as high-performance electrode materials for lithium-sulfur batteries, sodium-ion batteries and supercapacitors [7], or for strain sensing composite structures [8].

Acknowledgements

This work developed under the M-era.Net research project titled NANO2COM, the research was funded by grants No. M-ERANET-18-414-Nano2Com from Slovak Academy of Sciences, and by project VEGA 02/0010/18 (Slovakia).

References

[1] M. Naguib, M. Kurtoglu, V. Presser, J. Lu, J. Niu, M. Heon, L. Hultman, Y. Gogotsi, M. W. Barsoum, Adv. Mat. **23** (2011) 4248.
[2] S. Dinesh Kumar, M. Ravichandran, S.V. Alagarsamy, C. Chanakyan, M. Meignanamoorthy, S. Sakthivelu, Materials Today: Proceedings, **27** (2020) 1152-1156.
[3] A. Allaoui, S. Bai, H. M. Cheng, J. B. Bai, Compos. Sci. Technol. **62** (2002) 1993-1998.
[4] S. A. Meguid, Y. Sun, Mater. Des. **25** (2004) 289-296.
[5] M. Q. Zhao, C. E. Ren, Z. Ling, M. R. Lukatskaya, C. Zhang, K. L. Van Aken, Y. Gogotsi, Adv. Mat. **27** (2014) 339-345.
[6] K. Mosnáčková, Z. Špitálský, J. Kuliček, J. Prokeš, A. Skarmoutsou, C. A. Charitidis, M. Omastová, J. Appl. Polym. Sci. 132 (2015) Art. №. 41721.
[7] R. Kang, Z. Zhang, L. Guo, J. Cui, Y. Chen, X. Hou, J. Yu, Scientific Reports, **9** (2019) Art. №. 9135.
[8] G. Monastyreckis, A. Spepura, Y. Soyka, H. Maltanava, S. Poznyak, M. Omastová, A. Aniskevish, D. Zeleniakiene, Sensors, **21** (2021) Art. №. 2378,

 ISBN: 978-80-574-0039-4

Preparation and Characterization of Li-S Pouch Cells Using Composite Cathode Materials

Andrea Straková Fedorková[1*], Dominika Capková[1], Tomáš Kazda[2], Katarína Benková[1], Veronika Niščáková[1], Pedro Gómez-Romero[3], Elena Shembel[4], I. Šišoláková[a]

[1]Institute of Chemistry, Faculty of Science, P.J. Šafárik University, Moyzesova 11, SK-04154 Košice, Slovak Republic
[2]Department of Electrical and Electronic Technology, Faculty of Electrical Engineering and Communication, Brno University of Technology, Technicka 10, 616 00 Brno, Czech Republic
[3]Institut Català de Nanociència i Nanotecnologia, ICN2, CIN2 / Consejo Superior de Investigaciones Científicas (CSIC), Campus UAB, E-08193 Bellaterra, Barcelona, Spain
[4]Ukrainian State University of Chemical Technology, Dnipro, 49005, Ukraine

Abstract

Composite materials are an integral part of current secondary battery technologies, where typically thermal and electric pathways are provided by one material, mechanical integrity with another, and functional properties (storage of energy) by yet another one. Sulfur is a promising cathode material because of its high specific capacity and energy density [1-3]. Theoretically, for every gram of sulfur in the cathode, 433 mg of lithium is required for the reaction. Therefore, the theoretical gravimetric capacity of the lithium-sulfur battery with respect to the combined mass of sulfur and lithium is 1167 Ah/kg. With an average discharge voltage of approximately 2.2 V, the energy density of the battery is 2567 Wh/kg [4]. Present day lithium-sulfur batteries consist of solid-state sulfur composite cathodes, which incorporate a conductive carbon additive and an organic polymer binder (Fig 1).

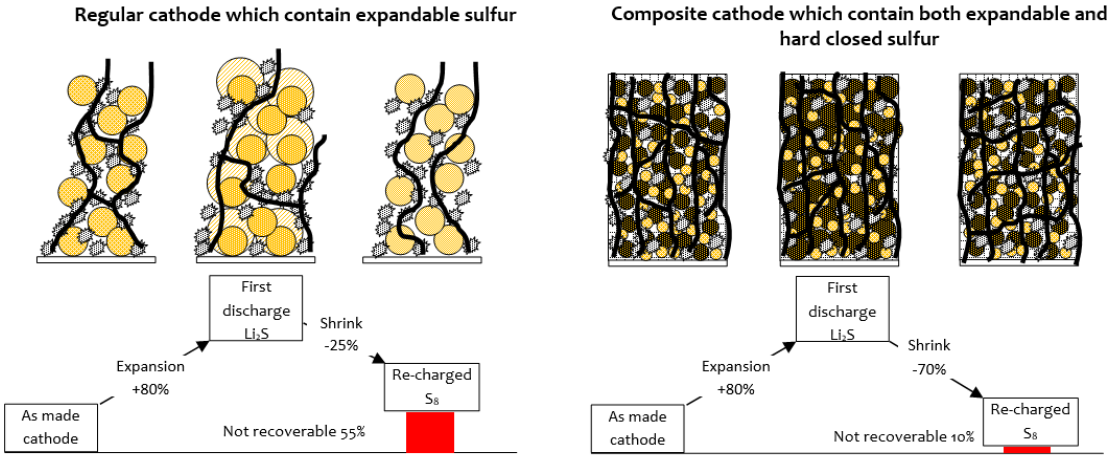

Fig. 1 Schematic presentation of new composite cathode materials based on sulfur

Our aim was to prepare new composite materials based on sulfur and conductive additive by different preparation techniques. Compatible electrolytes with improved fire safety or with addition of different fire retardants were also tested. Special attention is connected with using the nonflammable solid inorganic electrolytes, which allow to avoid the short circuit between the electrodes in the Li-S batteries during the cycling, and allow increase the operation range of the temperature without of the fire problems. This activity was based on the investigation the correlation between the nature and composition of the electrolyte, and parameters of the electrochemical processes during discharge/charge processes of the sulfur based cathodes and carbon or carbon-silicone anodes. Fabrication of

 ISBN: 978-80-574-0039-4

the final small Li cells with cathode based on the sulfur composite materials was important for evaluation of results from small cells. The energy density and cycle life of the resulting lithium-sulfur cells were significantly higher than the state-of-the-art commercially available cells increasing the viability of wide ranging environmental and technological goals of renewable storage and electro-mobility. Further to that, a thorough analysis of the whole value-chain, from sulphur cathode production, through composite carbon or carbon-silicone synthesis and optimisation to utilisation of the material in secondary batteries, was expected to result in a more sustainable battery technology and an increased understanding of the interdisciplinary area of composite materials for energy storage. Several samples with different composition were prepared and tested. The electrochemical properties of composites were investigated by cyclic voltammetry (CV), electrochemical impedance spectroscopy (EIS) and galvanostatic charge/discharge measurements. Structural, stability and safety tests were also performed. The best samples were chosen and tested in small laboratory prototypes (Fig. 1). Results obtained from electrochemical characterization of final prototypes showed improved stability, performance and sustained cycle stability and low decay rate after 200 cycles.

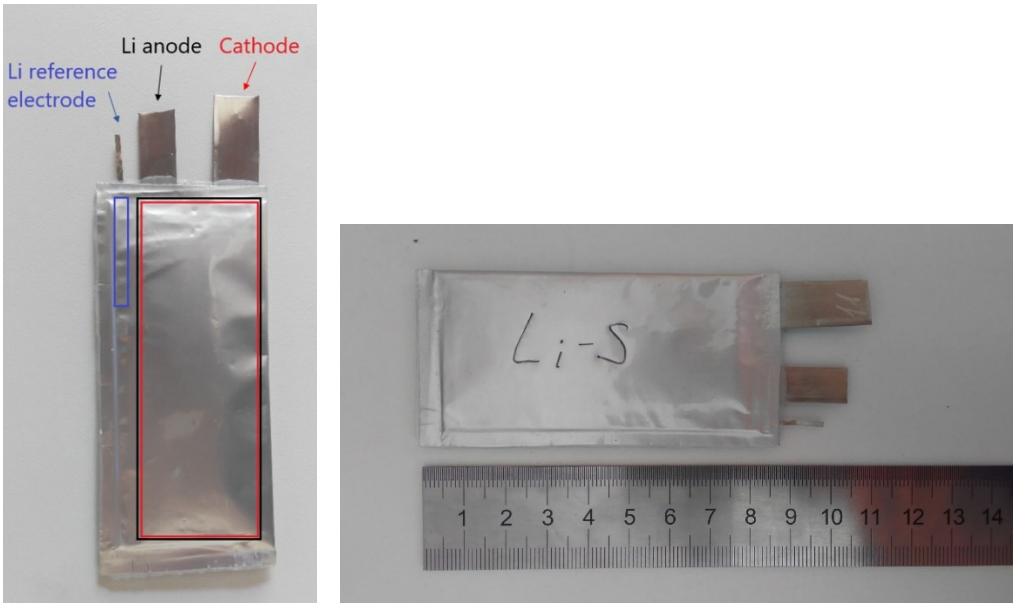

Fig. 2 Li-S laboratory pouch cell prototypes

Acknowledgement

This publication was supported by the Operational program Integrated Infrastructure within the project: Innovative Solutions for Propulsion, Power and Safety Components of Transport Vehicles, 313011V334, cofinanced by the European Regional Development Fund and of the Slovak Research and Development Agency APVV-20-0138 and APVV-20-0111.

References

[1] Kazda, T.; Capková, D.; Jaššo, K.; Fedorková Straková, A.; Shembel, E.; Markevich, A.; Sedlaříková, Materials (2021), 14, 5578.
[2] H. Kim, H.-D. Lim, J. Kim, K. Kang, J. Mater. Chem. A, 2 (2014), 33.
[3] P.G. Bruce, S.A. Freunberger, L.J. Hardwick, J.M. Tarascon, Nat. Mater., 11 (2012), 19.
[4] M.K. Song, Y.G. Zhang, E.J. Cairns, Nano Lett., 13 (2013), 5891.

 ISBN: 978-80-574-0039-4

Porous carbon fibers for HER

M. Strečková[a]*, O. Petruš[a]. A. Gubóová[b], C. Bera[a], R. Oriňaková[b]

[a] Institute of Materials Research, Slovak Academy of Sciences, Watsonova 47, 040 01 Kosice, Slovak Republic
[b] Institute of Chemistry, Faculty of Science, P.J. Safarik University, Moyzesova 11, 040 01 Kosice, Slovak Republic
*mstreckova@saske.sk

The high costs of coal and gas, together with negative impact of fossil fuels on the environment and human life, have led to increased interest in the use of renewable energy. Unfortunately, fossil fuels still cover almost 60% of global electricity supply, so water, wind and solar energy as alternative energy sources present new challenges in the field of safety of energy supply, independent distribution, production, storage and use of surplus energy. Hydrogen is considered a suitable energy carrier for the future due to its high energy density, high incidence and positive impact on the environment in terms of greenhouse gas emissions [1]. Electrolysis of water using a direct current derived from sustainable energy is highly eco-friendly method for production of hydrogen, as it uses renewable H_2O and produces only pure oxygen as a by-product. According to the experimentally measured electrochemical parameters of HER (exchange current density, overpotential, electron transfer kinetics, etc.) and DFT (density functional theory) calculated from the Gibbs free energy ΔG_H of the adsorbed atomic hydrogen, three most perspective alternatives for catalysts are: metals and alloys, transition metal compounds, and carbonaceous compounds.

According to the literature and authors` knowledge, three main factors affect the catalytic behavior of carbon fibers prepared by needle-less electrospinning: i. structure of CF [2] morphology and porosity of the fibers (size and diameters of CF, defect-less structure, distribution of incorporated nanoparticles, etc.); ii. modification of CF [1] – surface or interior modification by additional nanoparticles or additives (CNT growth on the surface, type of TMN, etc.); iii. final heat treatment, which can influence the building of the carbon matrix and affect the distribution of TMN and growth of CNTs [3].

Needle-less electrospinning (NLES) or electrospinning of free liquid surfaces can simultaneously generate a number of streams from the solution surface, which increases the amount of fibers prepared by an order of magnitude, thus significantly reducing the time required to produce fibers [4]. NLES is a promising technology for mass-scale production of nanofibers. Although there are some issues with the practical application, NLES is still the first choice for industrial production of nanofibers, considering its advantages and potential for continual improvement. Thanks to close collaboration between electrospinners, chemists, designers, machinery, electricians, and automation controls engineers, NLES will produce high-quality nanofibers in a well-controlled way at low cost, and be beneficial to our daily life, health care, and various industrial sectors [5].

This contributions dials with the investigation of the effect of polymer solution composition, heat treatment conditions on the morphology and electrocatalytic activity of CFs modified by cobalt phosphide nanoparticles (CoP, Co_2P) for HER. Polymeric fibers containing the source compounds for Co_2P nanoparticles formation have been produced by NLES. These compounds are represented by cobalt nitride and phosphoric acid. The further main step of modified carbon fibers preparation was sintering at 1200 °C in Ar atmosphere. The heat treatment process is responsible for carbon ladder matrix formation with incorporated Co_2P nanoparticles [6]. Cobalt phosphate nanoparticles have been incorporated into the carbon matrix in situ in the heat treatment process and act as the catalysts for CNT growth during sintering. The specific surface area of the fibers increased rapidly with increasing content of Co_2P nanoparticles in the carbon matrix. The usage of nitrate cobalt salts led to the formation of large quantities of multi-walled carbon nanotubes (MWCNTs) perpendicular to the carbon matrix (Fig.1a-f). The growth of CNT was performed according to the "Tip growth model" (Fig.2 a-f) [1]. No additional surface modification was necessary. The used sintering conditions had a great influence on the morphology, porosity, and growth of CNTs on the CF surface, which had a positive effect on the active surface area for HER. CNT growth was catalyzed by the presence of Co_2P nanoparticles. Fiber morphology and CNT growth were observed by SEM and TEM. The type of phosphides was determined by XRD and the amount of Co in the fibers was determined by atomic absorption spectroscopy (AAS). The electrocatalytic activity of fibers and the effect on hydrogen evolution were analyzed using linear sweep voltammetry and Tafel slopes.

 ISBN: 978-80-574-0039-4

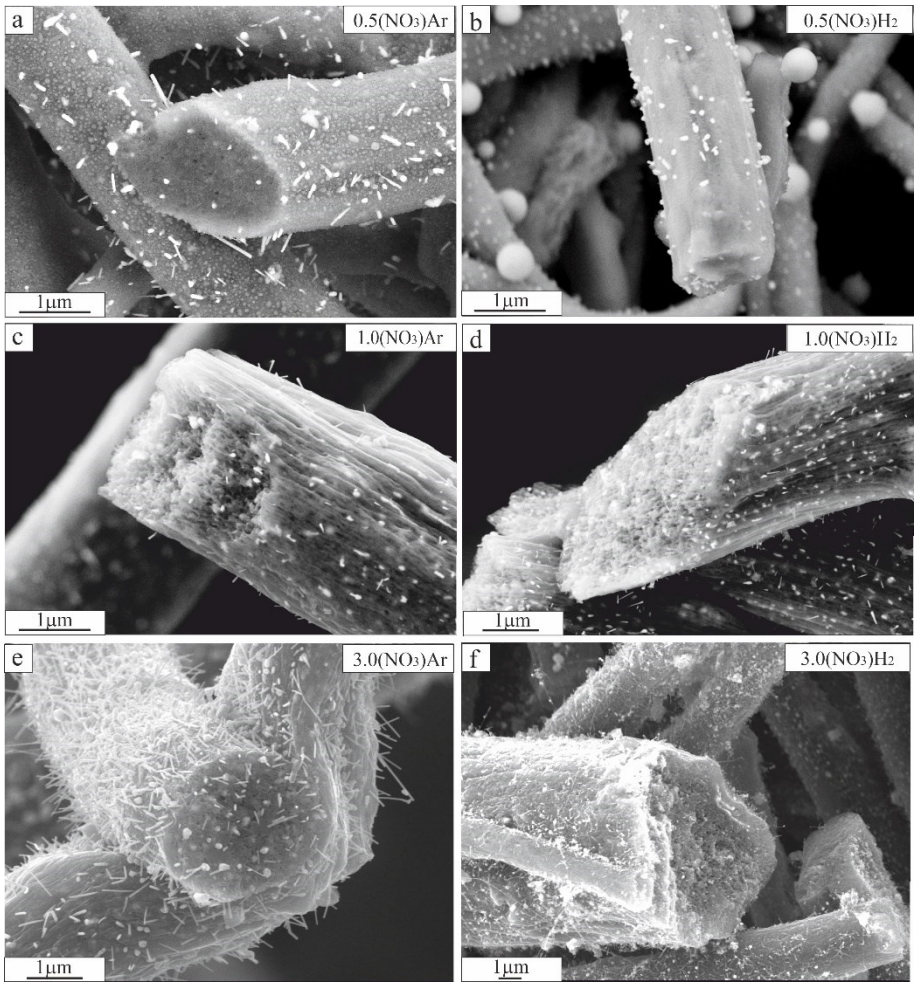

Fig. 1 SEM images of carbon fibers with incorporated Co_2P nanoparticles prepared from different amount of $Co(NO_3)_2$/30 ml DMF in spinned solution:
a) 0.5g/30 ml DMF carbonized in Ar, b) 0.5g/30 ml DMF carbonized in Ar/H_2
c) 1.0g /30 ml DMF carbonized in Ar, d) 1.0g/30 ml DMF carbonized in Ar/H_2
e) 3.0g/30 ml DMF carbonized in Ar, f) 3.0g/ 30 ml DMF carbonized in Ar/H_2

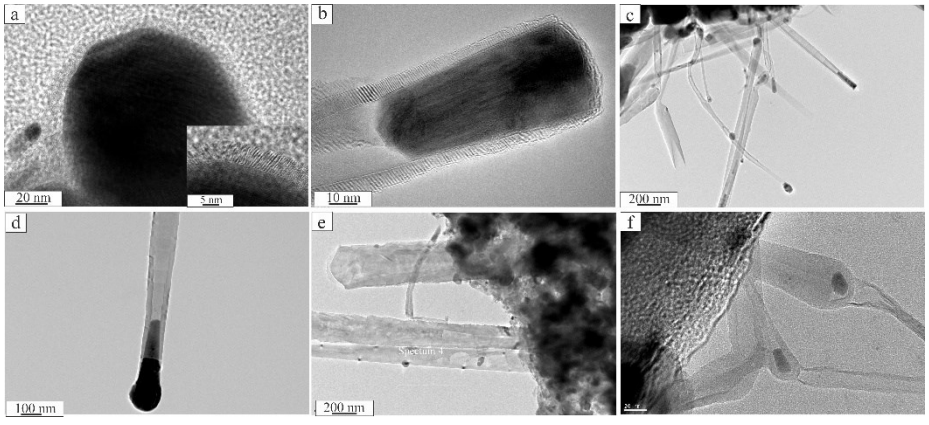

ISBN: 978-80-574-0039-4

Fig. 2 HRTEM of CNTs growth from fibrous carbon matrix initiated by Co_2P nanoparticles
a) Co_2P nanoparticle surrounded with multi-walled graphene shell,
b) the conical shape of Co_2P during growth of CNT, surrounded with multi-walled graphene shell
c) banboo-like nanotubes
d) Co_2P nanoparticle falling out from CNT
e) Finished growth of CNT, open-ended hollow CNT
f) secondary growth of carbon nanotubes

Acknowledgements

This work was supported by Slovak Research and Development Agency under the contract no. APVV 20-0229 and Grant Agency of Slovak Academy of Sciences, projects No. VEGA 2/0036/20, VEGA 1/0095/21.

References

[1] M. Streckova, R. Orinakova, J. Hovancova, M. Heckova, A. Guboova, V. Girman, E. Mudra, Z. Dankova, A. Bekenyiova, J. Dusza, Appl Surf Sci, **507** (2020) 144927.
[2] M. Heckova, M. Streckova, R. Orinakova, J. Hovancova, A. Guboova, T. Sopcak, A. Kovalcikova, B. Plesingerova, D. Medved, J. Szabo, J. Dusza, Appl Surf Sci **506** (2020) 144955.
[3] M. Streckova, E. Mudra, R. Orinakova, L. Markusova-Buckova, M. Sebek, A. Kovalcikova, T. Sopcak, V. Girman, Z. Dankova, M. Micusik, J. Dusza, Chem. Eng. J. **303** (2016) 167–181.
[4] H. Niu, H. Zhou, H. Wang, *Electrospinning: an advanced nanofiber production technology electrospinning: an advanced nanofiber production technology. In: Energy harvesting properties of electrospun nanofibers.* IOP Publishing chapter 1 (2019) 1-44.
[5] B. Ding, X. Wang, J. Yu, *Electrospinning, Nanofabrication and Applications* (2019) Elsevier.
[6] M. Streckova, R. Orinakova, E. Mudra, Z. Dankova, M. Sabalova, V. Girman A. Kovalcikova, J. Hovancova, M. Heckova, F. Kalavsky, J. Dusza, Energy Technol., 6 (2018) 1310 – 1331.

 ISBN: 978-80-574-0039-4

In-situ Studies of Lead Sulfate Crystal Growth on Negative Electrode for Lead Acid Batteries

L. Chladil[a]*, H. Hálová[a], J. Smejkal[a] and O. Čech[a]

[a] Brno University of Technology, Department of Electrical and Electronic Technology, Technická 10, 616 00, Brno, Czech Republic
*chladil@vut.cz

Introduction

The lead-acid battery is one of the oldest electrochemical systems used as chemical energy storage devices. Despite their many years of development, these energy sources are still the subject of research attempts and especially with regard to longevity in both partial and deep cycling. [1-2] Basically, we can distinguish between two different types of electrochemical storage systems - those that use insertion/intercalation mechanisms (charged and discharged state occurs by insertion or intercalation into the internal structure of the solid material) and those whose transition between charged and discharged state occurs through a soluble intermediate - i.e. precipitation systems.

First mentioned systems like Li-ion or Na-ion system suffers from slow degradation mechanisms wherein the original mass is gradually degraded either due to the dissolution of the active phase of the material, the formation of a secondary electrochemically inactive phase, or due to the loss of electrical or ionic contact of the active particles. In these systems the active materials exhibit the same structure or the phase transitions during cycling occur within the solid phase. The electrode porosity of such systems is generally set during the material synthesis process and then could be influenced by the slow Oswald ripening process (recrystallization) or by micropore generation (cracking) under high loads.

In the second type of system, referred to as dissolution/precipitation systems, there is a massive transformation of the active mass in each cycle. These systems include, for example, the negative mass of Ni-Zn batteries, metal Li electrode, the positive electrode of Li-Sulfur batteries, or also the above-mentioned negative electrode of lead-acid batteries. These systems inherently must go through massive recrystallization processes during each cycle and therefore this process needs to be carefully controlled and not eliminated for a good long-term lifespan.

The negative electrode of lead acid batteries passes from metallic lead in a charged state to lead-sulfate in a discharged state. Under normal conditions, reversible sulfation occurs in the lead-acid battery - the formed lead sulfate crystals easily decompose into the metallic lead sponge and sulfuric acid ions during charging. [3] In case of prolonged standing of the battery in a partially charged state, the crystals cannot disintegrate sufficiently during subsequent charging, and thus lead sulfate is preferentially deposited on the previously formed crystals. The resulting presence of large crystals can clog the pores in the active materials then and thus reduces the effective area of the electrodes - gradually reducing both the battery capacity and increasing the internal resistance and stress on the cells [4] [5]. The rate of sulfation can be influenced to some extent by additives added to the negative mass – eg the use of $BaSO_4$, carbon [5], or carbon-coated SnO2 particles [4], etc. All these additives have a certain positive effect on the size reduction and subsequent slower growth of lead sulfate crystals.

Our work is therefore focused on the evaluation of electrode changes by two different in-situ techniques like Laser Confocal Scanning Microscopy (CLSM) and X-ray Powder Diffraction (XRD) that has the potential to online monitoring as the material composition in different states of charge but also evaluate the changes in crystal size both on nano-scale (using XRD) and on micro-scale (CLSM). The indirect connection of these methods could bring a new perspective on the recrystallization process and bring new knowledge about the effect of different types of additives on irreversible processes limiting the activity of lead-acid batteries.

Experimental

For the X-ray study, a special holder was designed for the possibility of repeated measurement of the surface of the cycled lead electrode, which enables both cycling of the electrodes in the measuring electrolyte and direct mounting in the diffractometer chamber and X-ray diffraction of the electrode surface without air access. Thus the 1 mm thick pasted electrode could be measured in different states of charge without affecting the surface by post-treatment washing methods. The whole measurement procedure takes approximately 15-25 minutes to obtain a complete spectrum in the range of 5-90 ° theta-2theta and then follow cycling could be performed.

CLSM operando study of the pasted electrodes was performed using Olympus Lext OLS4100 confocal laser microscope equipped by ECC-Opto-std electrochemical cell by EL-CELL®. In the first phase, the cell was adapted

 ISBN: 978-80-574-0039-4

to the highly corrosive environment of battery sulfuric acid, and the working pasted electrode was optimized for small cell dimensions. Automatic surface scanning at time intervals of 1 to 5 minutes allows you to obtain a high-quality image from which you can compose a time-lapse video recording. It monitors in detail the development of surface morphology and is especially suitable for assessing irreversible changes in large lead sulfate crystals.
Figure 3 shows the typical morphology of the lead sulfate layer prepared on the metallic lead substrate. The layer contains sub-micron (nano) $PbSO_4$ crystals that tightly adhere to the metallic lead, and much larger crystals, which represents a possible beginning of an irreversible sulfation process at the electrode. While the size evolution of nano-dimensional crystals can be monitored by X-ray diffraction technique, because they cause the broadening of the measured diffraction peaks, for the growth monitoring and evaluation of large crystals changes, is necessary to use a different technique such as confocal laser scanning microscopy.

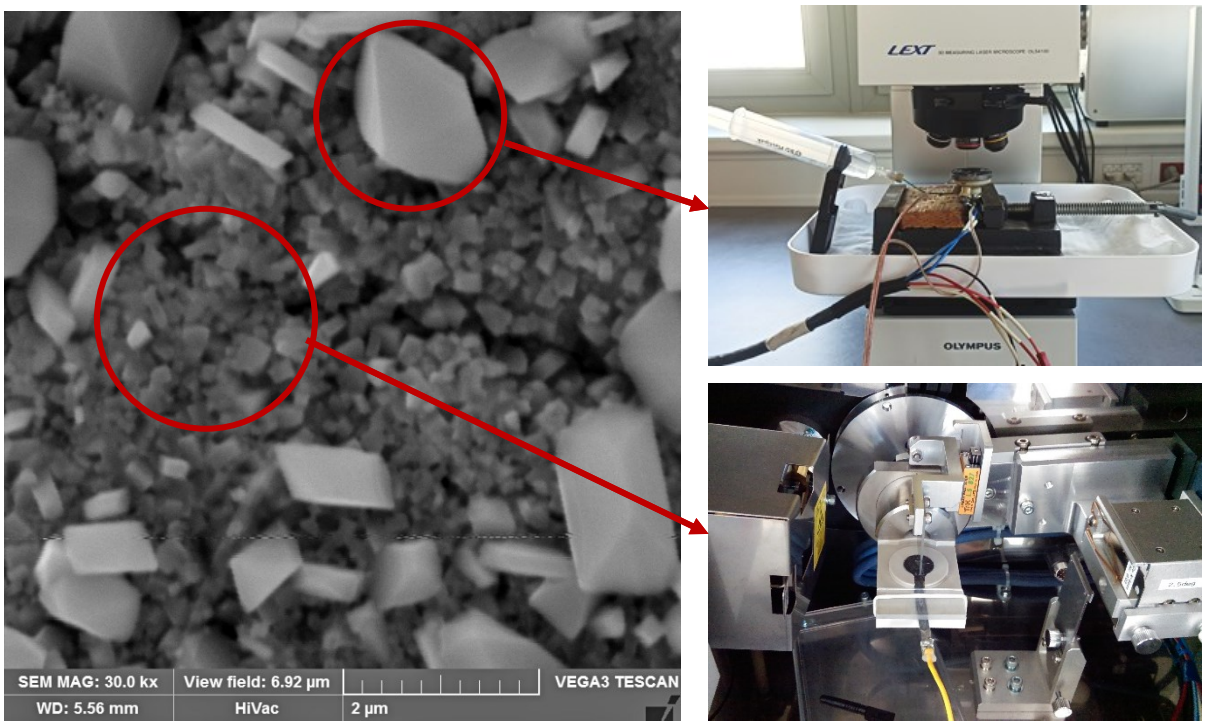

Fig. 1 SEM image of morphology of $PbSO_4$ layer on metallic lead substrate prepared at 15 minutes with marked areas of interest of in-situ confocal laser scanning microscopy (CLSM) and X-ray powder diffraction (XRD) techniques

Figure 2 a) shows the result of crystallite size analysis calculated by the Scherrer equation. The first part of the curve corresponds to discharging of the pasted mass. In this part, we can detect, at first, a slight decrease of crystallite size that could be explained by the initial precipitation of new crystal nuclei, and after only a gradual increase in $PbSO_4$ crystal size was detected. During charging, we can see the gradual decrease of lead sulfate particles at first, but at 50 % state of charge (SOC) a significant increase in average crystallite size was detected. This could be explained by the preferred dissolution of small crystals that lead to a gradual increase in the amount of larger crystals that remain on the electrode surface for a longer time and until later stages of charging. These larger lead sulfate crystals thus dissolute rapidly at the last stage of charging i.e. under 75 % of SOC.
This explanation is supported by CLSM monitoring of the behavior of large lead sulfate crystals (Fig 2 b). Whereas the growth of the crystal is fast in all stage of discharging, dissolution proceeds mainly at higher overpotential that corresponds to potential in later stages of charging.

ISBN: 978-80-574-0039-4

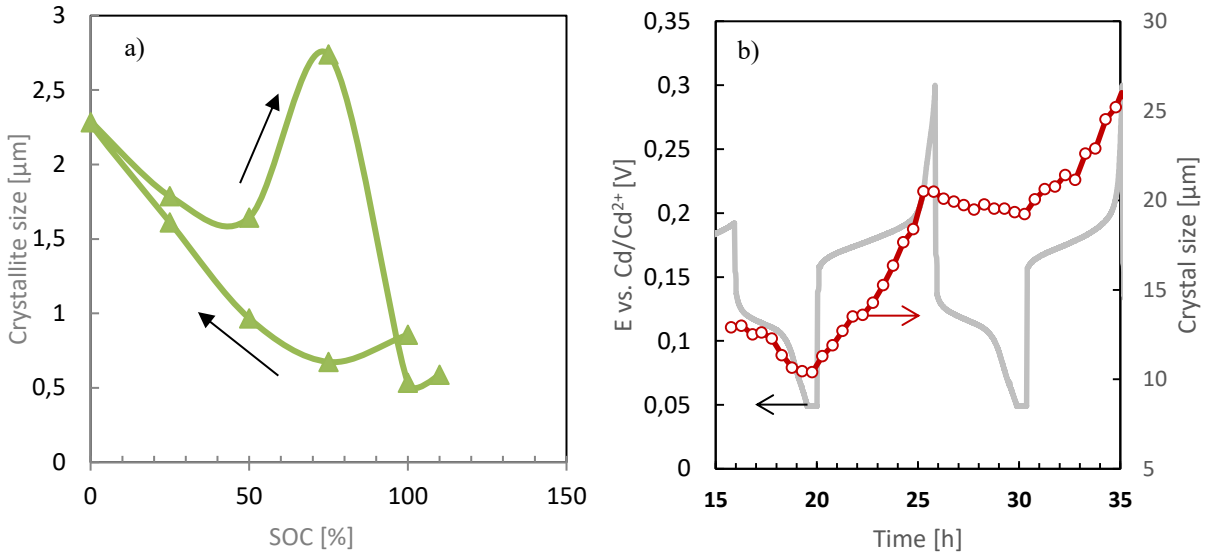

Fig. 2 Crystallite size evolution in different state of charge monitored by X-ray powder diffraction (a) and crystal size evolution of selected crystals during galvanostatic cycling from analysis of images from confocal laser scanning microscopy (b)

Conclusion

In-situ XRD technique and confocal laser scanning laser microscopy bring new insight on lead sulfate crystal propagation in lead-acid batteries. The connection of these techniques brings a powerful tool for monitoring both the nano-sized lead sulfate crystal evolution on the lead sponge and also the evolution of preferably grown lead sulfate crystals on a micro-scale. This could be helpful mainly in planned studies evaluation of additives influence on their ability to reduce irreversible changes of lead sulfate crystals (sulfation) and thus improve the long-term lifespan of such systems.

Acknowledgements

Authors gratefully acknowledge the financial support from the Ministry of Education, Youth and Sports of the Czech Republic under project No. LTT19001 and BUT specific research programme (project No. FEKT-S-20-6206).

References

[1] J. Valenciano, A. Sanchez, F. Trinidad, A.F. Hollenkamp, *J. Power Sources*, 158 (2006).
[2] M. Cenek, Akumulátory od principu k praxi, FCC Public, Prague (2003)
[3] D. Pavlov, in *Lead-Acid Batteries: Science and Technology: A Handbook of Lead-Acid Battery Technology and Its Influence on the Product*, 2nd edition, editor, Elsevier, 2017.
[4] V. Naresh and S. K. Martha, *J. Electrochem. Soc.*, **166**, 4, A551, (2019).
[5] P. T. Moseley, D. A. Rand, A. Davidson and B. Monahov, *J. Energy Storage*, **19**, (2018).

ISBN: 978-80-574-0039-4

Mechanically Induced Chemistry

V. Šepelák[a]*

[a] Institute of Nanotechnology, Karlsruhe Institute of Technology, Hermann-von-Helmholtz-Platz 1, 76344 Eggenstein-Leopoldshafen, Germany
*vladimir.sepelak@kit.edu

Mechanically induced chemistry (the so-called *mechanochemistry*) has a long history and continues to be of high importance. The presentation is focused on the mechanochemical phenomena in oxides, where an external mechanical force is exerted for the size reduction of solid particles even to the nanometer range, for the mixing and combination of chemical elements down to the atomic scale, and for the initiation or acceleration of solid state chemical reactions [1]. Heterogeneous processes shall be illustrated with the specific case of the mechanically induced formation reactions (mechanosyntheses) of complex oxides.

Acknowledgements
The present work is supported by the DFG (project SE 1407/4-2) and the CAPES.

References
[1] V. Šepelák, K. L. Da Silva, R. S. Trautwein, K. D. Becker, H. Hahn, Z. Phys. Chem. (2021) pp. 000010151520213101. https://doi.org/10.1515/zpch-2021-3101

 ISBN: 978-80-574-0039-4

Numerical Modelling of Heterogenous Catalysis on Porous Particles

M. Mačák[a]*, P. Vyroubal[a]

[a] Department of Electrical and Electronic Technology, Brno University of Technology, Brno 616 00, Czech Republic
*E-mail address: Martin.Macak@vut.cz

Introduction

Heterogenous catalysis is a widely applied process in many chemical technologies as it can significantly accelerate and direct the reaction process. The range of application varies from chemical manufacturing to energy storage. Most of the catalysts consist of active nanoparticles dispersed on host materials with large surface. Metal nanoparticles are one of the most used catalysts for broad range of industrial processes. Such catalysts usually have complex structure, which makes the atomistic understanding of the structure quite challenging [1, 2].

Numerical simulations of heterogenous catalytic reactions attract great interest as they can accelerate the design and optimisation of processes. Usually, atomistic modelling of catalysts is unsustainable for the modelling of large-scale processes as the length scales would range from nanometres to meters [1, 2]. It is then necessary to develop simpler descriptions, which could be used for macroscopic simulation while still being accurate. This simplification is mainly carried out through the description of reaction kinetics at the liquid-solid interface. Additionally, the interaction between fluid flow and diffusion might also influence the effectivity of catalyst materials. This process can be studied at micro-scale and its results can be then simplified and transferred to macro-scale dimensions. Computational fluid dynamics (CFD) simulations can bring overall insight into these processes, which might be experimentally difficult and time consuming.

This article describes a model of a reaction process on a catalyst particle focusing on the interaction between fluid flow and diffusion of species. Catalytic hydrogenation (catalyst particles from Pt, Pl, Ru or Ni [3, 4]) of nitrobenzene (NB) was chosen as a model process. Liquid hydrogenation, which is a gas-liquid-solid system, is a favourable process to the classic gaseous process due to higher productivity [3-5]. Even though, this process is widely used, numerical simulations in this area are relatively rare [5, 6]. The application of simulations might decrease energy demand of the process while increase the effectivity of the process (shorter rise time, higher purity of the product or higher volume production). This model can be used for modelling of free particle catalysts as well as for fixed bed catalysts.

Chemistry and Numerical Model

The mechanism of liquid hydrogenation of nitrobenzene is very complicated but can be generally summarised into two steps [5, 7]. First AN is produced from NB and H_2. In the second phase (higher temperature), side products (cyclohexylamine (CHA)) are produced from deep hydrogenation of AN.

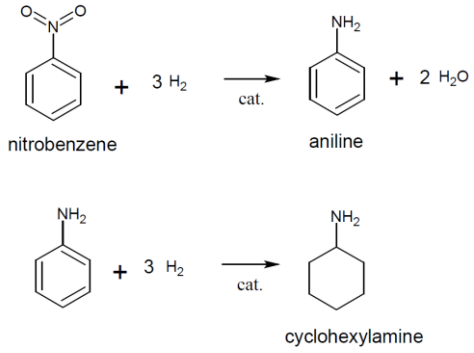

Fig. 9 Simplified reaction mechanism. First reaction describes the main process of AN production. Second reaction describes the side reaction of CHA

 ISBN: 978-80-574-0039-4

CFD software Ansys Fluent was used to carry out the simulations. The process is described as a single-phase reacting flow, which uses a Eulerian mixture approach governed by Navier-Stokes equations [8]. Transport of species (NB, H_2, AN, H_20 and CHA) is defined by a convection-diffusion equation [8]. In this case, the catalyst particles are considered as a stationary porous host material. Reactions on active sites were defined through Arrhenius equation. The reaction rates were based on a model presented by Turek et al [5]. In this model, the effects of NB adsorption on the catalyst surface were implemented directly into the reaction rate. As a result, it was not necessary to consider site deactivation. A sample geometry is shown in Figure 2.

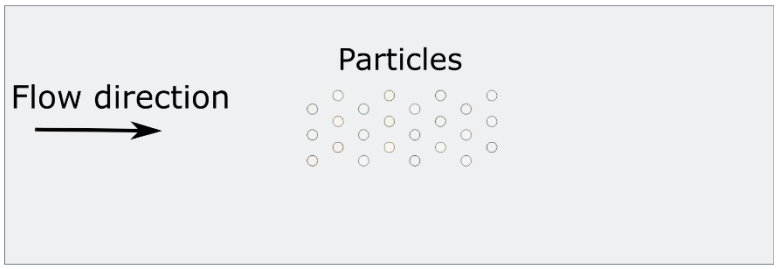

Fig. 2 Comupational domain. Porous catalyst particles have a diameter of 10 μm

Results

First simulations studied concentration and temperature dependence of the reactions. The reaction ratio based on the concentration of NB is shown in Figure 3. For low concentrations of NB, the side reaction (r2) will overtake the main reaction (r1) and CHA will be produced. On the other hand, higher concentrations of NB will inhibit the main reaction due to NB adsorption on the catalyst. These results suggest that it is necessary to maintain the NB concentration in the range of 10 mol·m^{-3} to 100 mol·m^{-3}. Figure 3 also shows the temperature dependence on the reaction ratio. Generally, as the temperature increased, the side reaction became more prominent. The results also suggest that the lower concentrations of NB are more susceptible to temperature changes.

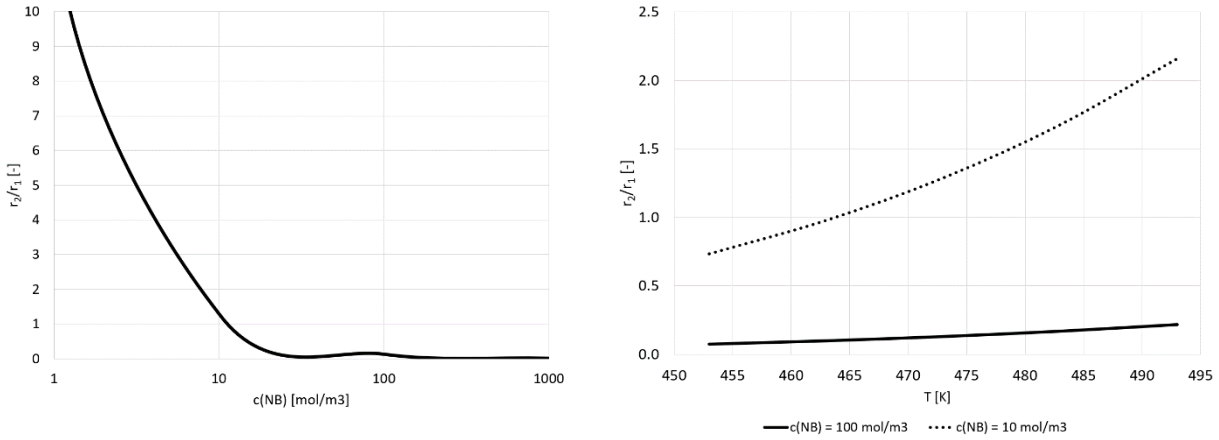

Fig. 3 Concentration (left) and temperature dependence (right) of the reaction ratio (r2 signifies the side reaction while r1 represents the main reaction)

As a second step, the influence of the diffusion of species towards and through porous particles was investigated. Additionally, a fluid flow was introduced to the computational domain (Figure 2). Overall, results from the simulations show that it is possible to predict the influence of the catalyst particle structure as well as the influence of environment proportion on the chemical process. Figure 4 shows the mass fraction of AN, where it is possible to see a gradual increase in AN mass fraction, which signifies that the main reaction is dominant. Increasing the amount of particles would naturally increase the final AN concentration up to a point, in which the side reaction

 ISBN: 978-80-574-0039-4

would accelerate based on the concentration dependence (Figure 3). In this case, only a small amount of CHA was produced. Figure 5 shows the velocity field. The viscous resistance of the particles caused the fluid to slightly flow around the catalyst structure. Inside the structure, the species transport was mainly carried out by diffusion. Exothermic effects of the reactions are shown in Figure 6. Even with few particles, the temperature increased considerably. The ambient temperature was set to 440 K.

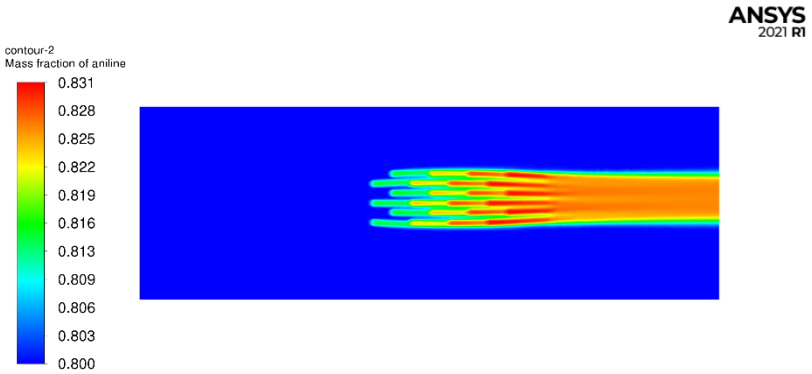

Fig. 4 Mass fraction of aniline

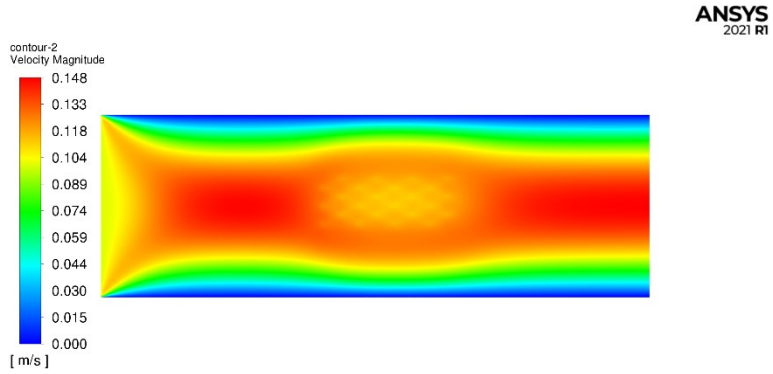

Fig. 5 Velocity field of the whole mixture

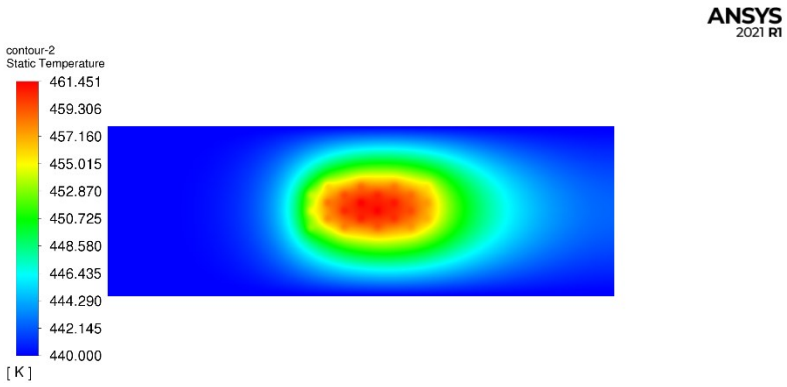

Fig. 6 Visualisation of exothermic effects of the reaction mechanism

ISBN: 978-80-574-0039-4

Acknowledgements
This work was supported by the BUT specific research program (project No. FEKT-S-20-6206).

References
[1] H. Wang and J. Lu, Chinese Journal of Chemistry, 38(2020)1422-1444.
[2] S. Schauermann, N. Nilius, S. Shaikhutdinov, and H. -J. Freund, Accounts of Chemical Research, 46(2013), 1673-1681 .
[3] V. Y. Doluda, A. E. Filatova, E. M. Sulman, V. G. Matveeva, S. P. Mikhailov, A. I. Sidorov, and Y. Y. Kosivtsov, Catalysis in Industry, 11(2019) 147-153.
[4] D. V. Sharma, A. W. Patwardhan, and V. V. Ranade, Industrial & Engineering Chemistry Research, 56(2017) 1404-1415.
[5] F. Turek, R. Geike, and R. Lange, Chemical Engineering and Processing: Process Intensification, 20(1986) 213-219.
[6] Y. Mo, J. Imbrogno, H. Zhang, and K. F. Jensen, Green Chemistry, 20(2018), 3867-3874.
[7] C. S. Couto, L. M. Madeira, C. P. Nunes, and P. Araújo, Chemical Engineering & Technology, 38(2015) 1625-1636.
[8] A. Mühlbauer, M. W. Hlawitschka, and H. -J. Bart, Chemie Ingenieur Technik, 91(2019) 1747-1765.

 ISBN: 978-80-574-0039-4

Experimental and computational study directed towards heterogeneous catalytic hydrogenation of CO_2 to methanol

N. Podrojková[a]*, R. Oriňaková, A. Oriňak[a]

[a] Department of Physical Chemistry, Faculty of Science, P.J. Šafárik University, Moyzesova 11, 041 54 Košice, Slovakia
*natalia.podrojkova@student.upjs.sk

Excessive combustion of fossil fuels causes a constant increase in the concentration of CO_2 in the atmosphere, which leads to fundamental changes in the world's climate. CO_2 is also a highly chemically stable molecule, the decomposition of which requires considerable adjustment of physical conditions. Increasing the production and use of biofuels can affect the consumption of fossil fuels and the generation of CO_2, and the production of these biofuels can also be achieved by decomposing CO_2 in a suitable technological way. One of the most used CO_2 decomposition processes is heterogeneous hydrogenation to methanol. Methanol as one of the most valuable chemicals obtainable by CO_2 hydrogenation is not only considered as easily-transport liquid energy storage medium with high energy density, but also served as an essential chemical feedstock with a wide range of utilization ways to produce different chemicals such as formaldehyde, acetic acid, methyl methacrylate, dimethyl terephthalate, methylamines, dimethyl ether, methyl tert-butyl ether, chloromethanes, or light olefins.
The most commonly used catalyst is Cu together with different promoters (Zn, Zr, Ce, Al, Si, V, Ti, Ga, B, Cr, etc.). The synthesis of methanol using copper-based catalysts can occur via three different reversible reaction pathways (Figure 1) [1]. The first mechanism is the formate mechanism, where the reaction of CO_2 with atomic H leads to the formation of formate as an intermediate. Chemisorbed formate can be formed from CO_2 reaction with dissociated surface hydrogen. Then, surface-bound formate is hydrogenated, which is the rate-determining step, to produce dioxomethylene that can lose oxygen with the formation of formaldehyde or lose hydroxyl and form H_2CO*. H_2CO* can be further hydrogenated to methoxy and methanol. The second reaction pathway is called RWGS and it produces a carboxyl intermediate. RWGS pathway involves the formation of CO* through the loss of hydroxyl from hydrocarboxyl. HCO intermediate is then hydrogenated to formyl that leads to methanol. During the third hydroxycarbonyl mechanism a $C(OH)_2$ intermediate is formed. It assumes that hydrocarboxyl can be hydrogenated to form COOH* which may subsequently lose hydrogen to form *COH. *COH is then hydrogenated to hydroxymethylene. All three reaction pathways lead to the formation of formyl (H_2CO*) which is subsequently hydrogenated to methoxy (H_3CO*) and methanol (CH_3OH) [1].

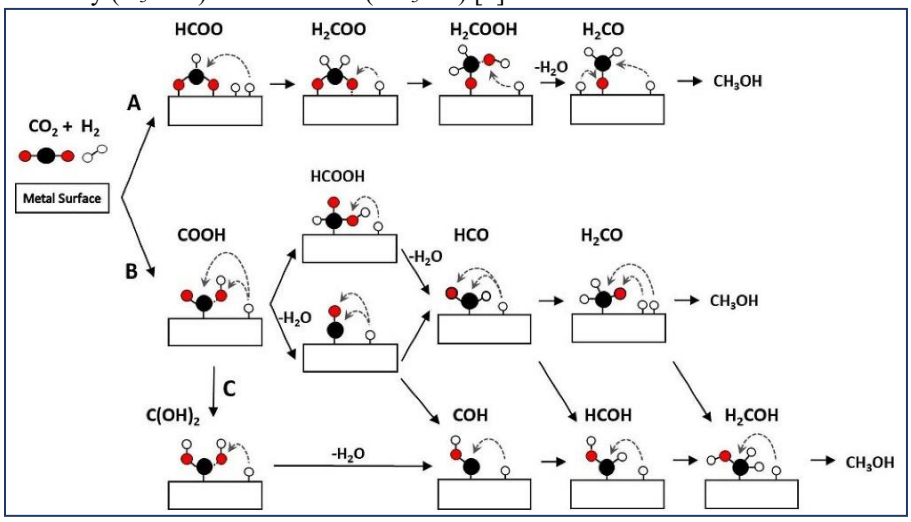

Fig. 10 Possible mechanism and intermediates of methanol synthesis via CO_2 hydrogenation according to different studies a) formate mechanism, b) RWGS mechanism, c) hydrocarboxyl mechanism [1]

 ISBN: 978-80-574-0039-4

The most used combination of catalysts in the low-pressure methanol synthesis is based on ZnO, Cu, and Al_2O_3. However, $Cu/ZnO/Al_2O_3$ catalysts suffer from the limited selectivity (< 70 %) for methanol and stringent reaction conditions (50 – 100 bar, 200 – 300 °C). Mentioned catalysts are characterized by low stability and low activity due to water formation and strong hydrophilic character of Al_2O_3. Besides, although the most used catalyst is Cu, there are still open questions rising about the active sites. One has suggested that metallic copper is the active site and addition of oxides would sustain the large copper surface and reduce CuO to metallic copper. Other suggested the effect of "Cu-Zn" synergy for being essential for the active site where methanol is synthesized over Cu^+ at the Cu/ZnO interface, or over Cu cations that dissolve in the ZnO matrix and metallic copper only promotes the dissociation of H_2 [1]. Liang et al. investigated the deactivation behaviour of a CuZnAl catalyst in CO_2 hydrogenation to methanol where the agglomeration of ZnO species and the oxidation of metallic Cu were the main reasons for catalyst deactivation [2]. After 10 h of the reaction ZnO agglomerated which led to reduction of Zn-Cu interface leaving the Cu surface more revealed towards CuO production and deactivation of the whole catalyst. Liang et al. observed the formation of CuO on the revealed Cu sites after 720 h.

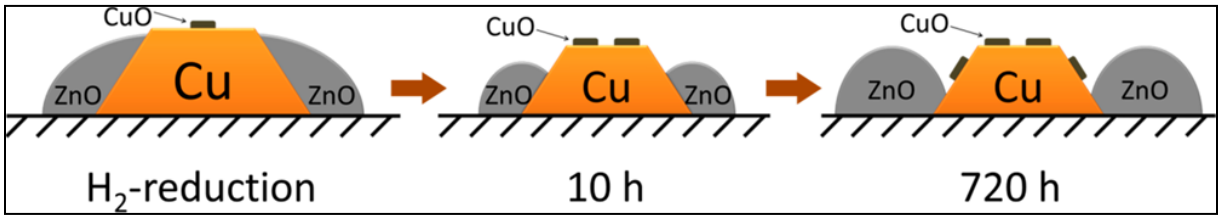

Fig. 11 Schematic representation of the structure changes of CuZnAl catalyst at different stages proposed by Liang et al. [2]

The use of quantum mechanics simulations for understanding the CO_2 hydrogenation process is effective in finding new intermediates, searching for new catalysts, and identifying reaction pathways. The density functional theory (DFT) simulation of CO_2 behaviour on the surface of the catalysts can provide invaluable insights about the C=O bond activation, help to understand the evolution adsorbed species on the surface of the catalyst, information about rate-determining step, and overall insight into reaction mechanism which can speed up and diminish the system cost significantly and contribute to obtain a better understanding of the catalyst role [1].

Our theoretical studies were oriented towards the effect of CuO on the mechanism of CO_2 hydrogenation to methanol to better understand the deactivation process of the catalyst. Using the DFT+U calculations in GPAW software we were able to optimize the CuO cell structure with calculation of U parameter at value 8,0 eV. Also, values of lattice parameters were optimized (a = 4,88 Å, b = 3,341 Å, c = 5,198 Å and β = 101,5°) and CuO (111) surface structure was prepared for CO_2 adsorption simulations. Energetically the most stable surface was CuO(111) with adsorption energy of -95,038 kJ/mol. These results provided the possibility to find the transition states (Figure 3) and pathways of CO_2 hydrogenation to methanol which are the main goal of the work.

ISBN: 978-80-574-0039-4

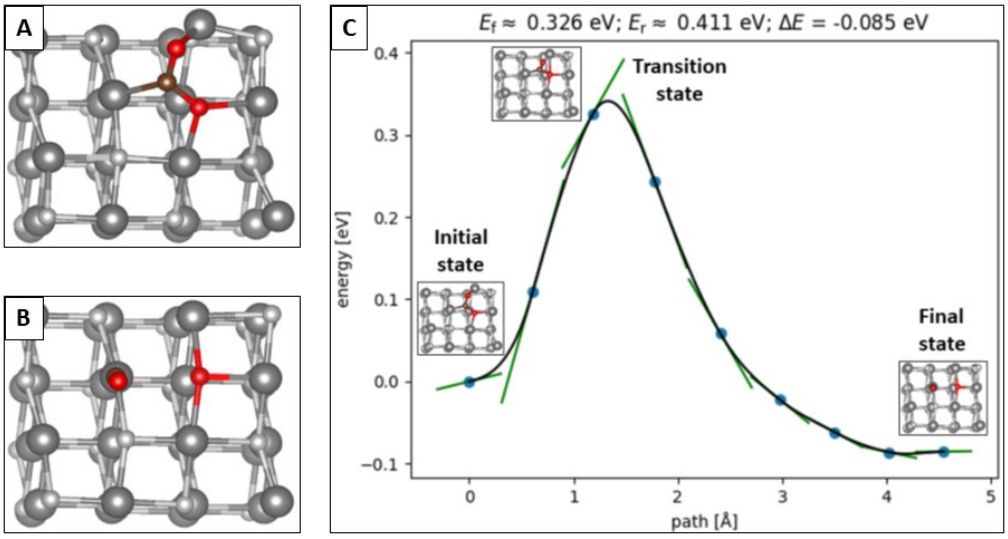

Fig. 12 Transition state of CO_2 cleavage on the CuO surface with the initial state of adsorbed CO_2 and final state of separated CO and O adsorbed on CuO surface

Acknowledgements
This work was supported by the Internal Scientific Grant System of Faculty of Science of Pavol Jozef Šafárik University in Košice, Slovak republic project no. VVGS-PF-2019-1052 and by Scientific Grant Agency of the Ministry of Education, Science, Research, and Sport of the Slovak Republic project no. VEGA 1/0074/17.

References

[1] N. Podrojková et al., ChemCatChem **12** (2020) 1802-1825.
[2] B. Liang et al., Ind. Eng. Chem. Res. **58** (2019) 9030-9037.

ISBN: 978-80-574-0039-4

Novel Ni based catalyst for Hydrogen production by catalytic thermal decomposition of methane

K. Sisáková[a]*, R. Oriňaková[a], A. Oriňak[a]

[a] Department of Physical Chemistry, Faculty of Science, P. J. Šafárik University, Moyzesova 11, 04001 Košice, Slovakia
*corresponding author e-mail

Introduction

Methane is widely used as a hydrogen source because of its high H/C ratio and abundance in natural gas fields. Green hydrogen can be produced by utilizing renewable energy sources, such as landfill gas and biogas from livestock manure and food processing waste, and methane feedstock and solar thermal energy as a heat source. Catalytic methane decomposition, CMD ($CH_4 \rightarrow 2H_2 + C$, $\triangle H_{298K} = 75.6$ kJ/mol) has attracted much attention as an alternative to conventional SMR process in terms of economic and environmental aspects. It is reported to produce COx-free hydrogen directly applicable for PEM fuel cells, and to dramatically reduce CO_2 emissions when coupled with heating source such as solar systems.

However, the thermal decomposition of methane to produce COx-free hydrogen entails several obstacles that need to be overcome. One of the disadvantages of the process is the high temperature at which the reaction takes place. Decomposition of methane without the use of a catalyst takes place at temperatures higher than 1200 ° C. The development of high-efficiency catalysts and the optimization of reactors are essential for the industrial production of TCDs [1]. Catalysts can reduce activation energy and shorten reaction times. Therefore, the selection of a suitable catalyst plays a crucial role in the TCD catalysed process. At present, research is mainly focused on Ni-based catalysts, noble metal doped catalysts, carbon catalysts and iron-based catalysts [2]. Another disadvantage is that the carbon formed is adsorbed on the active sites of the catalyst and causes the catalyst to be deactivated. At present, many industrial catalysts consist of Ni or Ni and other metal alloys supported on a suitable support. The main reason for this support is to keep the catalytically active phase in a highly dispersed state. The most important factors influencing carbon deposition during metal-catalysed methane decomposition are particle size, dispersion, and stabilization of the metal catalyst particles, which can be controlled by selecting a suitable support. In recent years, special attention has been focused on the use of SiO_2 as a support for a suitable catalyst for the process of thermal decomposition of methane [3]. The addition of a noble metal to a nickel-based catalyst, such as palladium, leads to a significant increase in stability and overall hydrogen yields, but modification with other noble metals reduces nickel activity.

Material and methods

Hydrochloric acid (HCl), ammonia solution (NH_3), ethanol (C_2H_6O), palladium chloride ($PdCl_2$), and silica nanoparticles (SiO_2, 200 m^2/g) were purchased from Sigma Aldrich (Missouri, USA). Nickel acetate tetrahydrate ($Ni(CH_3COO)_2$*4 H_2O) and iron acetate ($Fe(CH_3COO)_2$) were used as a source of nickel-iron oxide nanoparticles, which were together with polyvinylpyrrolidone (PVP, $(C_6H_9NO)n$), which was used for coating palladium nanoparticles, purchased from CentralCheme (Bratislava, Slovakia). Nanoparticles were prepared by alcohol reduction.

TEM, SEM and AAS methods were used to characterize the structure of nanocatalysts. Microscopic images of the samples were taken with a HITACHI SU 6600 scanning electron microscope (SEM), which provides a resolution of up to 1.3 nm and a magnification of 60-600 000x. A Jeol 2100 (TEM) instrument was used for transmission electron microscopy, which provides a resolution of up to 0.19 nm and a magnification of 1000-800 000x. A ContrAA 300 atomic absorption spectrometer (Analytik Jena AG, Germany) with a flame ionization with a continuous radiation source was used to measure atomic absorption spectroscopy.

The DFT method was used to simulate and model the thermal decomposition of methane. The General Gradient Approximation (GGA), which modifies the functional, is commonly used in catalysis and is referred to as the revised Perdew-Burke-Ernzerhof (rPBE), which uses double numerical plus polarization (dnp). This functional was used in conjunction with FD mode. The base set was used to balance electron exchange and correlation. The most

 ISBN: 978-80-574-0039-4

stable crystallographic surface of palladium (fcc 111) was studied. The adsorption energy per 1 molecule can be calculated from the relation:

$$Eads = E_{surf + mol} - (E_{surf} + E_{mol}) \qquad (1)$$

where $E_{surf+mol}$ is the total energy of the adsorbate-substrate system; The E_{surf} is the energy of an uncovered surface cell; and E_{mol} is the energy of the isolated CH_4 molecule.
The nudged elastic band (NEB) was used to simulate the cleavage of C-H covalent bonds from a CH_4 molecule.

Results and Discussion

The structure of the catalysts was studied using a scanning and transmission electron microscope. Figure 1A, 1B and 1C shows TEM and SEM images of Pd nanoparticles deposited on a SiO_2 support. From the TEM images we can observe that palladium nanoparticles are deposited both on the surface and inside the pores of SiO_2. The Pd size of the nanoparticles is approximately 8 nm. In the figure 1G and 1H SEM and TEM images of $NiFe_2O_4$ nanoparticles deposited on a SiO_2 support are shown. From the TEM images we see that $NiFe_2O_4$ nanoparticles are absorbed mainly in the pores of SiO_2. $NiFe_2O_4$ nanoparticles are also more homogeneously dispersed compared to palladium nanoparticles. The average size of $NiFe_2O_4$ nanoparticles is approximately 10 nm. The TEM and SEM images of $Pd/NiFe_2O_4/SiO_2$ catalyst are shown in the figure 1D, 1E and 1F. The orange circle indicates palladium nanoparticles, while the blue circle indicates $NiFe_2O_4$ nanoparticles. From the TEM images we can observe that the Pd nanoparticles are surrounded by $NiFe_2O_4$ nanoparticles. It is also possible to observe empty pores of SiO_2. The nanoparticles are located mainly in the open pores of SiO_2.

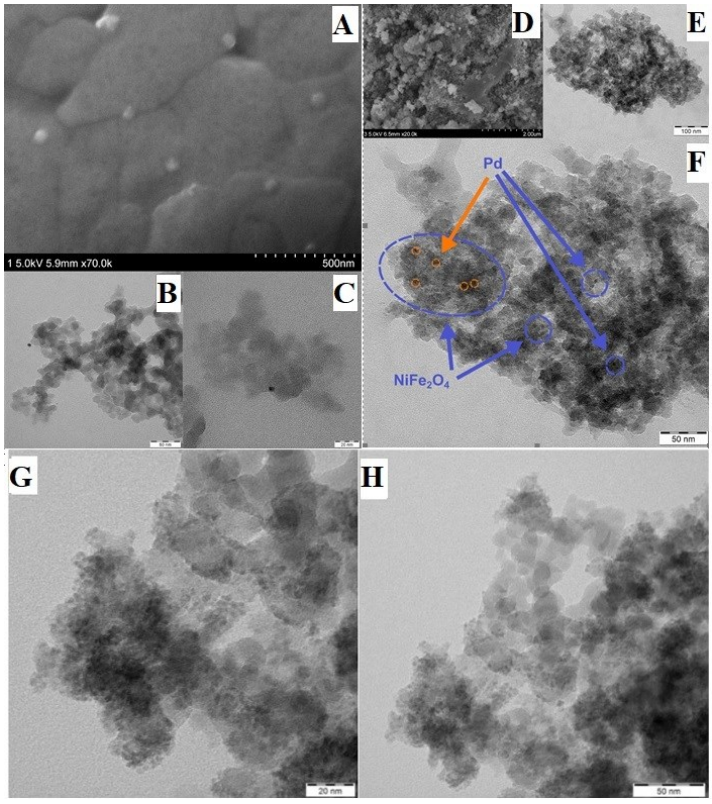

Fig. 1 A- SEM images of Pd/SiO_2, B, C - TEM images of Pd/SiO_2, D - SEM images of $Pd/NiFe_2O_4/SiO_2$ catalyst, E, F - TEM images of $Pd/NiFe_2O_4/SiO_2$ catalyst, G, H- TEM images of $NiFe_2O_4$ nanoparticles deposited on SiO_2

The prepared samples were also characterized by Atomic Absorption Spectroscopy (AAS). Under optimal conditions, a calibration dependence was made for all determined elements. Five calibration points were measured for palladium, nickel and iron. For Pd and Fe, a concentration range of 1-5 mg/L was determined. A calibration dependence in the range of 0.05-2 mg/L was determined for Ni.

 ISBN: 978-80-574-0039-4

	Amount of metal [mg/L]		
Catalyst	*Palladium*	*Nickel*	Iron
Pd/SiO_2	4,045	-	-
$NiFe_2O_4/SiO_2$	-	0,731	3,098
$Pd/NiFe_2O_4/SiO_2$	0,246	1,456	4,121

Tab. 1 Summarised values of amount of metal in samples

The first step in the calculations and simulations of the TCD process using the DFT method was to optimize the surface of hydrogen and methane and calculate their adsorption energies. The adsorption energy of optimized methane is -23.973 eV and the adsorption energy of hydrogen is -6.704 eV.
The adsorption energy of the Pd is -138,815 eV. In order to achieve the most accurate energy value, the grid parameter was also optimized in the values of 3.933 to 3.945 Å. The lowest value of adsorption energy was reached at the lattice parameter a = 3.942 Å. This value was used for surface creation and subsequent optimization. The distance between Pd atoms after optimization was 2.779 Å. In order to find out how the methane molecule is rotated during adsorption on the Pd surface, several possibilities have been optimized. It was shown that the lowest adsorption energy was achieved by methane, which was placed on the surface of the atom Pd, turned 1 with hydrogen downwards - towards the surface of Pd. This location corresponds to the literature [4]. The lowest value of adsorption energy was -162.914 eV.
The activation barrier required to dissociate the first hydrogen bond from the methane molecule was calculated using the NEB calculation method.
The adsorption energy of the system before the cleavage of the hydrogen bond from the methane molecule on the palladium surface was -162.914 eV and after the cleavage of the bond: -162.333 eV. The calculated activation barrier is 0.581 eV for the palladium surface, indicating that from a thermodynamic point of view, this step does not require a large activation energy for dissociation. Arevalo et. al. studied using NEB simulation of DFT calculations of TCD methane on the surface of nickel and ruthenium [5]. The activation barrier they calculated for the nickel surface was 0.49 eV, while for the ruthenium surface it was 1.10 eV. From the given results we can see that while, from a thermodynamic point of view, the surface of ruthenium requires a high activation energy, on the contrary the surfaces of palladium and nickel do not need a large activation energy for dissociation. Liu et. al. studied the thermal decomposition of methane on the surface of palladium and ruthenium [6]. They calculated an activation barrier for the dissociation of the first hydrogen bond from a methane molecule on the palladium surface of 0.3 eV. Compared to the values presented in this work, their value is half lower. Such different values may be due to the use of other calculation methods than in the case of the simulations of Liu et. al., where they used the VASP program with the PW method for simulations and in the case of the DFT method they used the PBE functional with Dudarev correction instead of the Tkatchenko-Scheffler correction.
Similar to the first methane dissociation reaction on the palladium surface, the structures and adsorption energy were optimized for the other dissociation reactions. The adsorption energy calculated in this work for the CH_3 radical was 1.258 eV, for the CH_2 radical 3.198 eV, for the CH radical 5.655 eV.

Conclusion
A catalyst based on palladium, nickel and iron supported on SiO_2 support - $Pd/NiFe_2O_4/SiO_2$ was prepared. As part of a better study of properties, Pd/SiO_2, $NiFe_2O_4/SiO_2$ catalysts were also prepared. These catalysts were studied for their structure by SEM, TEM and AAS methods. From TEM and SEM analysis we know that the Pd size of the nanoparticles in the case of the Pd/SiO_2 catalyst was 8 nm. The AAS provided us with information on the palladium concentration, which was 4.045 mg/L. For $NiFe_2O_4/SiO_2$, the particle size averaged 10 nm and the metal concentration was 0.731 mg/L for nickel and 3.098 mg/L for iron. With a $Pd/NiFe_2O_4/SiO_2$ catalyst, we can observe that the palladium nanoparticles are surrounded by $NiFe_2O_4$ nanoparticles. Both types of nanoparticles are adsorbed mainly inside the pores of SiO_2, but also on the surface. The metal concentration in the catalyst was Pd - 0.246 mg/L, Ni - 1.456 mg/L, Fe - 4.121 mg/L.

 ISBN: 978-80-574-0039-4

Using the DFT method, we studied Pd nanoparticles for the TCD process. We used the GPAW program for calculation and simulation, and the ASE program for surface modeling. The implementation of a given program for the study of the TCD process brings new possibilities for the study of catalyst surfaces. The results are comparable to current research. The surfaces of methane, hydrogen, palladium and methane radicals were modeled and optimized. In addition, we implemented NEB calculations. We found that the activation barrier for the first hydrogen dissociation reaction from the methane molecule on the palladium surface is 0.581 eV. This value is higher than stated in the articles, but these minor differences were due to the use of other calculation methods. The adsorption energy calculated in this work for the CH_3 radical was 1.258 eV, for the CH_2 radical 3.198 eV, for the CH radical 5.655 eV.

Acknowledgements
This work was supported by the Scientific Grant Agency of the Ministry of Education, Science, Research, and Sport of the Slovak Republic Projects No. VEGA 1/0095/21, Research and Development Support Agency No. APVV-20-0299 and the Internal Scientific grant system PF UPJŠ vvgs-pf-2021-1783.

References
[1] K. Sisáková, A. Oriňak, R. Oriňaková, M. Strečková, J. Patera, A. Welle, Z. Kostecká, V. Girman, Catalysis Letters **150** (2020) 781-793
[2] M. Pudukudy, Z. Yaakob, N. Dahani, M. Takriff, N. Hasaan, Journal of Cluster Science **28** (2017) 292-300
[3] J. Qian, T. Chen, L. Enakonda, D. Liu, G. Mignani, J. Basset, L. Zhou, Int. J. Hydrogen Energy **45** (2020) 7981-8001
[4] S. Kozlov, K. Neyman, Insights from methane decomposition on nanostructured palladium, Journal of Catalysis **337** (2016) 111-121
[5] R. Arevalo, S. Aspera, M. Sison Escaño, H. Nakanishi, H. Kasai, Tuning methane decomposition on stepped Ni surface: The role of subsurface atoms in catalyst design, Scientific Reports **7** (2017) 13963
[6] Z. Liu, P. Hu, General Rules for Predicting Where a Catalytic Reaction Should Occur on Metal Surfaces: A Density Functional Theory Study of C−H and C−O Bond Breaking/Making on Flat, Stepped, and Kinked Metal Surfaces, J. Am. Chem. Soc. **125** (2003) 1958-1967

 ISBN: 978-80-574-0039-4

Simulation model of battery cell based on LiFePO4 technology

Marek Šimčák, Michal Frivaldský

Department of mechatronics and electronics
Faculty of electrical engeneering and information technology
Univerzity of Zilina
Žilina 010 01, Slovakia
marek.simcak@feit.uniza.sk

Abstract
This article provides a partial description of the LiFePO4 technology. A real electrochemical cell (NPB 60AH) based on LiFePO4 in pouch packaging is described here. Description of the measurements of the charging and discharging process are given, while procedure for development of equivalent simulation behavioral model is consequently given and evaluated. A simulation model of selected battery is then developed, while results of the operational characteristics are then compared to the real measurements.

Keywords
LiFePO4, Equivalent battery scheme, battery simulation model,

Introduction

Nowadays, there is a great development in power electronics systems. These systems, such as electromobility or the production and storage of energy from renewable sources, are pushing the battery market. This pressure is mainly applied to maximize safety, maximize capacity and maximize battery life. Under this market pressure, the development came with LiFePO4-based catode batteries. These batteries belong to the Lithium battery group. LiFePO4 technology offers certain advantages and disadvantages. The advantages of these batteries are mainly in thermal stability, safety, electrochemical stability and very low toxicity. The availability of materials also significantly reduces the cost of these batteries. On the contrary, the disadvantage of this cell is, for example, in the lower energy density, compared to lithium cells containing cobalt. Electrochemical cells based on LiFePO4 are manufactured with high capacities. This fact predestines them for application in traction or in energy storage. These attributes were crucial for work and development in this area, specifically with electrochemical cells based on LiFePO4.

Battery cell description

Equivalent battery scheme

The equivalent battery scheme (Fig. 1) represents a battery model through passive electrical components. This scheme is used to model the charging / discharging of a given cell. Using this scheme, the dynamic parameters of the cell can also be modeled. This scheme consists of a DC source. This source represents an open circuit voltage (OCV). The element R_S represents the series resistance of the cell. Elements R_1 and C_1 represent the so-called fast time constant and elements R_2 and C_2 so-called slow time constant.

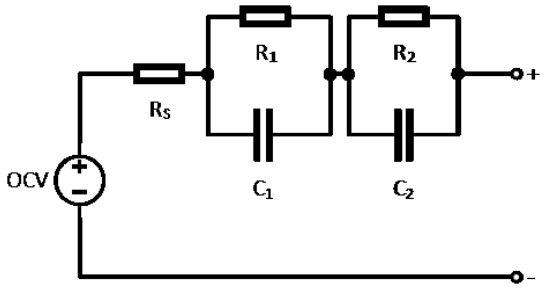

Fig. 1 Equivalent battery scheme (R2C2)

 ISBN: 978-80-574-0039-4

Selected battery cell type

This electrochemical cell represents the lowest level of a high voltage battery. This cell has a cathode made of LiFePO4 material. The manufacturer of this cell declares the basic parameters, which are shown in Table I. [2] This cell does not have a pressure valve. The design of this cell (Fig. 2) assumes that in the event of a critical condition where the electrolyte begins to evaporate, the cell will inflate. Unlike other cells where the pressure valve is located and this electrolyte blows out of the cell. Thus, if the electrolyte remains in the cell, its capacity can be better regenerated over time. This advantage is offered by this pouch type of cell.

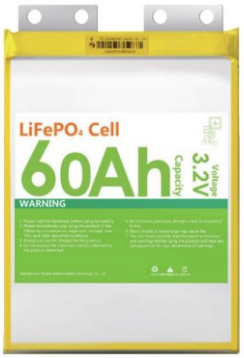

Parameters	Values
Nominal voltage	3,2 V
Nominal capacity	60 Ah
Minimal voltage	2,5 V
Maximal voltage	3,8 V
Rated discharge/charge current	18 A (0,3 C)
Maximal continuous discharge/charge current	60 A
Maximal working temperature	50 °C

Experimental measurements for equivalent schematics identification

Capacity characteristic

The capacitance characteristics (Fig. 3 - left) serve to determine the value of the capacitance of which cell is able to supply and at the same time during charging what capacity it is able to receive. From this characteristic we can find out that the capacity charged to the cell is 62.282 Ah and the capacity discharged from the cell is 62.568 Ah. This characteristic represents the range from 0% SOC (State of charge) to 100%. Where 0% SOC of cell is on the left side of the graph and 100% SOC of cell is on the right side of the graph. Therefore, the discharge characteristic is reversed because it discharges the cell from 100% SOC to 0% SOC.

The OCV characteristic (Fig. 3 - right) represents the process of charging the cell and the process of discharging the cell. The average value of these characteristics is the OCV characteristic. This waveform represents the approximate values of voltage during the pause in the capacity characteristic. OCV represents the voltage change in the range from 0% SOC (State of charge) to 100% SOC. This OCV is in the replacement equivalent battery scheme that DC power supply. SOC orientation of the graph in this case is identical to the capacity characteristics.

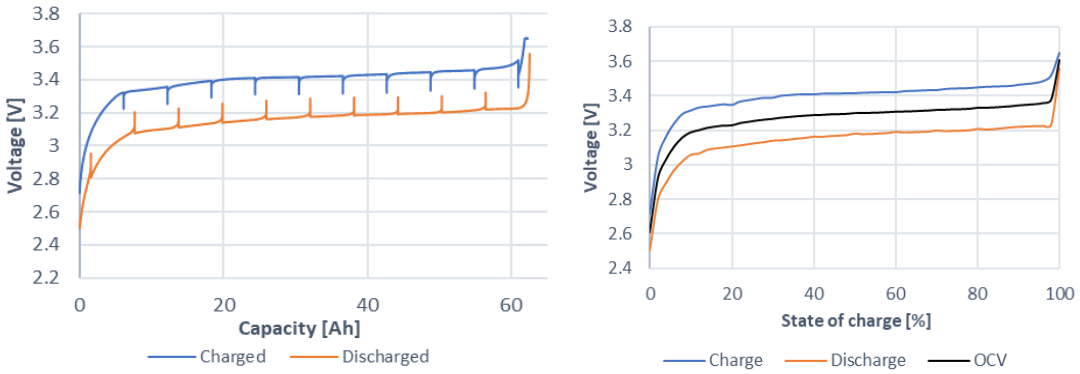

Fig. 3 Characteristic showing the dependence of cell voltage on cell capacity during charging and discharging (with pauses) – left, characteristic showing the approximate value of open circuit voltage (OCV) – right Charging and discharging process for the equivalent circuit identification

ISBN: 978-80-574-0039-4

The voltage waveform during charging over time is shown in Figure 4 - left. Here, the charging style is shown, where it can be seen that charging has been interrupted. This interruption was in order to identify the elements of the replacement scheme. This interruption occurred every 10% of the SOC (State of charge). This is to detect a change in the elements of the replacement equivalent battery scheme in the range from 0% SOC to 100% SOC. This course is compared below with the simulation model of the cell.
Discharging was similar to charging. The discharge of the cell was also interrupted. The course of intermittent discharge of the cell is shown in Figure 4 - right. Discharging was like charging. The discharge of the cell was also interrupted. The course of intermittent discharging of the cell is shown in Figure 4 - right. Similar to charging and discharging, pauses were analyzed, and elements of the replacement equivalent scheme were then determined from those pauses.

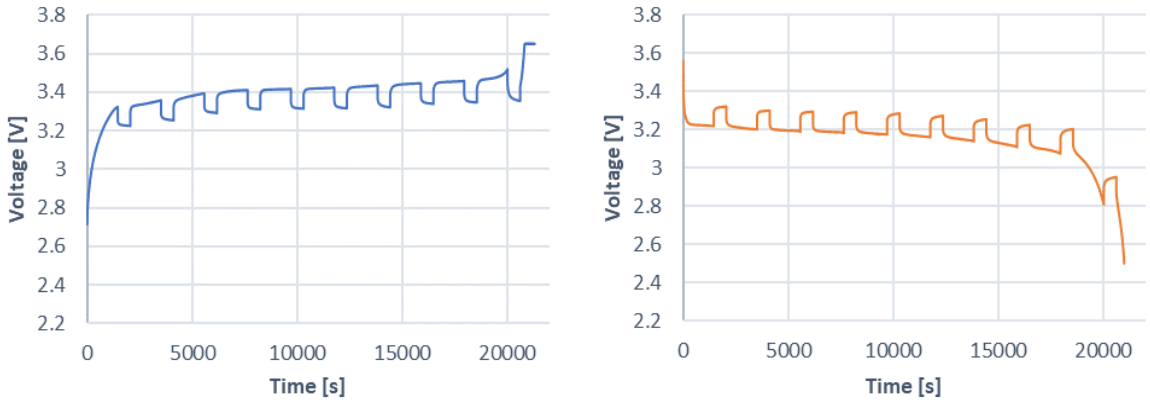

Fig. 4 The waveform of the cell voltage during charging with pauses (left), the waveform of the cell voltage during discharging with pauses (right)

Simulation model and simulation results

This simulation model of an electrochemical cell consists of two parts (Fig. 5). The first part is the power part composed of the elements of the replacement scheme and the + and - terminals. The second part of the simulation model is the computational part. This section calculates the current SOC (State of charge) of the cell and the values of the replacement scheme elements. The values of the elements of the replacement scheme consist of polynomials that overlap the measured waveforms of OCV, R_S, R_1, C_1, R_2 and C_2 depending on the SOC of the cell. Two more initial parameters enter this simulation. The initial SOC value of the cell and the capacity of the cell. From these values, the SOC value is then converted based on the current flowing through the cell. The real voltage of the cell s in this simulation is calculated as OCV plus the voltage drop (V_D) of the elements of the replacement scheme (1).

$$V_{CELL} = OCV \pm V_D \quad (1)$$

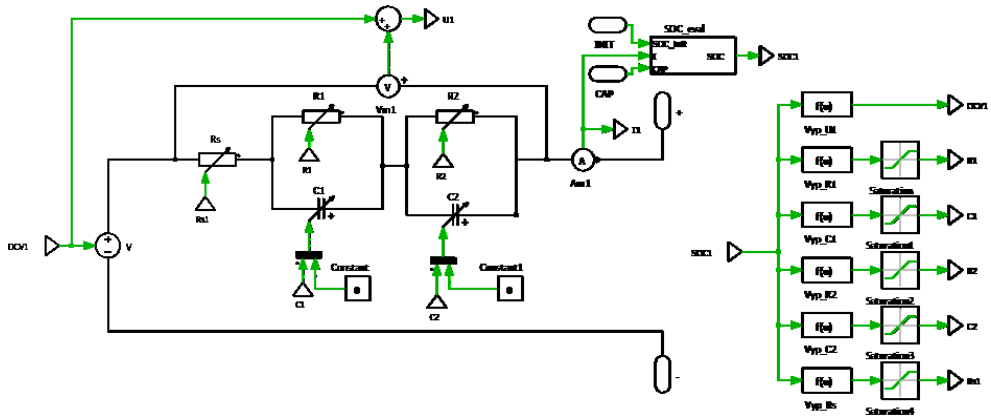

Fig. 5 Simulation model of selected battery cell

ISBN: 978-80-574-0039-4

In this simulation, 3 parameters of the cell are monitored. State of charge, open circuit voltage and cell voltage. Cell voltage for comparison with measured values. Initial values for charging were SOC INIT = 0 and for discharging SOC INIT = 1.

Simulation of the charging and discharging process

As a result of the simulation (Fig. 6 - left), it can be seen that the SOC and OCV gradually increase. However, during the course of the cell voltage, it is clear what influence the elements of the replacement equivalent scheme have on the cell voltage. During charging, the current flows in such a direction that a voltage drop occurs at the elements of the replacement equivalence scheme, so that it manifests itself in the resulting course as a pulsed charge. If we compare it with the measured values, the time of full charging of the cell corresponds almost exactly to the values that were measured. It can be seen similarly at the pulse rate. Thus, we can say that the results of the simulation almost 100% agree with the real measured values. The results of the simulations for discharging (Fig. 6 - right) look exactly opposite to charging. For comparison with the measured values, the discharge time is also the same, and the same applies to the height of the cell voltage pulses. When testing the discharge of this simulation model, we can also say that it is almost 100% the same as the measured values.

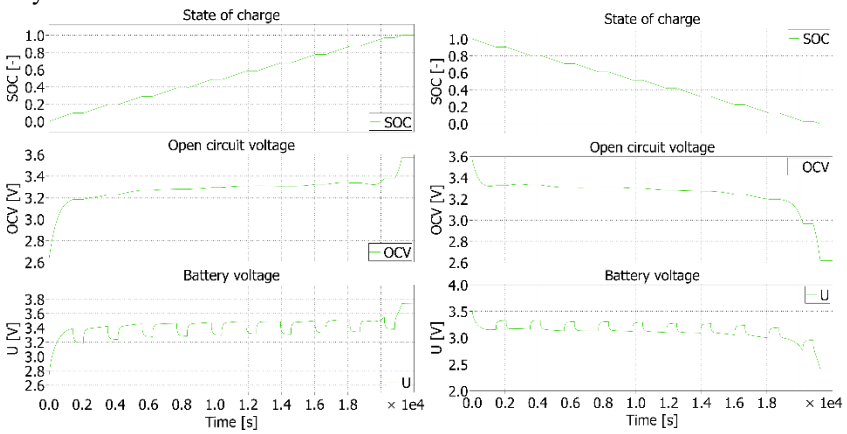

Fig. 6 Simulation results for charging (left) and discharging (right) process

Conclusion

The aim of this work was to build the most accurate simulation model of an electrochemical cell. A LiFePO4 based cell was selected for this purpose. With the help of an algorithm and a programmable load and source, the cell was discharged and charged by pauses. Subsequently, from the measured waveforms, the pauses from these pauses were analyzed and the parameters of the surrogate equivalent scheme of the cell were determined. From these measurements, a simulation model of this cell was constructed.

From the results (Fig. 7) of the simulations and the subsequent comparison, we can say that the simulation is accurate. Therefore, this cell simulation model can be used in more complicated simulation models as an energy source or energy storage. This model serves as a complete replacement for a single cell. By connecting this model in series-parallel, we can also disassemble high-voltage batteries and analyze them at the lowest level, at the level of the cell.

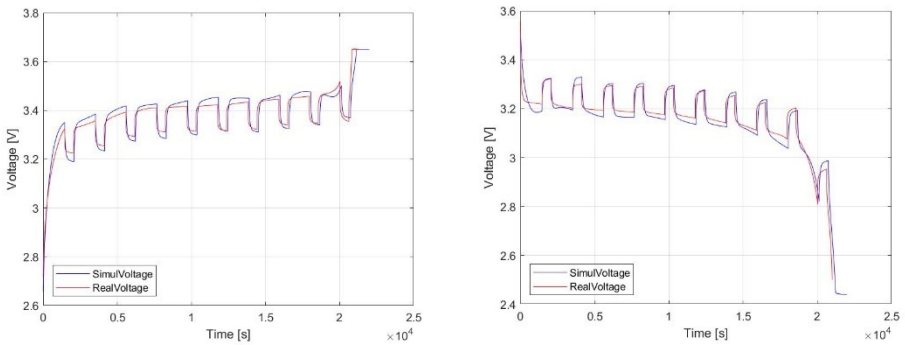

Fig. 7 Comparisson between simulation and experiment, charging process – left, discharging - right

ISBN: 978-80-574-0039-4

Acknowledgements

This publication was realized with support of Operational Program Integrated Infrastructure 2014 – 2020 of the project: Innovative Solutions for Propulsion, Power and Safety Components of Transport Vehicles, code ITMS 313011V334, co-financed by the European Regional Development Fund.

References

[1] Battery University, https://batteryuniversity.com/.
[2] GWL POWER, Technical specification, Datasheet NPB60AH, NPB100AH

 ISBN: 978-80-574-0039-4

Electrode materials based on metal-organic frameworks and polymers for sodium-ion batteries

T. Kazda [a]*

[a]Department of Electrical and Electronic Technology, Faculty of Electrical Engineering and Communication, Brno University of Technology, Technická 10, 616 00 Brno, Czech Republic
*kazda@feec.vutbr.cz

Today's world is dependent on modern technologies that are related to freely available connectivity by rapid transfer of information from anywhere and on the fast transport of goods and people. However, transport of people and goods brings the environmental burden caused by the combustion of fuels, which is from environmental point of view unsustainable from the long-term perspective. Modern communication technologies, on the other hand, work without an internal combustion engine but they need some compact portable source of power. The answer solving both problems are modern lithium-ion (Li-ion) batteries, which enable the operation of portable devices and the implementation of efficient electrical transport. This technology also has its limits, and in the future, it will be necessary to look for other types of batteries for energy storage. One of the further possibilities of development are sodium-lithium ion batteries which can provide reasonable energy density for public transport electric vehicles and also enough energy density for stationary energy storage applications whit sustainable battery technology based on abundant sodium.

Introduction

Modern technologies such as cell phones, notebooks and other wearable electronics would be useless without the use of today's Li-ion battery technologies. Only high energy density of cutting-edge Li-ion batteries can store enough energy for energy needs of this modern applications. Significant development of energy density of Li-ion batteries enabled the development of new mobility applications such as electric vehicles, e-bikes or drones as well. The disadvantage of using Li-ion batteries in the future may be the use of lithium, which is not represented in the earth's crust in high percenteg and is avability is complicated. Despite these disadvantages, current lithium reserves should be able to cover the development of all these applications in the future [1]. However it is unnecessary to use the most advanced technology for all types of applications if there is a sustainable alternative. This is the main reason why current battery research will focus on other types of technologies based on sodium, potassium, calcium or magnesium [2]. All these technologies are based on environmentally friendly and abundant materials and are also theoretically capable of achieving high energy densities. In this article, we will focus on materials that can be use in Na-ion batteries.

Na-ion batteries

Na-ion battery systems are very attractive because of sodium used as active element. Sodium, the sixth most common material in the earth's crust, is cheap and ecological. Another advantage of sodium usage is the possibility of using aluminum as a current collector on both electrodes. However, sodium has higher potential against standard hydrogen electrode -2.71 V compare to lithium -3.04 V and theoretical capacity of the sodium is significantly lower 1166 mAh/g compare to lithium 3860 mAh/g [3]. These properties limit Na-ion batteries in terms of the achievable gravimetric energy density and which will be lower than in the case of Li-ion batteries. However, this limitation would not be significant for less demanding applications or for stationary energy storage and the main prerequisite for a successful market application would be price and a sufficiently long cycle life. However, the short cycle life of anode materials in particular is one of the main shortcoming of this battery system. Compared to Li-ion batteries, use of the graphite as anode material is in the case of Na-ion batteries not possible. Diameter of sodium ions is about 34% higher compare to lithium ions which leads to decomposition of graphite layers during sodium intercalation and the consequent capacity loss [4]. This is a main reason why the research focuses on the development of anode materials that would have a sufficiently high cycle life and at the same time high capacity. One of the promising possibilities is the use of composite carbon materials combined with metal oxides based on metal-organic frameworks (MOFs). An example could be the use of the Co-C nanocomposite based on Co-Bpdc MOF after treatment at 340°C presented by Škoda at.al [5]. The Co-Bpdc-340 exhibit high electrochemical activity at low potential against sodium ~ 0.4 V, capacity over 200 mAh/g, low irreversible capacity in the firs cycle 18.7% and

 ISBN: 978-80-574-0039-4

capacity retention 71.6% after 100 cycles at 0.2 C. Other example of the MOFs can be V-NBpdc MOF converted to VO-NC composite by carbonization at 600°C in argon atmosphere presented by Škoda at. al.[6]. This VO-NC composite exhibit slightly higher potential against sodium ~ 0.8 V, capacity over 250 mAh/g, low irreversible capacity in the firs cycle 14.2%, however lower capacity retention 54% after 100 cycles at 0.2 C. As we can see, mainly low irreversible capacity is main advantage compare to hard carbons (irreversible capacity usually ~30%) which can be use as anode material for Na-ion batteries as well. Other materials that can be use in the MOFs for Na-ion anodes are titanates. Zhang at.al.[7] In his work present porous cake-like TiO_2 derived from metal-organic frameworks. Porous cake-like TiO_2 was obtained by MIL-125 calcination at 500°C. This porous cake-like TiO_2 exhibit potential against sodium ~ 0.6 V, capacity over 250 mAh/g, high capacity retention ~ 92% after 70 cycles at different C-rate, however high irreversible capacity in the firs cycle 43%. Other interesting option is using polymers like an electrode materials for Na-ion batteries. Syrový at. al presented us of poly(1,5-anthraquinonyl sulfide) (PASQ) in combination with Super C45 conductive aditive [8]. PAQS-C45 sample exhibit two steps discharge plateau ~2 V and ~1.6 V versus sodium. This type of material can be used as high voltage anode or like a low loltage cathode. PAQS-C45 exhibit low irreversible capacity just ~14%, capacity over 140 mAh/g and high capacity retention during cycling at 0.2 C see Figure 1. Guo at. al present 9,10-anthraquinone encapsulated in CMK-3 mesoporous carbon (AQ/CMK-3) low voltage cathode [9]. AQ/CMK-3 cathode exhibit potential against sodium ~ 1.7 V, capacity around 200 mAh/g, negligible irreversible capacity in the first cycle just 3% and high capacity retention 88% after 50 cycles at 0.2.

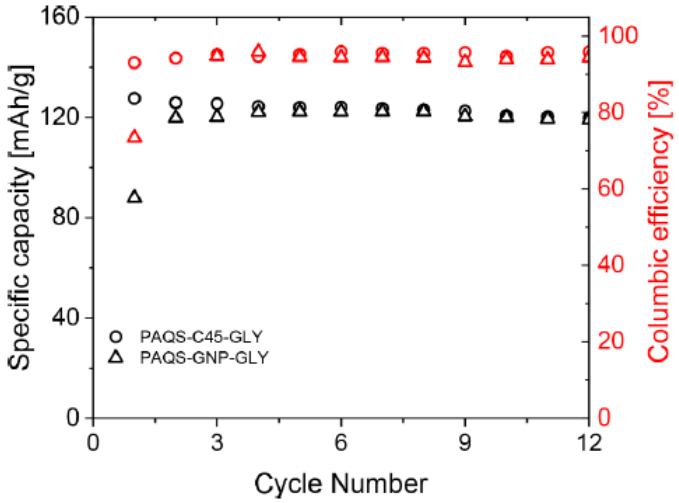

Fig. 1 Galvanostatic cycling of coin cell at 0.2 C rate for glymes-based type Na electrolyte for PAQS with conductive filler based on Super C45 and GNP [8]

Conclusions

This article serves as a brief review of sodium-ion technology and the possibilities of using metal-organic frameworks and polymer based electrodes to improve the properties of Na-ion batteries. It is clear that both MOFs and polymers offer a wide range of options for adjusting their properties in order to achieve the best possible properties for Na-ion batteries. MOFs generally offer higher capacity however lower stability during cycling on the other hand polymers offer lower capacity however lower irreversible capacity and quite good stability during cycling.

Acknowledgements

This work was supported by the specific graduate research of the Brno University of Technology No. FEKT-S-20-6206 and from the Ministry of Education, Youth and Sports of the Czech Republic under project No. LTT19001.

 ISBN: 978-80-574-0039-4

References

[1] GREIM, Peter, A. A. SOLOMON a Christian BREYER. Assessment of lithium criticality in the global energy transition and addressing policy gaps in transportation. *Nature Communications*. 2020, 11(1), 11. ISSN 2041-1723
[2] ELIA, Giuseppe Antonio, Krystan MARQUARDT, Katrin HOEPPNER, et al. An Overview and Future Perspectives of Aluminum Batteries. *Advanced Materials*. 2016, 28(35), 7564-7579. ISSN 09359648
[3] Yabuuchi N, Kubota K, Dahbi M, Komaba S (2014) Research Development on Sodium-Ion Batteries. *Chemical Reviews* 114:11636-11682
[4] Nayak PK, Yang L, Brehm W, Adelhelm P (2018) From Lithium-Ion to Sodium-Ion Batteries: Advantages, Challenges, and Surprises. *Angewandte Chemie International Edition* 57:102-120.
[5] SKODA, David, Tomas KAZDA, Lukas MUNSTER, et al. Microwave-assisted synthesis of platelet-like cobalt metal-organic framework, its transformation to porous layered cobalt-carbon nanocomposite discs and their utilization as anode materials in sodium-ion batteries. *Journal of Energy Storage.* 2020, 27(2), 13. ISSN 2352152X.
[6] SKODA, David, Tomas KAZDA, Barbora Hanulikova, et al. Vanadium Metal-Organic Frameworks Derived VOx/Carbon Nano-Sheets and Paperclip-Like VOx/Nitrogen-Doped Carbon Nanocomposites for Sodium-Ion Battery Electrodes. *Materials Chemistry and Physics.* 2021
[7] ZHANG, Xiaojie, Miao WANG, Guang ZHU, Dongsheng LI, Dong YAN, Ting LU a Likun PAN. Porous cake-like TiO2 derived from metal-organic frameworks as superior anode material for sodium ion batteries. *Ceramics International*. 2017, 43(2), 2398-2402. ISSN 02728842
[8] SYROVÝ, T., T. KAZDA, J. AKRMAN a L. SYROVÁ. Towards roll-to-roll printed batteries based on organic electrodes for printed electronics applications. *Journal of Energy Storage*. 2021, 40(5), 9. ISSN 2352152X.
[9] GUO, Chunyang, Kai ZHANG, Qing ZHAO, Longkai PEI a Jun CHEN. High-performance sodium batteries with the 9,10-anthraquinone/CMK-3 cathode and an ether-based electrolyte. *Chemical Communications*. 2015, 51(50), 10244-10247. ISSN 1359-7345.

 ISBN: 978-80-574-0039-4

Influence of low temperatures on LTO battery performance

M. Šedina[a]*, T. Kazda[a]

[a] Department of Electrical and Electronic Technology, Faculty of Electrical Engineering and Communication, Brno University of Technology, Technická 10, 616 00 Brno, Czech Republic
*xsedin00@vut.cz

Abstract
This text deals with the influence of low temperatures on LTO ($Li_4Ti_5O_{12}$) Li-ion battery. The behaviour of the Li-ion batteries under low temperatures is crucial for electric vehicles, which can operate in extreme weather, and we need to know if this low temperature won't have a negative effect on the battery.

Introduction
Li-ion batteries are the most advanced energy storage which we use on an everyday basis. We have them in our smartphones, wearables, laptops, etc. Last but not least we are using LIBs to powering electric vehicles (EV). Using Li-ion batteries in EV increase interest in battery lifetime, which is affected by battery working conditions such as current load, operating temperature, etc. Because EVs should work everywhere on the planet, operation temperature is one of the discussed topics, because if it is too high it can dramatically irreversibly reduce battery capacity or it can lead to damaging the battery.[1][2] On the other hand, if it is too low the electrolyte can freeze and it will lead to battery damage, but there are some possibilities how to adjusted the temperature working range of the electrolyte and it can lead to the liquidity of the electrolyte even in -40 °C. [3]

Experiment
For the experiment was chosen cell in 18650 shapes, LTO1865-13, made by GWL with cathode material LTO.

Tab.1 Parameters of battery GWL LTO1865-13 taken from datasheet [4]

Nominal capacity	1300mAh
Optimal charging	CCCV, 1 C, 2.8V (100 mA) cut-off
Optimal discharging	1 C, 1.85 V cut-off
Maximal discharge current	13 A (10 C)
Capacity after 250 cycles (25 °C)	≥ 1.200 mAh
Operating temperature	Charging: -15 °C to 45 °C
	Discharging: -25 °C to 55 °C

The battery was tested in the full voltage window and for charging was used mode constant current, constant voltage (CCCV). During each measurement did battery 10 cycles with 0.2 C, first started with room temperature 23 °C then 40 °C and then again room temperature. After that was battery measured under low temperatures -5 °C, -10 °C, -15 °C, -20 °C, -25 °C and - 30 °C with step -5 °C. Between every temperature step was battery measured under room temperature. In the end, was battery left 14 days resting and then last 10 cycles at room temperature. A small cycling current was set to prevent lithium plating and reduction of self-heating during current flow in the battery.

 ISBN: 978-80-574-0039-4

Figure 1 represents the results of the long-time battery cycling under different temperatures. As you can see the starting capacity of the battery was lower (6.3 %) than the nominal capacity of the battery declared by the producer. The first 30 cycles were made at room temperature and above room temperature (40°C). Measuring at -5 °C show a drop of the capacity on approximately 1114 mAh which is an 8.5 % drop. After the next measurement on room temperature raised back with little drop. Measuring at -10 °C show a drop of the capacity on approximately 1036 mAh which is a 15 % drop. And room temperature showed no change in capacity. At -15 °C the average capacity was 964 mAh which is a 21 % drop. The room temperature showing a little decrease in capacity, but it is just an effect of ageing the battery. At -20 °C capacity dropped at 892 mAh which is 27 % less than a new battery. At -25 °C you can see a significant drop in the first three cycles and the average capacity was 795 mAh, which is a 35 % drop. Measurement at room temperature didn't show any capacity drop. Measurement at -30 °C showed a large difference between the values, capacity stabilised after five cycles and the average capacity was 559 mAh, which means 64 % capacity drop. After the next measurement on room temperature capacity showed no significant drop. For the last ten cycles battery was left 14 days at room temperature and then cycled. Results show a linear drop in capacity. After 160 cycles battery ended with a capacity of 1181 mAh, which is a 3% drop from the capacity of the new battery.

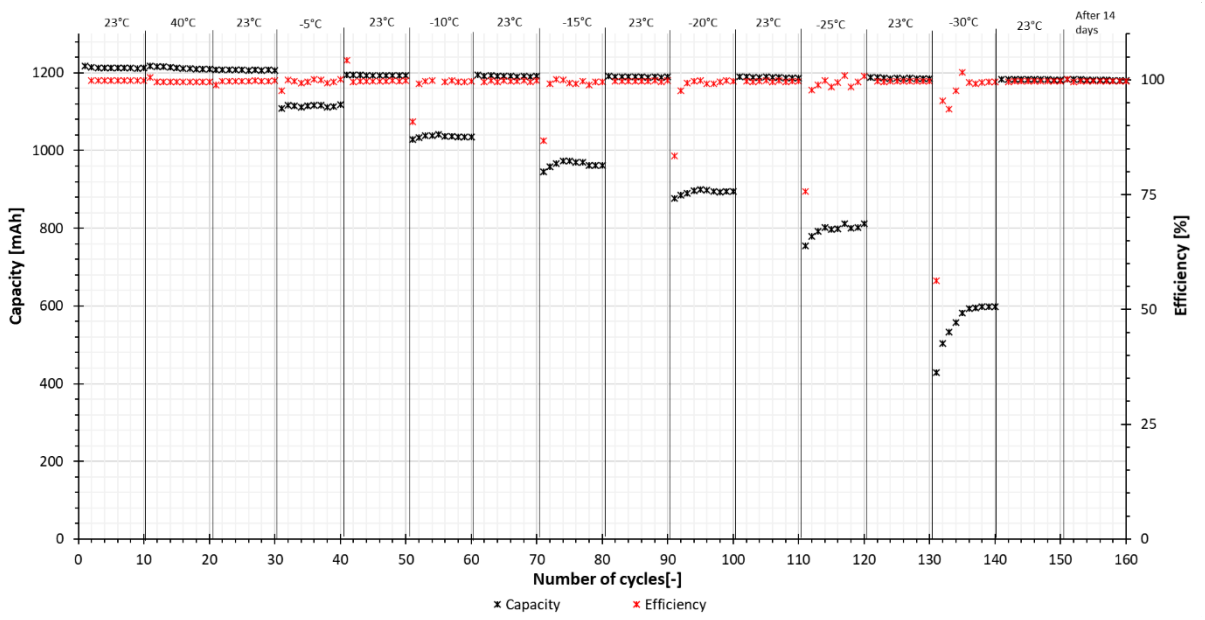

Fig. 1 Capacity and coulombic efficiency of the battery under measured temperatures

Conclusion

The experiment showed that Li-ion batteries based on LTO can work in low temperatures. If we choose the right battery technology, the temperature has almost no irreversible effect on battery capacity. In low temperatures is visible capacity drift which can be made by battery self-heating made by current flow during cycling.

Acknowledgements

This work was supported by the specific graduate research of the Brno University of Technology No. FEKT-S-20-6206.

References

[1] LENG, Feng, Cher Ming TAN a Michael PECHT. Effect of Temperature on the Aging rate of Li Ion Battery Operating above Room Temperature. *Scientific Reports*. 2015, **5**(1), 1-12. DOI: 10.1038/srep12967. ISSN 2045-2322. Dostupné také z: http://www.nature.com/articles/srep12967

 ISBN: 978-80-574-0039-4

[2] HIETANIEMI, Marianna. *Thermal stability of chemical compounds used in lithium-ion batteries* [online]. 1. Oulu: Oulu University Library, 2015 [cit. 2021-09-23]. Dostupné z: http://jultika.oulu.fi/files/nbnfioulu-201512032229.pdf

[3] HUANG, C. -K., J. S. SAKAMOTO, J. WOLFENSTINE a S. SURAMPUDI. The Limits of Low-Temperature Performance of Li-Ion Cells. *Journal of The Electrochemical Society*. 2000, **147**(8), 2893-2896. DOI: 10.1149/1.1393622. ISSN 00134651. Dostupné také z:https://iopscience.iop.org/article/10.1149/1.1393622

[4] GWL a.s.. [online datasheet]. *LTO1865-13*. ©2010 [cit. 17.4.2018]. Dostupné z: https://files.gwl.eu/inc/_doc/attach/StoItem/4576/GWL-LTO1865-13-Spec.pdf¨

 ISBN: 978-80-574-0039-4

Low-temperature Synthesis of Lithium Titanate Nanoparticles Assisted by Ball Milling and Their Structural and Electrochemical Performance as Anode Materials for Li-ion Batteries

M. Fabián[a]*, M. Žukalová[b], L. Kavan[b], M. Senna[c]
[a] Institute of Geotechnics, Slovak Academy of Sciences, 040 01 Košice, Slovakia
[b] J. Heyrovsky Institute of Physical Chemistry, Academy of Sciences of the Czech Republic, CZ-18223 Prague 8, Czech Republic
[c] Faculty of Science and Technology, Keio University, 232-8522, Yokohama, Japan

*corresponding author e-mail: fabianm@saske.sk

In this work, we refer on simple synthesis of spinel based $Li_4Ti_5O_{12}$ (LTO) by combination of mechanical pre-activation of precursors followed by low-temperature calcination at 600°C. The phase evaluation and its purity is examined by analyses of data provided X-ray powder diffraction and ^6Li MAS NMR. The charge capacity of the LTO with average crystallite size 150 nm was found to be 142 mAh/g, i.e. ~ 81 % of theoretical capacity. The capacity of our optimised material is superior to that of commercially available spinel, although the as-synthesized LTO is characterized by small BET-specific surface area. The superior properties of our material were also demonstrated by galvanostatic charging/discharging. In order to modify crystallite size and BET-specific surface area, as-prepared samples were further treated by ball milling. X-ray diffraction analysis proves the presence of majority of $Li_4Ti_5O_{12}$ phase with small amount of rutile and WC impurities with negligible effect on electrochemical properties. Transmission electron microscopy analysis revealed presence of $Li_4Ti_5O_{12}$ in different morphologies. Cyclic voltammetry of Li insertion and galvanostatic chronopotentiometry at 1C rate confirm the highest charge capacity for $Li_4Ti_5O_{12}$ spinel with surface area of 21 $m^2 g^{-1}$. Due to optimized ratio of two particular morphologies this material possesses excellent long time cycling stability during galvanostatic chronopotentiometry at 1, 2 and 5C. Its discharge capacities reach 170 mAh g^{-1} at 1C (~ 97% of theoretical value), 167 mAh g^{-1} at 2C and 160 mAh g^{-1} at 5C rates with 100% coulombic efficiency. The capacity drop was less than 1% for charging rates of 1 and 2C and about 5% at 5C. Accordingly, the effect of crystallite size and BET-surface area on the electrochemical properties of synthesized LTO are discussed within this work.

ISBN: 978-80-574-0039-4

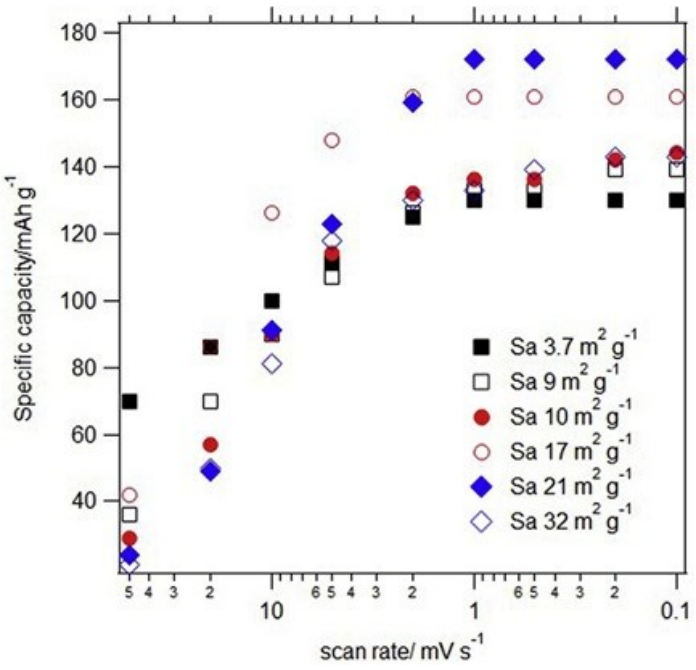

Fig. 1 Effect of B.E.T. surface area on capacity in as-prepared LTO powders.

Acknowledgements

This work was supported by the Slovak Research and Development Agency APVV (No. 19-0526) and Scientific Grant Agency VEGA (No. 2/0055/19).

ISBN: 978-80-574-0039-4

ISBN: 978-80-574-0039-4

ISBN: 978-80-574-0039-4

ISBN: 978-80-574-0039-4

The 5th International Conference on Nanomaterials: Fundamentals and Applications
Book of Abstracts

Edited by: Veronika Niščáková, Ivana Šišoláková

Publisher: Pavol Jozef Šafárik University in Košice
Publishing ŠafárikPress

Year: 2021
Pages: 90
Author's sheets: 4.5
Edition: first

ISBN 978-80-574-0039-4 (e-publication)

ISBN: 978-80-574-0039-4